

Information Theory and Pattern Recognition

by M.F. Daemi, B.Sc.

Thesis Submitted to the University of Nottingham for the degree of
Doctor of Philosophy, May, 1990

Contents

Chapter 1 - Introduction	1
1.1. Objective	1
1.2. The concept	2
1.3. Previous work in this area	2
1.4. The Thesis	3
Chapter 2 - Pattern Recognition and Theory of Information Assessment	5
2.1. Pattern Recognition	5
2.1.1. Approaches to pattern recognition	5
2.1.1.1. Template-matching	6
2.1.1.2. Decision-theoretic approach	6
2.1.1.3. Structural and syntactic approach	7
2.1.2. Pattern recognition techniques and relation with other disciplines	7
2.2. Information Theory	9
2.2.1. A brief history of information theory	10
2.2.2. Information content and entropy	11
2.3. Information theory in pattern recognition	13
Chapter 3 - Basic information assessment - Preliminary Investigation	15
3.1. Information assessment of simple binary patterns	15
3.1.1. The concept	15
3.1.2. Method in detail	17
3.1.3. Results	18
3.1.4. Analysis of the results	19
3.2. Basic Rotational and translational information assessment	20
3.2.1. Rotational information assessment	20
3.2.1.1. Technique of calculation	22
3.2.1.2. Results	22
3.2.1.3. Maximal and minimal limits of rotational information	24
3.2.2. Translational information assessment	26
3.2.2.1. Coarse and fine translation information	26
3.2.2.2. Results	27

3.2.2.2.1. Sets IIA and IIE	28
3.2.2.2.2. Sets IIB and IID	28
3.2.2.2.3. Set IIC	30
3.2.2.3. Further consideration of the results	30
 Chapter 4 - Automatic Information Assessment of Simple Patterns	 33
4.1. The algorithms in detail	33
4.1.1. Definition of the pixel grid and the image under investigation	33
4.1.2. Identification of sensor output patterns	35
4.2. Fine translational information assessment	38
4.3. Rotational information assessment	40
 Chapter 5 - Assessment of Rotational, Translational and Total Information Content for Two Dimensional Patterns	 41
5.1. Translational, rotational and overall information	41
5.2. Information assessment of simple binary images	43
5.2.1. Patterns under study	43
5.2.2. Translational information assessment	44
5.2.2.1. The 4x2 rectangular pattern	45
5.2.2.2. Other patterns	46
5.2.3. Rotational information assessment	47
5.2.4. Overall information assessment	49
5.2.5. Shared information (s)	52
5.3. Information assessment of more detailed patterns	53
5.3.1. Patterns under study	53
5.3.2. Group 1	55
5.3.3. Group 2	56
5.3.4. Group 3	57

Chapter 6 -	Analysis of information distinguishing between patterns	58
6.1.	The comparison method	59
6.2.	Accuracy of discrimination between patterns	60
6.2.1.	Combining two images	60
6.2.2.	Combining multiple images	62
6.3.	Comparing very similar patterns	65
6.4.	pitch and roll information carried by aircraft silhouettes	66
6.5.	Comparison with a proposed pattern recognition method	69
Chapter 7 -	Conclusion and further considerations	71
7.1.	Summary of the conclusions	71
7.1.1.	Preliminary investigation	71
7.1.2.	Advanced information assessment	72
7.1.2.1.	Summary of the results	72
7.1.2.2.	Discussion and further conclusions	74
7.1.3.	Assessment of performance of pattern recognition systems	75
7.2.	Further development of the investigation	76
7.3.	Wider implications of information assessment methods	77
References		79
Appendices		

ABSTRACT

This thesis presents an account of an investigation into the use of information theory measures in pattern recognition problems. The objectives were firstly to determine the information content of the set of representations of an input image which are found at the output of an array of sensors; secondly to assess the information which may be used to allocate different patterns to appropriate classes in order to provide a means of recognition; and thirdly to assess the recognition capability of pattern recognition systems and their efficiency of utilization of information. Information assessment techniques were developed using fundamental principles of information theory. These techniques were used to assess the information associated with attributes, such as orientation and location, of a variety of input images. The techniques were extended to permit the assessment of recognition capability and to provide a measure of the efficiency with which pattern recognition systems use the information available.

Acknowledgements

My sincere thanks go to Professor R.L. Beurle for his invaluable guidance and advice over the years of this project. Gratitude is also due to R.S.R.E. for funding part of the investigation. My thanks also to Dr. Richard J. Petheram for his help and contributions. I would also like to thank my family for their support and encouragement. This thesis is dedicated to my brother, Mr. Farhad Daemi without whom all this would not have been possible.

Farhang Daemi

CHAPTER 1 - INTRODUCTION

1.1. Objective

This is an account of an investigation into the use of information theory measures in pattern recognition problems. The objective is to determine the information content of a set of representations of a given pattern, to assess the information which may be used to allocate different patterns to appropriate classes in order to provide a means of recognition, and to assess the recognition capability and efficiency of utilization of information of pattern recognition systems.

Pattern recognition situations can vary greatly, primarily because of the nature of patterns under investigation [1][2]. Patterns may be one dimensional (e.g. waveforms), or multi-dimensional (e.g. 2-dimensional images or 3-dimensional solid shapes, or indeed relationships between many variables). Consequently many different techniques are used which are usually problem dependent [3][4]. However there are certain considerations which apply to almost all pattern recognition problems. The most common difficulty is usually the vast amount of information which has to be dealt with. For example a pattern in the form of a two-dimensional half tone image in a n array of 1024×1024 pixels, each of which may record one of 256 grey levels, contains over 8 Mega-bits of information. The analysis of the pattern without any foreknowledge would constitute a formidable task [5].

It is evidently advantageous if one can reduce this massive information into manageable proportions by isolating and extracting just that part of the information which is relevant for the recognition process, from the mass of irrelevant information which often accompanies it. The definition, identification, assessment and analysis of this *useful information* is the main concern of this investigation.

1.2. The Concept

By making an estimate of the information content of a two dimensional image picked up on an array of light sensitive pixels, one can assess the limitations necessarily imposed on any pattern recognition system which seeks to make use of this information.

In order to meet the objectives of this investigation, various sets of two-dimensional, two state (binary) input images were chosen for study. These patterns range from simple square and rectangular shapes in earlier work (as described in chapters 3 and 5), to somewhat more detailed silhouettes of aircraft shapes viewed from different angles (chapters 5 and 6).

These patterns were deemed to be adequate for the purpose of this work since, as already mentioned, the main emphasis is placed on developing methods of assessment of the useful information in a pattern. Moreover, most recognition processes involve thresholding, segmentation and extraction of the edges of grey scale images at an early stage [6][7][8][9][10]. This effectively results in patterns of the type under study here. It may be argued that by artificially defining such patterns some useful information has been eliminated. This is desirable because the work is concerned with investigation of fundamental principles.

1.3. Previous work in this area

The current investigation commenced with an extensive literature survey. This showed that little significant work has been undertaken into the implementation of fundamental information theory principles in pattern recognition problems. It was found that most investigations in this area used information theory methods in tasks such as statistical pattern analysis, or image

coding and data compression which are similar to the long established uses of information theory in communications. Chapter 2 describes some of the work in this area as well as the theory of the techniques used in the current investigation.

1.3 The Thesis

This thesis is a presentation of the concepts and methods developed during the course of this work. The results obtained, and the conclusions drawn are discussed with particular reference to the potential of the process for further development and refinement.

Chapter 2 is dedicated to further introduction of common pattern recognition techniques and information theory concepts. In the case of pattern recognition theory the references cited enable the interested reader to further explore this area. A brief historical account of information theory is then given, which is followed by some basic theoretical treatment of the subject. Reference is made to previous attempts to apply information theory to pattern recognition, and the major differences from the approach adopted in this work are highlighted.

Chapter 3 deals with some of the preliminary work which aims to establish a better appreciation of the principles of information assessment. Simple two-dimensional binary patterns are considered here, and the results illustrate some of the potential uses of information assessment techniques in the context of pattern recognition. In particular, this chapter shows how specific information related to certain attributes of a pattern, such as its position and orientation (referred to as translational and rotational information) may be determined, and how it relates to the task of recognition.

Chapter 4 is concerned with implementation on a computer of the methods derived in

chapter 3. This results in the development of automated procedures applicable to realistic patterns. Various practical considerations are discussed in this chapter.

Chapter 5 further expands the investigation, by detailed algorithmically-based assessment of rotational, translational and total information content of patterns of a more general nature, such as aircraft silhouettes. The relationship between shape and the information content associated with each pattern is scrutinised in some detail.

Chapter 6 describes the assessment^{of} that part of the information content of a sensor array output pattern which enables different input images to be distinguished from one another. It shows how this may be used in assessing the recognition capability and efficiency of utilization of information of pattern recognition systems. Comparison is also made with a proposed practical pattern recognition system [12].

Chapter 7 draws conclusions from the results presented, and highlights the prospects for further use of the proposed methods and their potentials for further development and refinement.

CHAPTER 2 - PATTERN RECOGNITION AND THEORY OF INFORMATION ASSESSMENT

2.1. Pattern Recognition

Pattern Recognition (PR) has been with us for a long time, and yet it is still one of the fastest growing scientific areas with applications across a wide variety of disciplines. These applications range from industrial application such as automatic inspection [20][14], bio-medical applications such as abnormality detection [15][16], remote sensing [17], Power Engineering such as fast fault detection on transmission lines [18], and communication [13][19].

The tasks of pattern recognition are basically to remove the need for a trained operator to perform the recognition, or to enable recognition to be performed that would otherwise be impossible [12]. In examining a pattern one is very often interested only in extracting from it a description of what it depicts. The desired description may be merely a classification of the pattern into one of a small set of pre-specified classes; or it may involve properties of, and relationships among features that appear in the pattern [8].

2.1.1. Approaches to Pattern Recognition

There are many methods proposed for designing a pattern recognition system [31][29][32]. These methods can primarily be grouped into three approaches [20]; namely, *template matching* [21], *decision-theoretic* or *discriminant* approach [22][23], and *syntactic* and *structural*

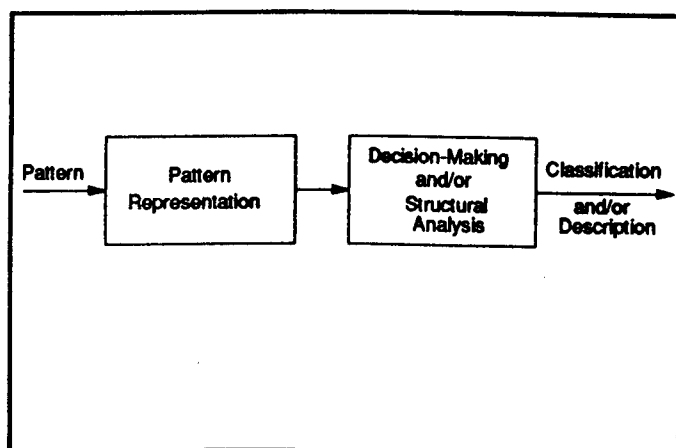


Figure 2.1. A general pattern recognition system (source: reference [20]).

approach [24]. A brief description of each of these three PR approaches is given below, additionally Figure 2.1 shows a block diagram of a pattern recognition system which is generally based in terms of pattern representation and decision making.

2.1.1.1. Template-Matching

In the template matching approach, a set of templates or prototypes, one for each pattern class, is stored in the machine. The input pattern with unknown classification is matched or compared with the template of each class, and the classification is based on a pre-selected matching criterion or similarity measure (eg. correlation). The template matching approach has been used in some existing printed-character recognizers and bank-cheque readers.

2.1.1.2. Decision-Theoretic Approach

In the decision-theoretic approach, a pattern is represented by a set of N features or N -dimensional feature vector, and the decision making process is based on a similarity measure which, in turn, is expressed in terms of a *distance measure* or *discrimination function*.

Statistical methods are commonly used in this approach for the purpose of taking noise and distortion into consideration. Furthermore statistical techniques such as fuzzy sets [25] are used for characterization of each pattern class, which lead to classification of patterns (decision making).

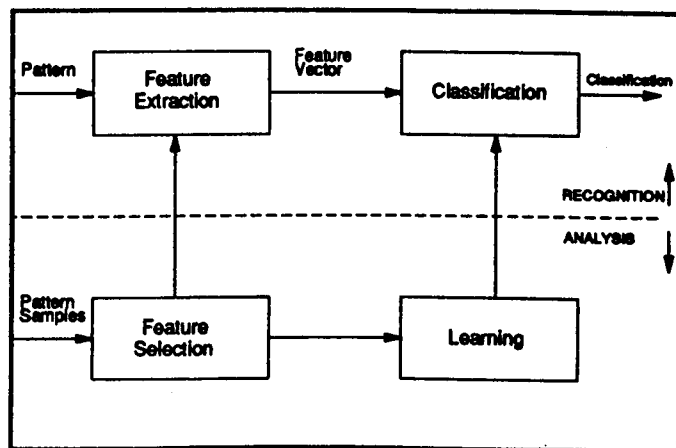


Figure 2.2. Block diagram of a decision-theoretic pattern recognition system (source: reference [20]).

More recently significant interest has been shown in use of information theoretic approaches to PR problems [11][26]. This is examined in more detail later in this chapter.

A block diagram of a decision-theoretic pattern recognition system is given in Figure 2.2. Applications of a decision-theoretic pattern recognition include character recognition, biomedical data analysis and diagnostics, remote sensing, target detection and identification, machine parts recognition and inspection in automation of manufacturing processes.

2.1.1.3. Structural and syntactic Approach

In the structural and syntactic approach, a pattern is often represented as a string, a tree or a graph of pattern primitives and their relations [4][6][27]. The decision making process is in general a syntax analysis or parsing procedure. Special cases include use of similarity (or distance) measures between two strings, two trees, or two

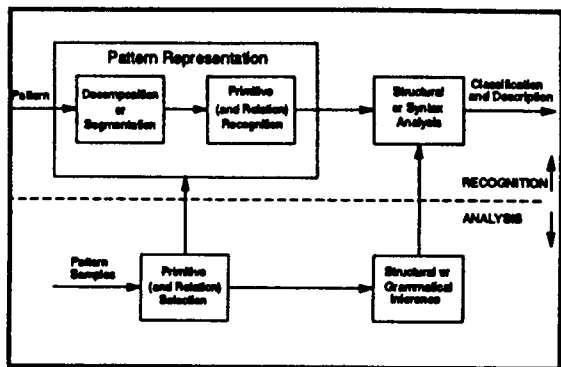


Figure 2.3. Block diagram of a structural/syntactic pattern recognition system (source: reference [34]).

graphs. A block diagram of structural/syntactic pattern recognition system is given in Figure 2.3.

Applications of syntactic pattern recognition include character recognition analysis, automatic inspection, speech recognition, geological data processing and remote sensing to name a few.

2.1.2. Pattern Recognition techniques and relation with other disciplines

The preceding sections have shown that techniques used in pattern recognition are numerous and can be extremely diverse. Figure 2.4 shows a family tree representation of PR techniques which may be regarded as a tentative attempt to put some of the PR techniques and their relationships into perspective.

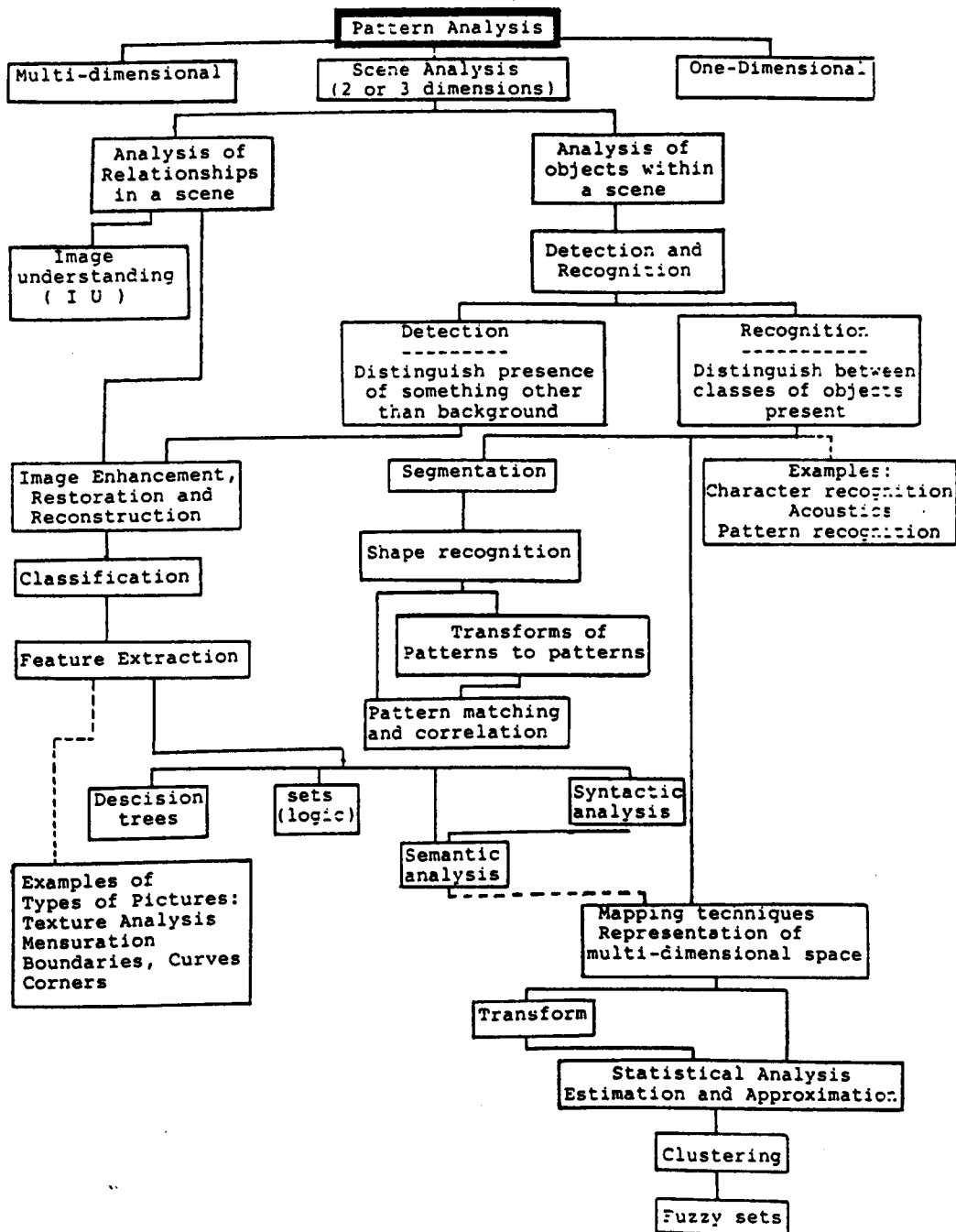


Figure 2.4. Family tree representation of Pattern Recognition techniques.

The relationship between PR and other disciplines is the subject of many publications, as seen in references [28], [29], [30] and [31]. Figure 2.5 (which is quoted from reference [28]) illustrates an indication of relations between automatic PR and a number of other disciplines. A detailed study most of these relations is beyond

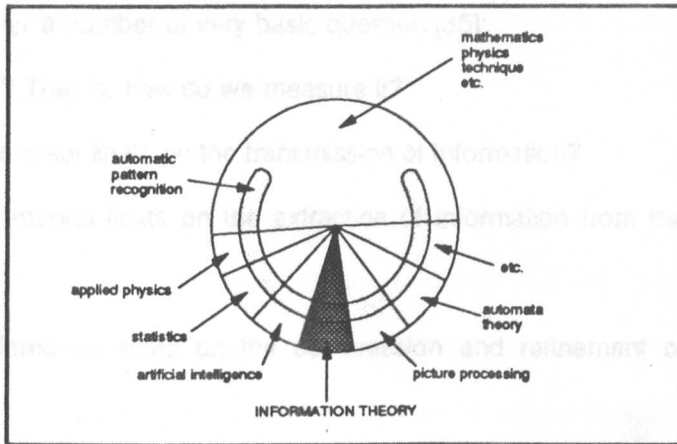


Figure 2.5. Global indication of relations between automatic pattern recognition and a number of disciplines in the world of mathematics, physics, technique, etc. (source: reference [28]).

the scope of this work. However, we shall focus on the topic of information theory and its application in Pattern Recognition.

2.2. Information Theory

Information theory, which may be regarded as "a branch of mathematical theory of probability and statistics" [11], is a discipline centred around a common mathematical approach to the study of the collection and manipulation of information [35]. It provides a theoretic basis for such activities as observation, measurement, data compression, data storage, decision making and *pattern recognition*.

Information theory provides a guide for development of information transmission systems based on a study of the possibilities and limitations inherent in natural law [35]. It is the study of how laws of probability, and of mathematics in general imply limits on the design of information transmission systems. The nature of information theory enables it to be applied to any probabilistic or statistical system of observations [11]. It is the application of information theory in pattern recognition which is of interest in this thesis.

Information theory attempts to answer a number of very basic question [35]:

1. What is information? That is, how do we measure it?
2. What are the fundamental limits on the transmission of information?
3. What are the fundamental limits on the extraction of information from the environment?
4. What are the fundamental limits on the compression and refinement of information?
5. How should devices be designed to approach limits?
6. How closely do existing devices approach these limits?

Although these questions may initially appear vague and unscientific, in a theoretical sense information theory has been spectacularly successful in interpretation of answers to such questions. In a practical sense, information theory has affected the design and development of many systems. It provides guidance to those who are searching for new, more advanced systems [35]. The work presented in this thesis is an illustration of the power and flexibility of information theory in application to pattern recognition situations.

2.2.1. A brief history of Information theory

Claud Shannon is universally known as the father of information theory. In 1948 he published his classic paper "A mathematical theory of communication" [36] in which he created a completely new branch of applied mathematics. Earlier attempts to define a measure of information were made by the communication theorists Nyquist in 1924 [37] and Hartley in 1928 [38], and by statistician Fisher in 1925 [39]. In addition to these, in 1946 Gabor [45] arrived at the idea of a *logon* or unit of information, which really related to Nyquist's work on signalling speed and was nonstatistical in nature [46]. However the subject did not take its present shape until publication of Shannon's work [36]. Wiener [40] and Kotel'nikov [41] also

published in this area at around the same time, but failed to create the same depth and impact as Shannon's work.

Shannon gave mathematical definition of the information rate or entropy of a source and the capacity of a communication channel, noiseless or noisy. This led to significantly improved redesign and new design of communication systems; and also to development of numerous other important techniques such as further development of coding theory for design of error-correcting codes [42].

During the decade of 1970s, related topics in decision and estimation theory were under development. Kulback in 1959 [11] took the position that these topics were a part of information theory. He introduced a function that he called the *discrimination* and developed its relationship to the study of statistics. This function is of great importance since it serves as means of expressing the links between statistics and information theory [35].

2.2.2. Information Content and Entropy

The essence of Shannon's theory can be summed up as follows:

Suppose X is a discrete random variable, that is, one whose range $R=\{x_1, x_2, \dots\}$ is finite or countable. Let $p_i = P\{X=x_i\}$ (where P is the probability measure). The *information content* is defined by [43][44]:

$$I(x_i) = \text{Log} \frac{1}{p(x_i)} \quad (2.1)$$

The function I can be interpreted as the amount of information provided by the event $\{X=x_i\}$, as shown in Figure 2.6. According to this interpretation, the less probable an event is, the more information we receive when it occurs. A certain event (one that occurs with probability 1)

provides no information, whereas an unlikely event provides a very large amount of information [44].

In the spirit of Shannon's theory, it may be said that *information content* of an event should be described in such terms that it

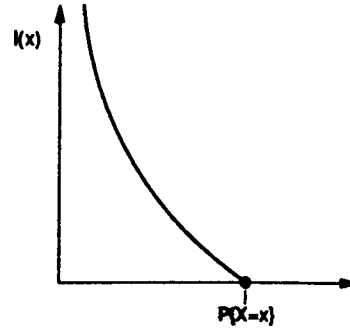


Figure 2.6. The Function $I(x)$.

monotonically decreases with increasing probability and goes to zero for a probability of unity [44].

Entropy, which is the average information per message, may be obtained by taking the various symbols used to transmit the message and weight each by the fraction of time that we expect that particular message to occur (ie. its probability of occurrence). Thus, given n messages x_1 through x_n , the entropy is defined by:

$$H(X) = \sum_{i=1}^n p(x_i) I(x_i) = \sum_{i=1}^n p(x_i) \log \frac{1}{p(x_i)} \quad (2.2)$$

Entropy can be used to measure the prior uncertainty in the outcome of a random experiment, or equivalently, to measure the information obtained when the outcome is observed [35]. In other words, entropy can be thought of as a measure of the following things [44]:

- (a) The amount of *information* provided by an observation X .
- (b) Our prior uncertainty about X which is reduced by making the observation.
- (c) The randomness of X .

The descriptions given above help to clarify the common confusion about what is meant when entropy is referred to as negative information in some texts. One may simply think of entropy as a measure of uncertainty about an event before it is observed (thus the term negative

information or lack of information). Thus the information received on the occurrence of the event can be thought of as negative entropy, because it has reduced the uncertainty.

The base of the logarithm is usually 2 when applying entropy in discrete (digital) problems, the units in this case are *bits* (binary digits). However, sometimes base-e is used in which case units are called *nats* (natural digits) [44].

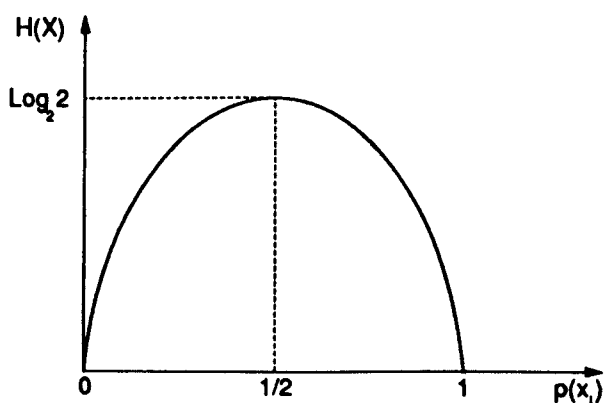


Figure 2.7. Response of the binary entropy function.

For a binary system where the message is made up of two possible symbols x_1 and x_2 and probabilities $p(x_1) = 1 - p(x_2)$, the entropy is given by:

$$H(X) = p(x_1) \log_2 \frac{1}{p(x_1)} + [1 - p(x_1)] \log_2 \left[\frac{1}{1 - p(x_1)} \right] \quad (2.3)$$

Figure 2.7. illustrates the response of binary entropy function

2.3 Information theory in pattern recognition

The preceding sections of this chapter have dealt with pattern recognition and information theory mostly as independent concepts. Let us now consider how information theory may be used in solution of pattern recognition problems, and survey the developments and trend of work.

The most significant impact of information theory has been in the field of communications. As

Shannon's theorems were digested by the mathematical/engineering community, it became clear that he had created a brand-new science, and many others began to make contributions of their own [44]. However the majority of the subsequent work was focused around communications applications [47]. It was not until 1970s that work on decision and estimation theory was under further consideration and development that information theory was first considered seriously in pattern recognition applications [48][53] (see also section 2.2.1).

A majority of work since then has been concerned with enhancement of statistical (or stochastic) methods used commonly in pattern recognition by exploitation of similarities with information theory. These include work on pattern texture analysis [6][55], pattern classification [49][50][51][54][21]; image enhancement using techniques such as fuzzy sets [25][52] and maximization of entropy [56][57][62]; and coding [7].

More recently, there has been some interest in critical examination of pattern recognition systems using information theory [58][59][60][61]. It may appear somewhat surprising that researchers have until now neglected use of information theory principles in their simplest form to pattern recognition situations. However, the concept of pattern recognition was not so far advanced nor so universally of importance as for communication theory at the time of publication of Shannon's paper. It may be that as interest in pattern recognition developed, researchers were slow to realise the possibility of using principles of information theory in reviewing the performance of pattern recognition systems and techniques. The work presented in this thesis may be considered as an ensemble of critical applications of simple information theory principles to pattern recognition systems, in the belief that simplest approaches are often the best!

CHAPTER 3 - BASIC INFORMATION ASSESSMENT - PRELIMINARY INVESTIGATION

This chapter describes some of the initial work on the information content of simple artificial images. The objective of this work was to provide practical experience of information assessment techniques. This initial work paved the way for the application of information assessment techniques to more realistic digitized images described in later chapters.

3.1. Information Assessment of Simple Binary Patterns

A series of experiments in measurement of information content of a set of simple, binary, artificial images were carried out by applying the fundamental formulae for entropy.

Images of one, two and three black pixels against a white background were considered in various positions and orientations and the amount of the information conveyed by each pattern was assessed using both the non-conditional and the conditional entropy formulae. The non-conditional entropy assessment was used as an independent check on the validity of the measurements made using conditional entropy.

3.1.1. The Concept

As discussed in chapter 2, *Entropy* which is the average information per message may be obtained by taking the information content associated with each message weighted by the fraction of time we can expect that particular message to occur (ie. its probability of occurrence)[35][40]

Thus, given n messages, x_1 to x_n , the entropy is defined by:

$$H(x) = - \sum_{i=1}^n p(x_i) \log_2 p(x_i) \quad (3.1)$$

$$H(x) = - \sum_{i=1}^n p(x_i) \log_2 \frac{1}{p(x_i)} \quad (3.2)$$

This reflects the fact that an event which is certain (one with probability 1) provides no information, whereas an unlikely event provides very large amount of information when it does occur.

Conditional Entropy (or equivocation) for a pair of random variables x_1 and x_2 , is the entropy of x_2 given x_1 , $H(x_2 | x_1)$, and is defined by:

$$H(x_2 | x_1) = - \sum_{x_1, x_2} p(x_1, x_2) \log_2 \frac{1}{p(x_2 | x_1)} \quad (3.3)$$

but since

$$p(x_2 | x_1) = \frac{p(x_1, x_2)}{p(x_1)} \quad (\text{from Bays' theorem})$$

and total entropy is

$$H(x) = H(x_1) + H(x_2 | x_1)$$

we have

$$H(x) = - \sum_{x_1, x_2} \left\{ p(x_1) \log_2 \frac{1}{p(x_1)} + p(x_2 | x_1) p(x_1) \log_2 \frac{1}{p(x_2 | x_1)} \right\} \quad (3.4)$$

3.1.2. Method in detail

Three simple shapes were considered during this part of the investigation which is described in detail as an introduction to more sophisticated methods used later.

- (i) One single black pixel against a white background,
- (ii) Two black pixels against a white background,
- (iii) Three black pixels arranged in L-shape against a white background.

Figures 3.1, 3.2, and 3.3 demonstrate the shapes described above.

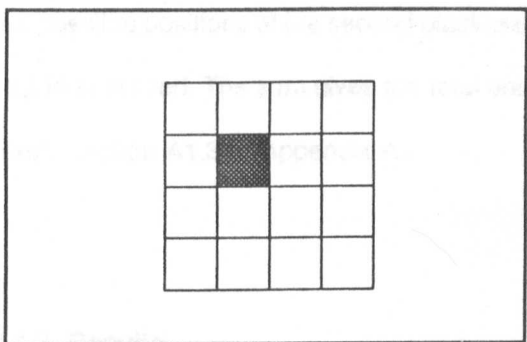


Figure 3.1. The single black pixel.

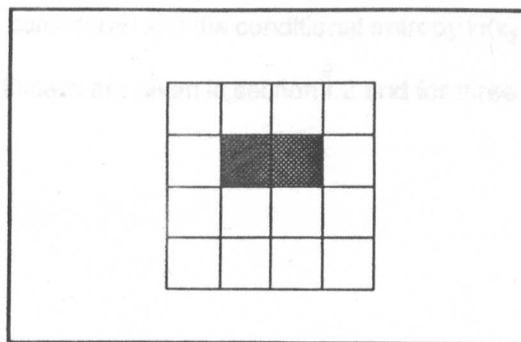


Figure 3.2. The two black pixels.

Each shape considered was assumed to be defined by binary levels, ie. black against a noise-free white background. It was further assumed that the shapes occupied an integral number of pixels, and that no part of the shapes lay outside the grid.

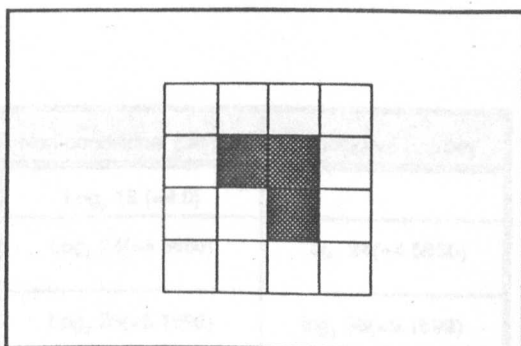


Figure 3.3. The L-shape.

For most cases a 4 by 4 grid was considered, however a 5 by 5 grid was also considered in the case of the 3 pixel L-shape in order to further establish the validity of the techniques used.

Both entropy formulae were used during these investigations. For patterns of two or more black pixels the first, non-conditional entropy formula was found to be a useful test to check the validity of the calculations made using the conditional entropy formula and vice-versa. The formulae are shown in equations 3.2 and 3.4:

Thus by non-conditional entropy the single black pixel may occupy any one of 16 positions for each of which therefore $p_i = 1/16$. Summed over the 16 positions this gives $\text{Log}_2 16$. See section A1.1 of Appendix I for details.

The calculation for a pair of black pixels follows similar principles. For the first black pixel on its own the information is assessed in terms of entropy as $H(x_1)$. Then, given this information, the possible positions of the second black pixel are considered and the conditional entropy $H(x_2 | x_1)$ is assessed. The sum gives the total entropy. Details are given in section A1.2 and for three pixels section A1.3 of Appendix A1.

3.1.3. Results

The results obtained are summarised in table 3.1. Further details of the calculations in each case are given in Appendix 1.

Case no.	Shape	Grid size	Non-conditional Entropy	Conditional Entropy
1	single pixel	4x4	$\text{Log}_2 16 (=4.0)$	-
2	two pixels (rectangle)	4x4	$\text{Log}_2 24(=4.5850)$	$\text{Log}_2 24(=4.5850)$
3	three pixels (L-shape)	4x4	$\text{Log}_2 36(=5.1699)$	$\text{Log}_2 36(=5.1699)$
4	three pixels (L-Shape)	5x5	$\text{Log}_2 64(=6.0)$	$\text{Log}_2 64(=6.0)$

Table 3.1. Summary of the results

It must be noted that the numerical values of the results shown above are, as might be expected, dependent on the size of the grid that contains the object and the background. However, the relative values may be used for comparative purposes under similar conditions.

3.1.4. Analysis of the Results

The results confirm that the information measured by the non-conditional entropy method agrees with that measured using the conditional entropy. This is both a check^{on the} validity of the results obtained by both methods and is of interest when more complex images are considered.

Furthermore, it may be noted that the measured values convey the information related to both the position and the orientation of the object under study. For example, in the 4x4 grid as shown in Appendix 1 (section A1.3.), the L-shape may have 4 possible orientations and occupy 9 different positions; thus giving 36 possibilities in the sample set. Therefore,

Positional information = $\log_2 9 = 3.17$ binary digits

Orientational information = $\log_2 4 = 2$ binary digits

Total information = $\log_2 9 + \log 4$
 = $\log_2 9 \times 4$
 = $\log_2 36$ binary digits, in agreement with the previous
 ----- calculations.

These results encouraged the idea that the concept of entropy could be used successfully for measurement of the information content of images. This measured information may then be

used to ascertain the efficiency of pattern recognition processes. In particular, splitting the information into two parts related to the position and the orientation of the object has been of great value in considering more complex shapes as has the notion of conditional entropy.

In view of these findings, it was decided that further investigation of the positional and the orientational information content of simple binary images would be beneficial, to provide a better appreciation of the underlying concepts and the practical difficulties before considering more complicated real images.

3.2. Basic Rotational and Translational Information Assessment

This section describes the assessment of the information content associated with rotational and translational movements of simple artificial images in which the components of the image were no longer restricted to the area of integral pixels.

A series of experiments in measurement of rotational and translational information content of a set of simple, binary, artificial images was carried out by applying the fundamental formulae of entropy. Black rectangles, of dimensions 4 by 2 pixels, against a white background are considered in various positions and orientations relative to a rectangular matrix of pixels. The average rotational and translational information conveyed by the pixel outputs is then assessed.

3.2.1. Rotational Information Assessment

In this part of the investigation, a simple rectangular image was placed with its centre of gravity in a fixed position in relation to the matrix of sensors. The image was progressively rotated

through a total of 180 degrees about its centre of gravity, and the set of output patterns produced on the sensors was examined and assessed for entropy. This was done for each of the four positions of centre of gravity shown in Figure 3.4(i).

An assumption had to be made regarding the response of the sensor situated in each pixel.

Two alternative assumptions are:

- (i) The sensor is uniformly sensitive over the whole pixel area and will switch from 0 to 1 when more than half pixel is covered
- (ii) The sensor is at the centre of the pixel

Depending on the nature of the actual sensors used, a real array of sensors may be anywhere between these two extremes. As in the previous section (section 3.1) the sensors are assumed to have a binary response, thus returning a zero or a one for each pixel. The two cases may be referred to as area detection and point detection respectively.

In these experiments determination of the exact area of each pixel covered (in accordance with the first assumption) as the image is rotated was found to be practically difficult, particularly at the edges of the image. Other possible assumptions regarding the response of the pixels were therefore considered. It was found that the use of point sensors, situated at the centre of the pixels (the second assumption) simplified calculations, and it was hoped that this would give acceptable results. That the point sensor results are equally indicative of the nature of the problem is demonstrated in the two results quoted for set IA in the results given in Table 3.2. It is interesting to note that the point detectors actually convey slightly more information. The other sets IB, IC and ID were analyzed using the point detection assumption alone.

3.2.1.1. Technique of calculation

Each pattern produced on the sensors, as the image of the rectangular shape rotates over them, persists over a range R_i of angular positions of the image. It is these sensor output patterns that carry the information regarding image position, which is what we are attempting to assess. If we assume that all angles of the rectangular input image are equally probable, then we may assess the probability $p(x_i)$ of any one sensor output pattern occurring, and hence the information $H(x_i)$ carried on average by this output pattern or *symbol*. Sensor output patterns that occur only fleetingly as the angle is changed, carry more information when they do occur, because when they occur they define very precisely the angular position of the image which has caused them. Thus the *information per unit range* of angle $H(x_i)/R_i$ is high for patterns that occur fleetingly. However, because they are less likely to occur, the overall information they carry is less when information is integrated with respect to the angle of the image.

3.2.1.2. Results

Figure 3.4(ii) shows a typical set of successive positions of the 4x2 rectangular image as it is rotated through 180 degrees about its centre of gravity at (a) in Figure 3.4(i). Figure 3.4(ii) also shows, for point detectors, the corresponding pixel sensor output patterns (set IA) from which the information content is assessed.

The third column in Table 3.2. gives the rotational information content assessed for each of the sample sets whose centre of gravity is defined in Fig. 3.4(i). Appendix 2 gives the tabulated details of the calculations, and diagrams in this Appendix show all the sensor output response patterns arising from each position of the centre of gravity. The assessment of the information carried by each sensor pattern, and the summation of the information content of all response patterns arising from each set of images is tabulated in Appendix 2.

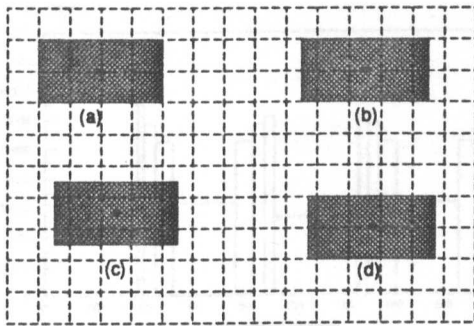


Figure 3.4(I) Position of centre of gravity of each sample set (each square represents one pixel).

- (a): Sample set IA
- (b): Sample set IB
- (c): Sample set IC
- (d): Sample set ID

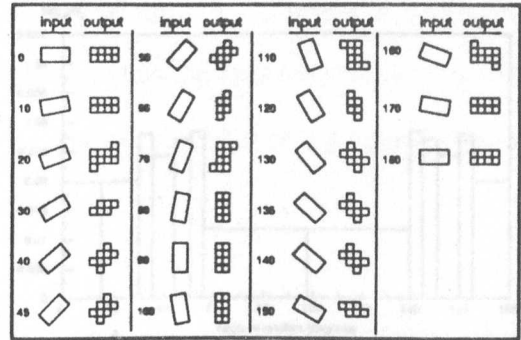


Figure 3.4 (II) The 4x2 rectangular image in case IA as it is rotated through 180 degrees and the corresponding pixel sensor output patterns.

Set	Maximal Information	Actual Information	Minimal Information
IA*	3.0000	2.7882	2.1134
IA	4.0000	3.3893	2.2879
IB	3.8074	3.2353	2.1059
IC	3.0000	2.5850	2.5850
ID	4.3219	3.8634	2.4148

* Set IA for area detector

Table 3.2. Summary of the assessment of Rotational Information content.

The tabulated results for point detectors for the four sets of images are shown in graphical form in figures 3.5, 3.6, 3.7 and 3.8. These histograms have ordinate heights which represent the "information per unit range" plotted against angle of rotation for each set of images. It can clearly be seen that sensor patterns restricted to a narrow angle convey a greater amount of information per unit range than other sensor patterns which persist through a greater angular range. However the contribution of each sensor pattern to the total amount of information conveyed, corresponds to the area under the corresponding histogram bar section. This is smallest for sensor patterns with a low probability of occurrence, as expected. This characteristic may be used to obtain *maximal* and *minimal* limits of information.

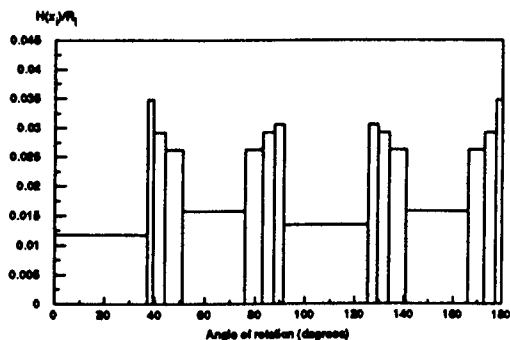


Figure 3.5. Histogram representation of the *information per unit range* $[H(x_i)/R]$ vs. angle of rotation for case IA. (for point detectors)

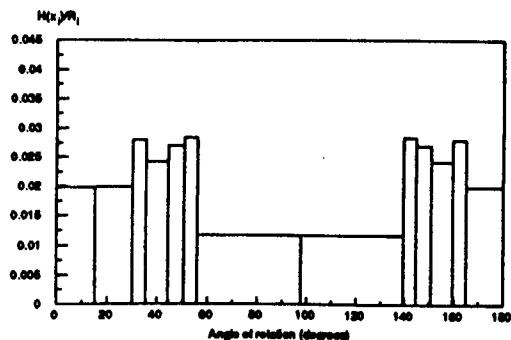


Figure 3.6. Histogram representation of the *information per unit range* $[H(x_i)/R]$ vs. angle of rotation for case IB.

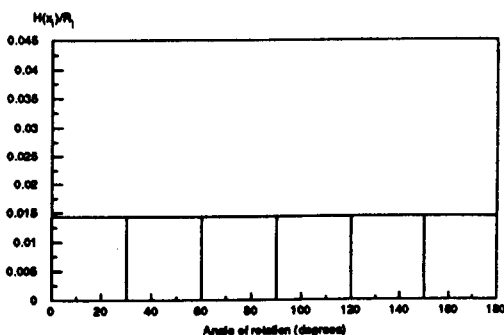


Figure 3.7. Histogram representation of the *information per unit range* $[H(x_i)/R]$ vs. angle of rotation for case IC.

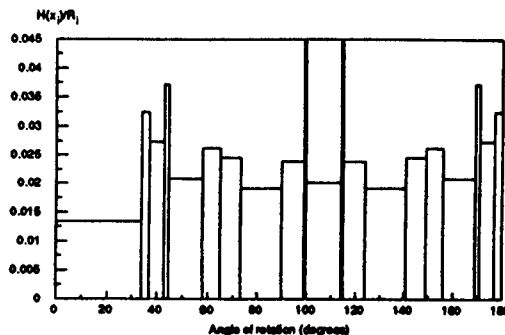


Figure 3.8. Histogram representation of the *information per unit range* $[H(x_i)/R]$ vs. angle of rotation for case ID.

3.2.1.3. Maximal and Minimal limits of rotational Information

The third column in Table 3.2 represents the total number of *binary digits* required to represent the information conveyed by each set of sensor patterns. This is arrived at in Appendix II by summing the information $H(X_i)$ conveyed by each of the separate sensor patterns that occur as the image is rotated. The whole process of deriving this sum for even a simple two by four element image is somewhat laborious, and could be excessively so for more extensive patterns. A method was therefore sought which would enable upper and lower limits for the information content to be estimated more easily.

A maximal measure of information may be obtained by considering *optimum information transfer*. That is assuming that all possible sensor patterns arising from the image set occupy an equal angular interval. This corresponds to a base-two logarithm of the total number of sample points.

A minimal measure of information may be obtained if the *worst case resolution* is taken as characterising the whole of each sample set. The worst resolution corresponds to the sensor pattern occupying the widest angular range. This in turn corresponds to the *shortest and the widest* bar on the histogram for the set, if extended over the whole of the angular range; or, in Appendix II the lowest value for $H(X_i)/R$ obtained for any sensor pattern when multiplied by the angular range which is in these examples 180 degrees.

The maximal measure of information may be used to obtain a quick estimate of the order of magnitude of the information content expected in each case. The minimal information is not as easily obtained, as a more detailed examination of the sample set is needed before this value can be evaluated. However, it sets a lower limit and is still easier than making a precise calculation of the information conveyed, and it is in some ways a more practically useful concept, as it represents the minimal accuracy of angular measurement of which the system is capable. Both maximal and minimal values are shown in Table 3.2. for comparison with the actual information.

3.2.2. Translational Information Assessment

This section considers the information associated with sideways translation of the centre of gravity of the input images limited to a distance equal to the spacing between pixels. Once again, the 4 x 2 rectangular shape was used as the test object. The image was considered at a number of pre-specified orientations (ie. at fixed inclinations to the pixel array) and at each orientation it was subjected to translation in directions perpendicular to the axis of the viewing system. The set of sensor patterns arising from point detectors positioned at the centre of each pixel, was examined. The relevant information assessment was made as for rotating images.

Owing to the complexity of the calculations, an assessment was only made for images inclined at zero degrees, 30 degrees, 45 degrees, and 90 degrees. The results are labelled sets IIA, IIB, IIC and IIE respectively in Table 3.3. The 60 degree case has been deduced from the 30 degree by symmetry and is labelled as set IID.

3.2.2.1. Coarse and Fine Translation Information

A clear distinction must be made here between the detection of image movement in increments equal to the pixel spacing, and the detection of changes of position of less than this magnitude. If, for example, on a rectangular array of sensors, the image moves in either coordinate direction by exactly one pixel, then the sensor pattern produced will be identical in shape but will also have moved to a different set of sensors displaced by one pixel spacing. Thus it is always possible to locate an image with the degree of accuracy corresponding to one pixel spacing, and this will be referred to as *coarse translation information*. However with many images, as they move through a distance not exceeding one pixel spacing, a sequence of different sensor patterns is produced as a result of individual sensors switching *on* or *off* at

different times. This enables the position of the image to be determined more accurately as though with a vernier gauge. The information carried by this sequence of patterns is referred to as *fine translation information*.

The coarse translation information tends to $\log_2 N$, where N is the number of pixels, as the array becomes larger relative to the image and the boundary effects less important. The fine translation information is the subject of the present study and is assessed in Appendix 2 by examining the detailed sequence of the sensor patterns produced as an image is moved through one pixel spacing in either coordinate direction.

3.2.2.2. Results

The fourth column in Table 3.3. gives the translational information content assessed for each set of sensor patterns. Appendix 2 gives the details of the calculations in each case. Diagrams in this Appendix show the successive areas occupied by each sample pattern as the respective 4x2 rectangular image when subjected to translation in either direction. The assessment of the information content for each pixel output pattern, and the summation of this is tabulated in Appendix 2.

Set	Angle	Maximal Information	Actual Information	Minimal Information
IIA	0	-	0.0000	-
IIB	30	4.8580	4.4381	3.4225
IIC	45	3.0000	2.6094	1.9037
IID	60	4.8580	4.4381	3.4225
IIE	90	-	0.0000	-

Table 3.3. Summary of the assessment of Translational Information content.

3.2.2.2.1. Sets IIA and IIE - Images inclined precisely at zero or 90 degrees

In these two cases, there can be only one sensor output pattern associated with each pixel with a probability of one. This is because the probability of occurrence of other sensor patterns is zero. Therefore the measure of the fine translation information is zero as expected. Further information about these two cases is given in sections A2.2.1 and A2.2.4 of Appendix 2.

3.2.2.2.2. Sets IIB and IID - Images inclined precisely at 30 or 60 degrees

In these two cases there are 29 different sensor patterns attributed to each pixel. Each sensor pattern occurs within a limited area of movement of the centre of gravity, and a map may be drawn, as in Figure 3.9, showing the *domain* associated with each of the 29 patterns. The information conveyed by this set of sensor patterns is summarised in Table 3.3. and further details about the set IIB are shown in section A2.2.2 of Appendix 2. The results for set IID are identical and were deduced by symmetry from set IIB. The tabulated results for these two cases are shown in graphical form in Figure 3.10. This histogram representation has ordinate heights which for each sensor pattern represent the *information per unit range* plotted against the fraction of one pixel area over which the pattern occurs.

As in the rotational information assessment case, it can clearly be seen that infrequent sensor patterns convey a greater amount of information per unit range than other sensor patterns having a higher probability. However the contribution of each sensor pattern to the total amount of information conveyed corresponds to the area under the corresponding histogram bar section. This is smallest for sensor patterns with a low probability of occurrence, as expected. This characteristic again may be used to obtain

maximal and minimal limits of information. These have been calculated following the principles used in section 3.1 and are given in table 3.3. for comparison with the actual information.

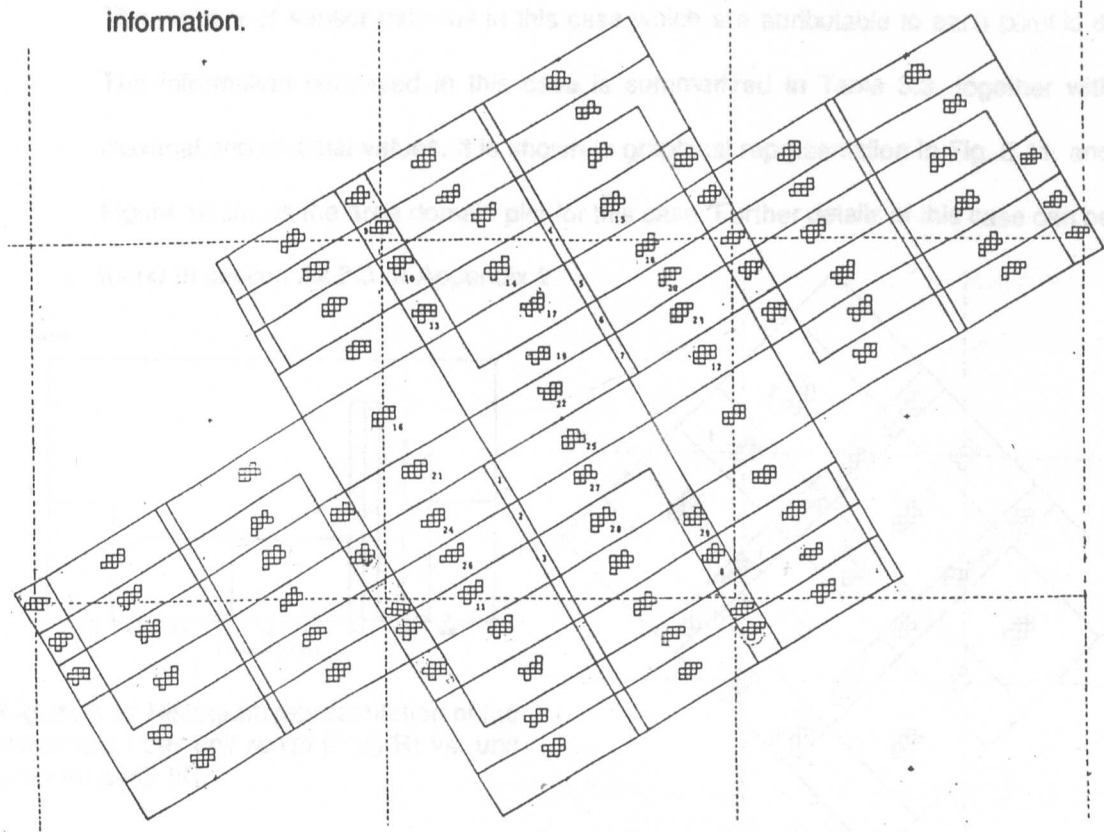


Figure 3.9. Area domain plot for case IIB at 30°.

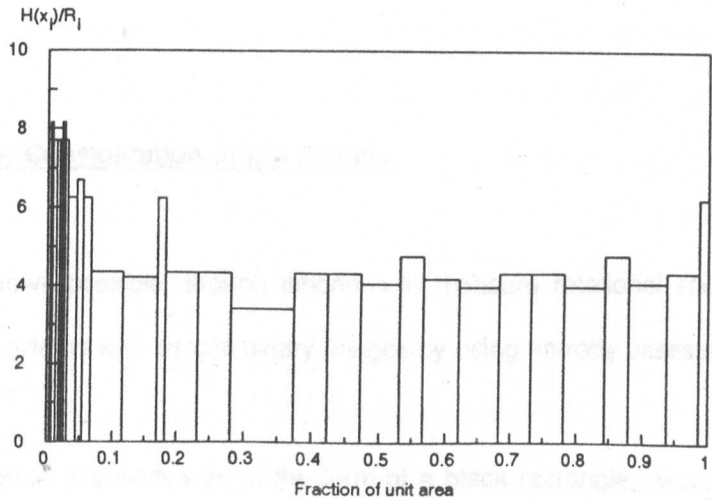


Figure 3.10. Histogram representation of the information per unit range $[H(x_i)/R]$ vs. unit area for cases IIB and IID.

3.2.2.2.3. Set IIC - Object inclined precisely at 45 degrees

The number of sensor patterns in this case which are attributable to each pixel is 8. The information conveyed in this case is summarized in Table 3.3. together with maximal and minimal values. It is shown in graphical representation in Fig. 3.11, and Figure 12 shows the area domain plot for this case. Further details of this case can be found in section A2.2.3 of Appendix 2.

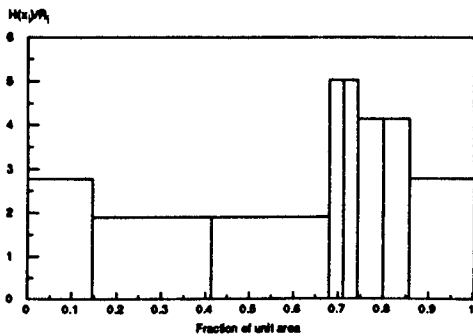


Figure 3.11 Histogram representation of the information per unit range $[H(x_i)/R]$ vs. unit area for case IIC.

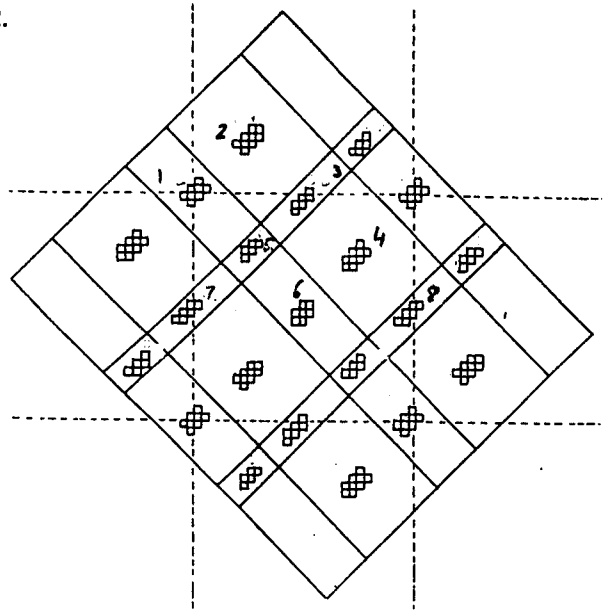


Figure 3.12. Area domain plot for case IIC at 45°.

3.2. 3. Further Consideration of the Results

It has been shown possible, though laborious to measure rotational and fine translational information associated with simple binary images by using entropy assessment methods.

The image used in this work was in the form of a black rectangle, measuring 4 by 2 pixel spacing, against a white background. The response of the sensors in each pixel was assumed to be that of a point detector, which permitted some simplification of calculations while returning realistic results. Separate tests were carried out for assessment of the rotational and the

translational information content. In the former case the object was rotated about its centre of gravity while keeping the position of the centre of gravity fixed in relation to the pixel array, and in the latter case translation of the object was achieved while maintaining a fixed inclination to the pixel array. Each distinct sensor pattern resulting from the rotation or translation of the object was then examined in turn and its contribution of information was calculated.

For each complete set of sensor patterns, the total amount of rotational or translational information was assessed by summing the information calculated for each sensor pattern in that particular set. The rotational information content of the object was found to be between 2.5850 and 3.8634 binary digits, depending on the position of the centre of gravity of the object in relation to the pixel grid. The translational information content of the object was found to be between zero and 4.4381 binary bits, depending on the inclination of the object to the pixel array.

Furthermore, maximal and minimal measures of information in each case were obtained. These relate to the information conveyed by considering the *optimum information transfer* in case of a maximal measure and the *worst case resolution* for a minimal measure, as described in sections 3.1. and 3.2. These values were found to differ from the actual value of the information measured by at most about one binary digit. The maximal and minimal measures of information may be used to obtain a quick estimate of the order of magnitude of the information content expected in each case.

The information assessment techniques developed in this work may in principle be extended to a wide range of images. The principal difficulty even with a simple 4x2 pixel rectangle has been the complexity of the calculations, which is why the rotational assessment was restricted to four positions of centre of gravity and the fine translational assessment to five angles, in two of which symmetry was used to deduce the results.

The next chapter describes how this technique may be applied to more practical cases, and to avoid being so restricted by the time consuming complexity it was necessary to seek extensive computing facilities so that a comprehensive analysis of the combined effect of continuous rotation and fine translation could be achieved

Chapter 4 - Automatic Information Assessment of Patterns

This chapter describes computerisation of the information assessment methods established in the preliminary investigations. This was necessary so that a comprehensive analysis of the combined effect of continuous rotation and fine translation could be achieved for more realistic patterns.

Various algorithms were developed to simulate the information assessment methods. Owing to the volume of calculation involved in these algorithms extensive computing facilities were necessary. The major part of the work was carried out using an ICL 3900 series mainframe computer as well as other powerful workstations such as a RISC architecture MIPS machine. The following sections briefly describe the development of these algorithms.

4.1. The algorithms in detail

The objective was to superimpose the binary image on a mosaic of pixels (the pixel grid), and then to rotate or translate the image in order to assess the rotational and fine translational information by identifying each unique sensor output pattern produced and measuring its probability of occurrence as the image passes over the pixels in the grid.

4.1.1. Definition of the pixel grid and the image under investigation

The first stage involved establishment of the pixel grid, and definition of the image within it. A 32 by 32 pixel grid was chosen, as it conveys adequate accuracy when a 15 bit word is used to denote positions across the full width of the grid. Thus with 2^{10} (=1024) increments for each single pixel width this allowed for an accuracy of 2^{15} (=32768) increments for the complete 32 pixel width.

As an example we may consider the first row of pixels shown in Figure 4.1. Using this convention means that the centre of each pixel moving from left to right is at location $(512,512)$, $(1536,512)$, $(2560,512)$, and so on to $(32256,512)$. Furthermore any

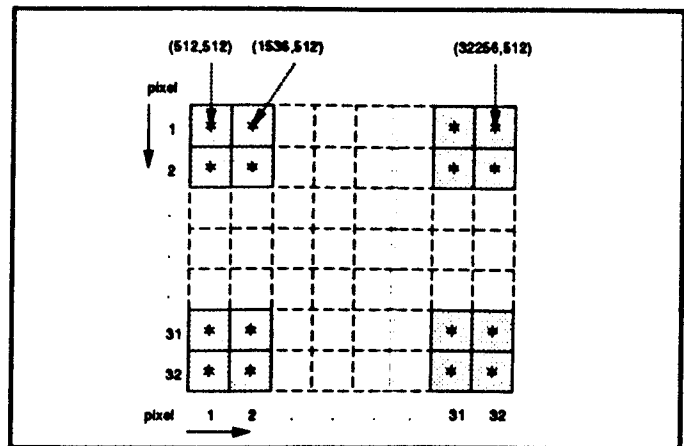


Figure 4.1. The pixel grid.

calculations regarding the location of the image may be carried out up to $1/1024$ th pixel width accuracy. In this investigation an approximately central pixel (16th pixel from the top left hand corner in horizontal and the vertical directions) was used as the *pivotal pixel* about which the images under study were generally located. All the major calculations are based upon the orientation and fine location of the image about this pivotal pixel and its neighbouring pixels. The size of the pixel grid ultimately limits the size of the image which can be analyzed.

The image may be set up by defining points on the boundary of the image with respect to its centre of gravity (ie. by contour description). The image may then be rotated as necessary and its centre of gravity appropriately located on the pixel grid. This

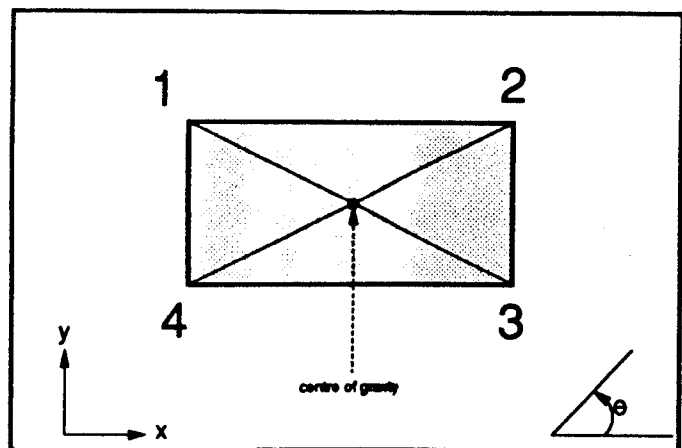


Figure 4.2. The 4x2 rectangular image.

procedure may be demonstrated by considering a 4 by 2 rectangular image as shown in Figure 4.2.

The boundaries of this image may be defined with respect to its centre of gravity as:

$$(x_1, y_1) = (-2, 1) \quad (x_2, y_2) = (2, 1) \quad (x_3, y_3) = (2, -1) \quad (x_4, y_4) = (-2, -1)$$

The image may then be rotated , if necessary, to an angle by using the equations 4.1 and 4.2.

$$x'_n = x_n \cos\theta - y_n \sin\theta \quad (4.1)$$

$$y'_n = x_n \sin\theta + y_n \cos\theta \quad (4.2)$$

The points may then be scaled by 1024 to take into account the pixel widths. Positioning of the image may then be achieved using the relationship shown in equation 4.3 and 4.4.

$$x'_n = cgx + [x_n \cos\theta - y_n \sin\theta] \times 1024 \quad (4.3)$$

$$y'_n = cgy + [x_n \sin\theta + y_n \cos\theta] \times 1024 \quad (4.4)$$

Where cgx and cgy are location of the centre of gravity of the image.

4.1.2. Identification of sensor output patterns

The next stage of the algorithm is concerned with identification of the pixels which are covered by the image, ie the pixels that are *on*. This facilitates tabulation of the various unique sensor output patterns together with their respective probability of occurrence which in turn leads to information assessment.

Starting from the top left hand corner, each pixel is taken in turn and tested to establish whether it lies horizontally in line with the image. This may be achieved by shifting the origin to the centre of the pixel under test. The 'y' coordinates of the boundary points describing the image are then listed sequentially in a clockwise direction. If a change of sign of y is encountered between two sequential points then the pixel under test is horizontally in line with the image. The type of the sign change (ie. positive to negative or negative to positive) is noted at this point. Figure 4.3. illustrates this procedure.

Once a change in sign of the y values of the boundary points has been found, the next stage is to determine if the pixel lies inside the image and therefore is *on* or not. The horizontal distances between the centre of the pixel and the boundaries of the image are measured using the relationship shown in equation 4.5. Figure 4.4. shows how this equation relates to physical distances.

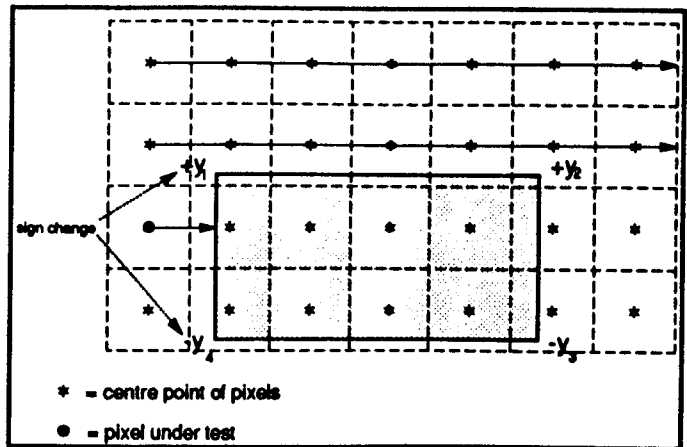


Figure 4.3. Finding pixels which lie horizontally in line with the image.

$$d = \frac{x_2 y_1 - x_1 y_2}{y_1 - y_2} \quad (4.5)$$

where: d = horizontal distance from the pixel centre
 x_1, y_1 = coordinates of the first boundary point
 x_2, y_2 = coordinates of the second boundary point

The image boundary may cross a horizontal line through the pixel centre more than once on either side, so this procedure is repeated until all such crossings have been covered. Clearly the minimum distances are of interest here since they indicate the nearest

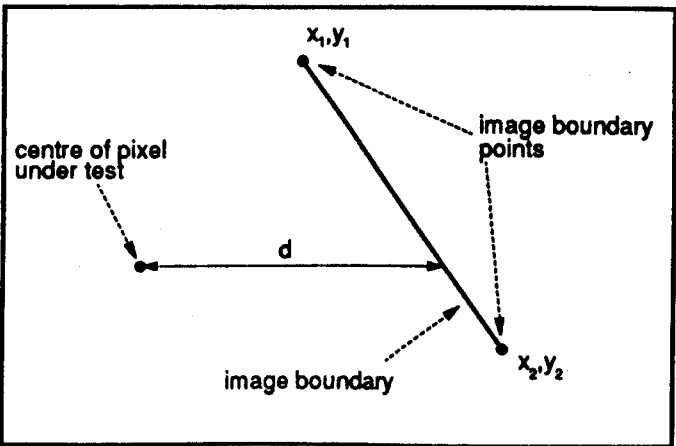


Figure 4.4. Calculation of the horizontal distance between the pixel under test and the image boundary.

boundary to the pixel under test. For a pixel to lie inside the image the following relationship must be true:

$$(dx_{pn} > 1) \text{ and } (dx_{np} < 1)$$

where:

dx_{pn} = horizontal distance of the nearest positive to negative going boundary from the pixel centre

dx_{np} = horizontal distance of the nearest negative to positive going boundary from the pixel centre.

In other words, for a pixel to be inside the image it must have a positive to negative transition of boundary points to its right and a negative to positive transition to its left. Figure 4.5. illustrates this principle. The magnitudes of dx_{pn} and dx_{np} are also important. A set of these values is obtained for all the *on* pixels for a given position of the centre of gravity of the image, and the minimum magnitude in each set is found for future use.

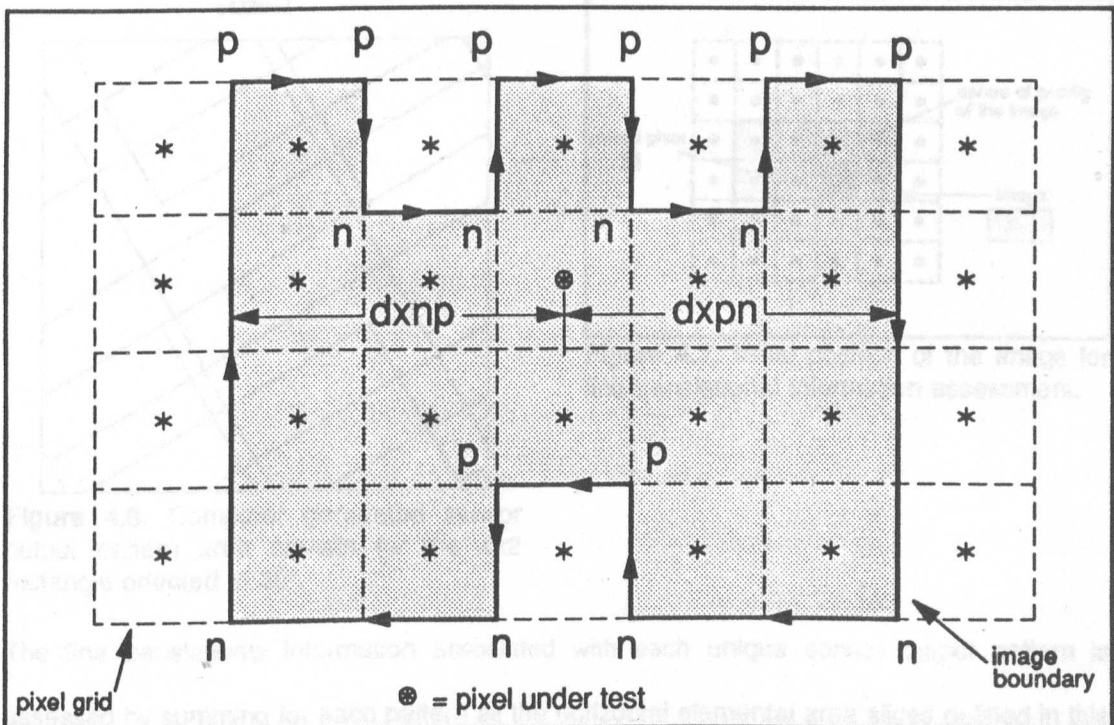


Figure 4.5. Illustration of discovering the *ON* pixels. In this example all the pixels which have a *n-p* boundary transition on the left and a *p-n* transition on the right are *ON*.

Once all the pixels are examined, the complete sensor output pattern of *on* pixels may be constructed, which may then be used to identify other positions of the centre of gravity of the image for which this particular sensor output pattern occurs. This in turn may be used in assessing the information content relevant to fine translation or rotation as follows.

4.2. Fine translational information assessment

One can imagine a map which shows the whole area within which the centre of gravity of the image may move without any change occurring in the sensor output pattern. Such a map was shown in Figure 3.9 in chapter 3. Figure 4.6 shows such a map generated by computer. This stage of calculations is concerned with evaluating the area attributable to each individual sensor pattern. The first step in evaluating the area for a particular pattern is to identify the extent of horizontal displacement which the centre of gravity of the image may undergo without changing the sensor output pattern.

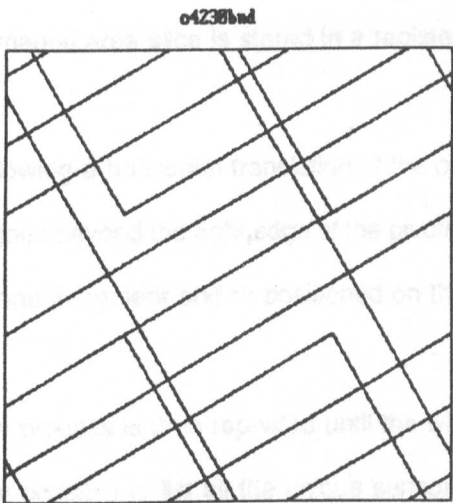


Figure 4.6. Computer generated sensor output pattern area domain for the 4x2 rectangle oriented at 30°.

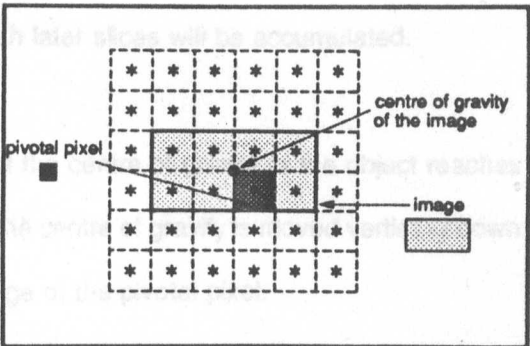


Figure 4.7. Initial position of the image for fine translational information assessment.

The fine translational information associated with each unique sensor output pattern is assessed by summing for each pattern all the horizontal elemental area slices defined in this way. This is done by firstly placing the centre of gravity of the image at the top left corner of the pivotal pixel [pixel at position (16,16)] as shown in Figure 4.7. The sensor output pattern

is then calculated using the algorithms described in the previous section. The minimum magnitudes found in each set of horizontal distance values dx_{pn} and dx_{np} indicate how far the centre of gravity of the image may move to left or right before the sensor output pattern changes. Therefore the sum of magnitudes of the minimum values of dx_{pn} and dx_{np} forms the first elemental area slice to be attributed to the first sensor pixel pattern.

The image is then translated horizontally by moving its centre of gravity to the right by the lesser of the two values $dx_{pn}+1$ and $dx_{np}+1$. This position will produce a different sensor output pattern which may be worked out using the fore-mentioned algorithms, together with its respective first elemental area. The whole procedure may then be repeated; each time a horizontal translation is imposed and a new sensor output pattern is found, it is compared with all the existing known output patterns. In case of a match the elemental area is added to the area already accumulated for the matched pattern. If no match is found, the sensor output pattern is labelled as a new unique pattern. Its record is added to the list of the unique patterns and its first elemental area slice is stored in a register in which later slices will be accumulated.

Following a horizontal translation, if the position of the centre of gravity of the object reaches or goes beyond the right edge of the pivotal pixel, the centre of gravity is moved vertically down by one increment and re-positioned on the left edge of the pivotal pixel.

This process is then repeated until the whole area of the pivotal pixel has been covered. It is then possible to list all the unique sensor output patterns with their respective contribution to the total area. Accordingly the fine translational information may be assessed as before, using the relationships described in chapter 3. Appendix 4 describes in detail these calculations with aid of an example.

4.3. Rotational Information assessment

Rotational information is assessed in a similar manner to that used for assessment of the translational information. The centre of gravity of the image is placed at one hundred equally spaced locations within the pivotal pixel, ten locations per row as shown in Figure 4.8. The image is then

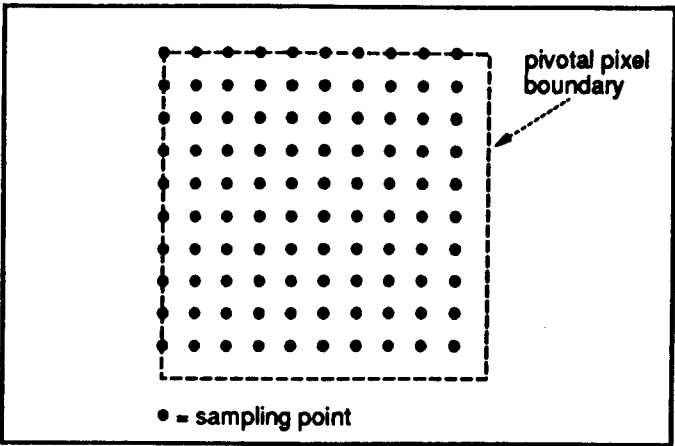


Figure 4.8. Location of centre of gravity of the image (sampling points) around the pivotal pixel for rotational information assessment.

rotated in 0.1 degree increments and the sensor output patterns are found and classified in unique patterns as before. The angular range (or ranges) over which a sensor output pattern remains unchanged is used to calculate the respective probability of occurrence and subsequently the rotational information of the image under study, again using the relationships from chapter 3.

The results obtained using such automated methods are presented for a variety of images in the following chapter.

Chapter 5 - Assessment of Translational, Rotational and overall information content of two dimensional patterns

This chapter describes the results obtained from analysis of the information content of two-dimensional patterns. Section 5.1 outlines the relationship between the translational, rotational and overall information content of patterns. Section 5.2 is concerned with simple binary patterns such as squares and rectangles of varying sizes. Translational, rotational and overall information related to these patterns are evaluated and discussed in detail. Comparisons are also made between some of these results and the results obtained in preliminary investigations described in chapter 3.

Section 5.3 describes rotational and overall information assessment of more detailed patterns such as cross and aircraft shapes. The relationship between the shape of a pattern and its information content are discussed.

5.1. Translational, rotational and overall Information

Fine translational and rotational information content of patterns under test may be calculated using the techniques described in chapter 4. For a given pattern these values may be combined to obtain the *overall information* of the pattern. The overall information is the information associated with a particular input pattern considering all its possible orientations and locations within the pivotal pixel and is not necessarily equal to the sum of translational and rotational information. We have already seen how a *domain map* may show the range of positions of centre of gravity of an input pattern for which a given sensor output pattern will arise. A similar domain map may show the range not only of position of centre of gravity, but also of orientation for which a given sensor output pattern will arise. Figure 5.1 is an example, and illustrates an interesting class of sensor output pattern for which there is correlation between the position and orientation of the input pattern from which it arises. This particular

sensor output pattern may either arise when the input pattern is in one location, A in Figure 5.1 or it may arise when input pattern is in location B. Thus when such a sensor output pattern arises, the information it provides is ambiguous, in that one cannot tell whether the input pattern is within the confined region at location A, or within the confined region at location B. If one knows that the orientation is, for example at A, then the position is known to be within the area A. Likewise if the orientation is at location B the position must be within the area B.

When the overall information is measured, the value obtained includes this correlated, ambiguous or shared information which will be denoted by (s). It also includes straightforward unambiguous *net* information about orientation (α) and position (τ) conveyed by sensor output pattern domains which correspond

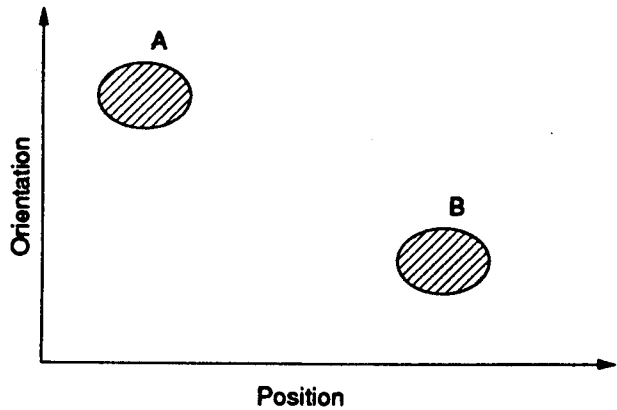


Figure 5.1. The occurrence of similar sensor output patterns in two different orientations and locations.

to single unambiguous locations. When measuring average rotational information (A) as described in Chapter 3 it was assumed that the position was known, so that the information measured therefore included ambiguous information (s) as well as unambiguous *net* rotational information (α). Similarly, when average translational information (T) was measured on the assumption that the angle was known, the result included (s) as well as *net* translational information (τ).

So we have the relationship:-

$$T = \tau + s \quad (5.1)$$

$$\text{and} \quad A = \alpha + s \quad (5.2)$$

and overall information

$$I = \alpha + \tau + s \tag{5.3}$$

or

$$I = A + T - s \tag{5.4}$$

Thus by measuring A and T as in Chapter 3, and by measuring *I* which is now possible with the calculating power of a computer, we may find the value of the shared information (s). Appendix 3 describes in detail the theory behind these relationships. It will be seen later that (s) has been measured for a few patterns and has a significant but not large value around 1 binary digit or 10% to 15% of the overall information *I*.

5.2. Information assessment of simple binary images

5.2.1. Patterns under study

A number of simple binary patterns were considered in this part of the investigation. These patterns were mainly in the form of squares and rectangles measuring from 1 up to 8 pixels in each dimension. Figures 5.1. and 5.2. illustrate the patterns used.

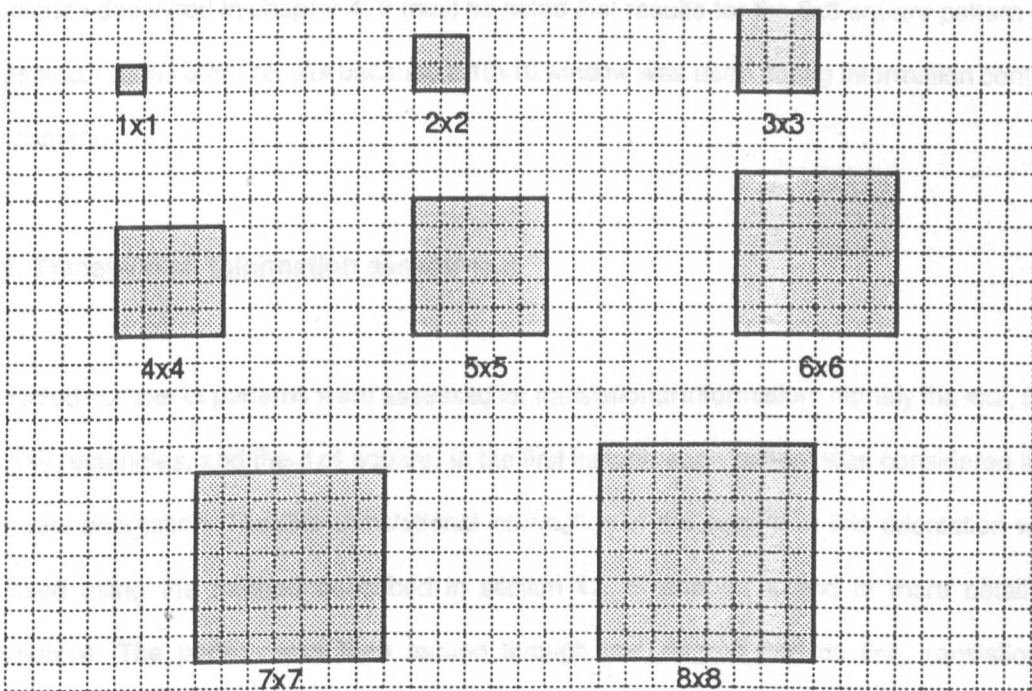


Figure 5.2. The square patterns under study.

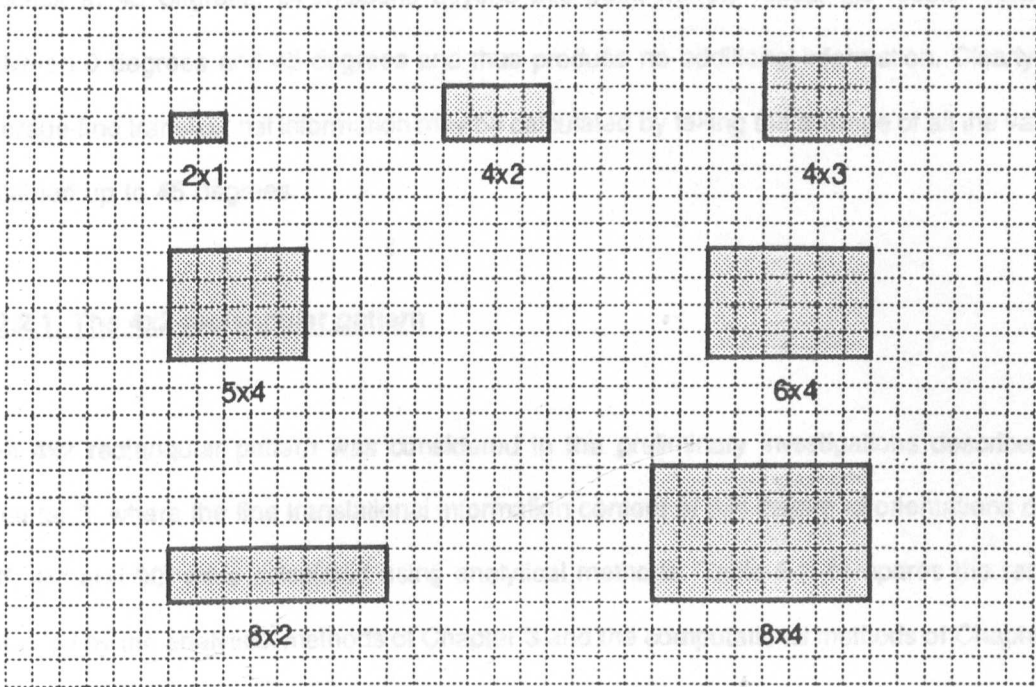


Figure 5.3. The rectangular patterns under study.

The translational and rotational information content of these patterns was calculated using the techniques described in chapter 4. It must be noted that results for the 8x8 square pattern are not as accurate as other results because a 10x10 window was used during information content assessment.

5.2.2. Translational Information assessment

A selected number of patterns were assessed for translational information; namely the 4x2, 8x2 and 8x4 rectangles, and the 4x4 square. In the first instant, each pattern was considered in a horizontal orientation. The fine translational information of the pattern in this orientation was assessed using the method described in section 4.2 of chapter 4 and in more detail in Appendix 4. The pattern was then rotated through one degree and its fine translational information at the new orientation was assessed in the same manner. This procedure was repeated for orientations up to 45 degrees in one degree increments. Since the patterns used were symmetrical about both horizontal and vertical axes, it was sufficient to terminate the

process at 45 degrees. Orientations beyond this point merely repeat the results obtained between 0 degrees and 45 degrees and thus produce no additional information. Clearly the average fine translational information may be calculated by taking the average of all the values obtained up to 45 degrees.

5.2.2.1. The 4x2 rectangular pattern

The 4x2 rectangular pattern was considered in the preliminary investigations described in Chapter 3, where the fine translational information content of this pattern at orientations of 0°, 30°, 45° and 90° were calculated using analytical methods. Table 5.1. compares the results obtained by the analytical methods of Chapter 3 and the computational methods of Chapter 4.

Orientation (degrees)	Translational information (bits)		Error (bits)
	Analytical results	Computed Results	
0	0.0000	0.0112	0.0112
30	4.4381	4.4381	0.0000
45	2.6094	2.5891	0.0203
60	4.4381	4.4381	0.0000
90	0.0000	0.0112	0.0112

Table 5.1. Comparison of the analytical and computed results for the 4x2 rectangle.

It can be seen that the computed results and the analytical results agree very closely. Furthermore, the computed area domains for sensor output patterns within the pivotal pixel were found to be the same as those plotted analytically. Figures 5.4 and 5.5 illustrate two typical area domain maps, which convey identical information to that shown in Figures 3.9 and 3.12 in Chapter 3.

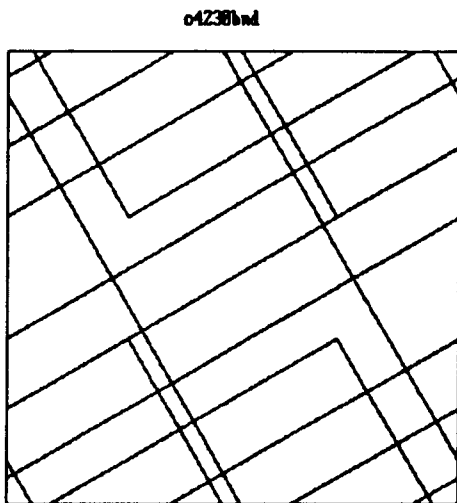


Figure 5.4. Sensor output pattern area domains for the 4x2 rectangle oriented at 30°.

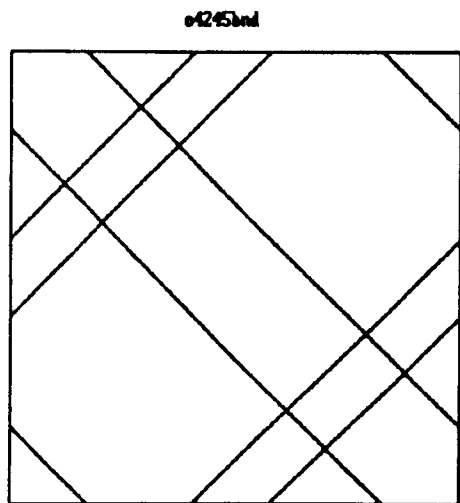


Figure 5.5. Sensor output pattern area domains for the 4x2 rectangle oriented at 45°.

5.2.2.2. Other patterns

The fine translational information assessed for all four patterns at all orientations from 0 to 45 degrees is tabulated in Appendix 4, and the results are illustrated graphically in Figure 5.6. The average fine translational information content for each pattern (as described in Appendix 4) is shown in Table 5.2.

Input pattern	Average translational information (binary digits)	Number of unique sensor output patterns
4x2 rectangle	3.6848	92
4x4 square	4.6588	240
8x2 rectangle	4.6000	696
8x4 rectangle	5.5376	1179

Table 5.2. Translational information results

Considering Figure 5.6, it can be seen that the value of the fine translational information *dips* at certain orientations such as at approximately 0°, 27°, 37° and 45°. This effect may be explained by considering interactions between the boundaries of the pattern under test and the pixel centres. At certain orientations the straight line boundaries of the pattern may be inclined

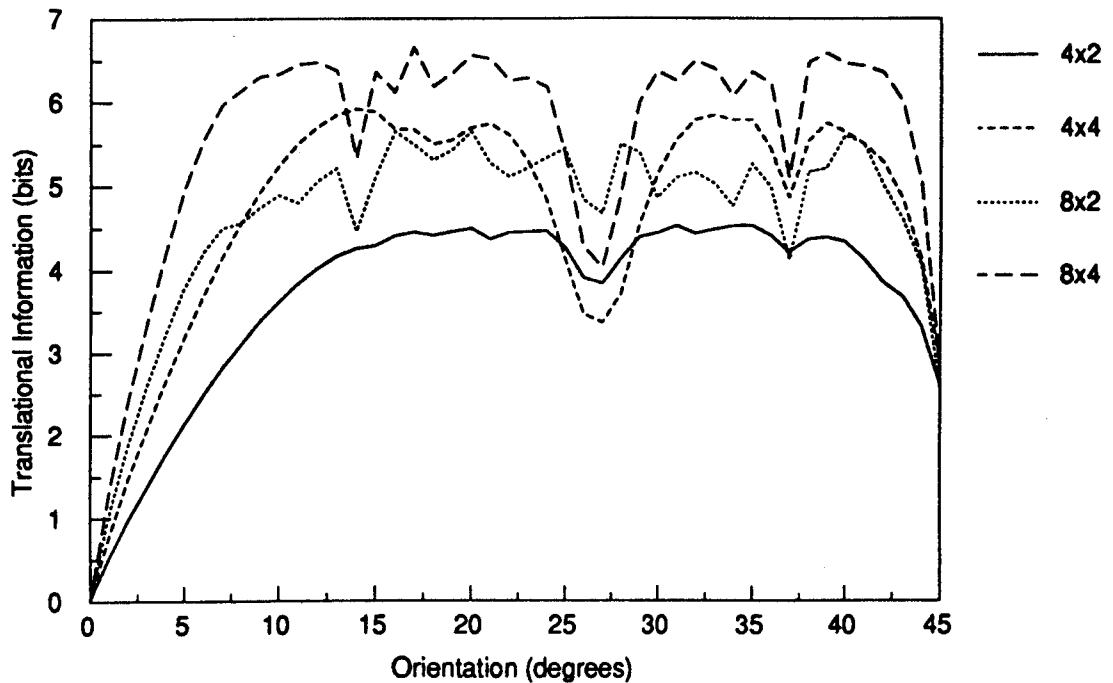


Figure 5.6. Translational information of simple patterns vs. orientation.

so that as they translate sideways they cross more than one pixel centre simultaneously. This leads to sudden major changes in the sensor output pattern but also to a reduction in number of different output sensor patterns. A direct consequence of fewer sensor output patterns each covering a larger area domain is that the assessed information is reduced. Appendix 5 describes this significant effect in detail and incorporates clear illustrations of the way in which this occurs.

5.2.3. Rotational Information assessment

The rotational information content was evaluated for a larger set of input patterns. This was partly because this could be readily done as a by-product of the calculation of overall information. The method described in section 4.3. of chapter 4 was used for the purpose of these analysis. One hundred samples of rotational information content were obtained within the pivotal pixel. The average information content was calculated by taking the average of these values. For clarity the results for square and rectangular patterns are shown separately in table 5.3. and Figures 5.7 and 5.8.

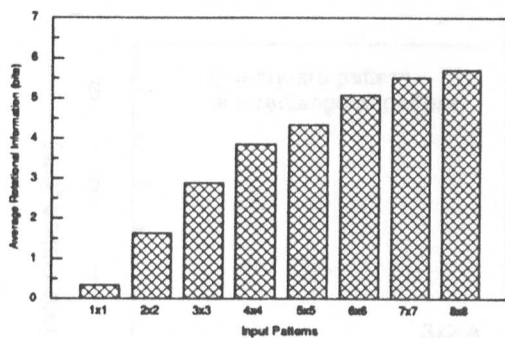


Figure 5.7. Average rotational information content of square patterns

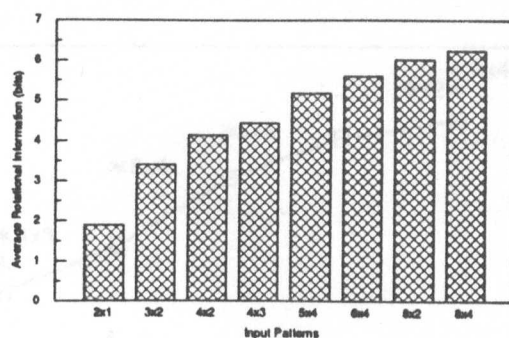


Figure 5.8. Average rotational information content of rectangular patterns.

Square Input Pattern	Average rotational information (binary bits)	Number of unique sensor output patterns
1x1	0.3383	4
2x2	1.6241	22
3x3	2.8827	70
4x4	3.8428	415
5x5	4.3382	851
6x6	5.0686	2135
7x7	5.5067	3367
8x8	5.7016	4004

Rectangular Input pattern	Average rotational information ((binary digits)	Number of unique sensor output patterns
2x1	1.8844	12
3x2	3.3979	108
4x2	4.1410	320
4x3	4.4512	523
5x4	5.1861	1295
6x4	5.5960	2205
8x2	6.0273	2501
8x4	6.2511	5018

Table 5.3. Average rotational information content

It can readily be seen that the amount of rotational information increases significantly with the size of the pattern under study. Furthermore it is interesting to note how the number of unique output sensor patterns increases sharply as the area of the input pattern and the length of its boundary increases. In Figure 5.9 information is plotted against the length of the longest side of the pattern and one may conclude:

- (i) That the length of the longest side is the most influential parameter in determining the information
- (ii) That, starting from a square, shortening one side by one pixel gives a gain in information of more than 15%

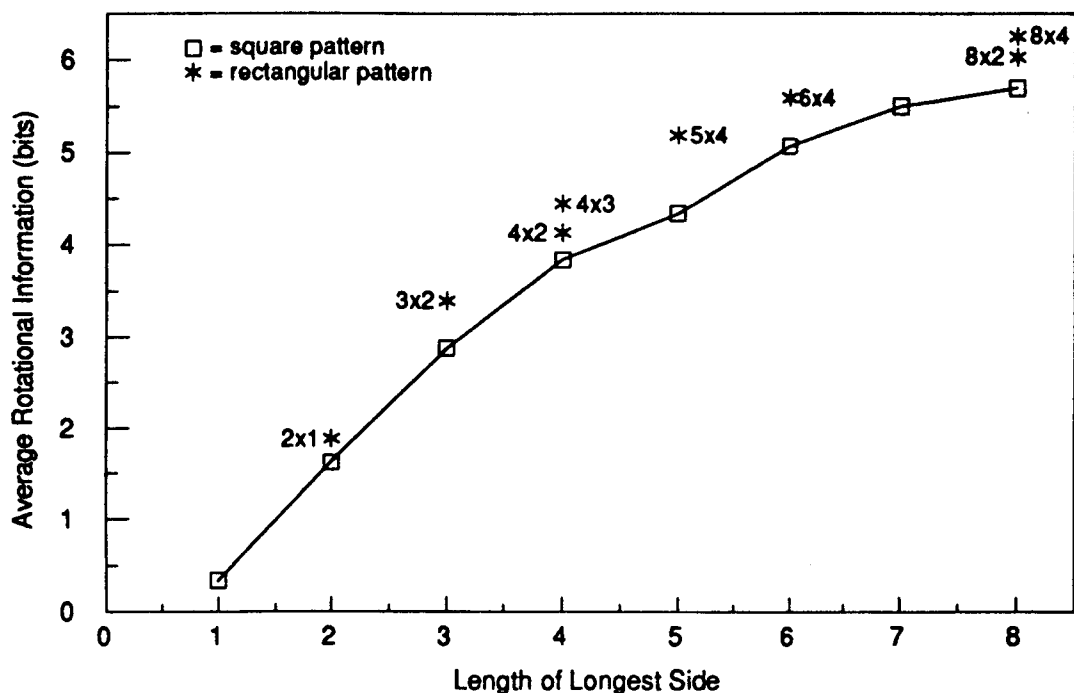


Figure 5.9. Variation of the average rotational information with change in the length of the boundaries.

- (iii) Further shortening of the one side relative to the other reduces the gain in information.

This outcome is not really surprising because a rectangle, having different lengths of sides is a more effective angular indicator or *pointer* than a square since the difference in length of side eliminates ambiguities. Nor is it surprising that a further reduction in width of the rectangle, which is normally accompanied by a reduction in the number of unique output sensor patterns should reduce the gain.

5.2.4. Overall Information assessment

The concept of overall information content was discussed earlier in section 5.1 of this chapter. Calculation of overall information was based on results obtained in evaluation of the rotational information, were used in these calculations since the 100 sample points used were found to produce adequate accuracy.

The overall *probability volume* of each unique sensor output pattern (see Appendix 4) was calculated by summing the probability values associated with each unique sensor output pattern over every one of the 100 sample points. The overall information was then calculated using these probability volumes as described in Appendix 4. Table 5.4, and Figures 5.10 and 5.11 show the results obtained for patterns under study.

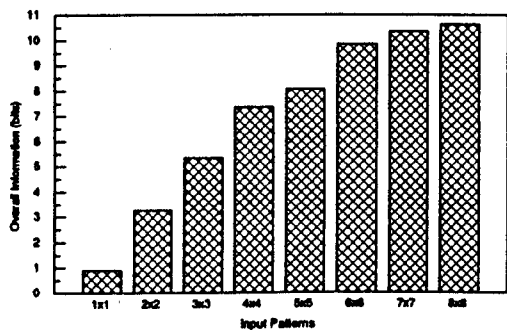


Figure 5.10. Overall information content of square patterns.

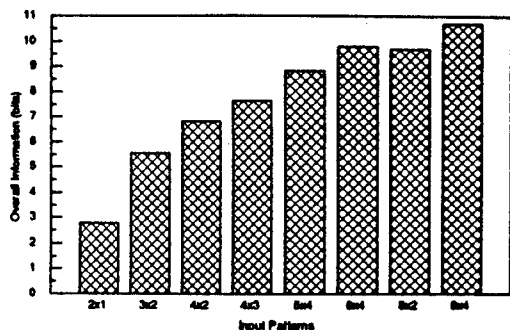


Figure 5.11. Overall information content of rectangular patterns.

Square Input Pattern	Overall information (binary bits)	Number of unique sensor output patterns
1x1	0.9067	4
2x2	3.25811	22
3x3	5.3478	70
4x4	7.3734	415
5x5	8.0756	851
6x6	9.8510	2135
7x7	10.3499	3367
8x8	10.6204	4004

Rectangular Input pattern	Overall information ((binary digits)	Number of unique sensor output patterns
2x1	2.7810	12
3x2	5.5562	108
4x2	6.8330	320
4x3	7.6487	523
5x4	8.8372	1295
6x4	9.7998	2205
8x2	9.6847	2501
8x4	10.6992	5018

Table 5.4 Overall information content.

As for rotational information it is interesting to note the increase in the overall information in line with the length of the longest side of the pattern. This effect is illustrated in Figure 5.12.

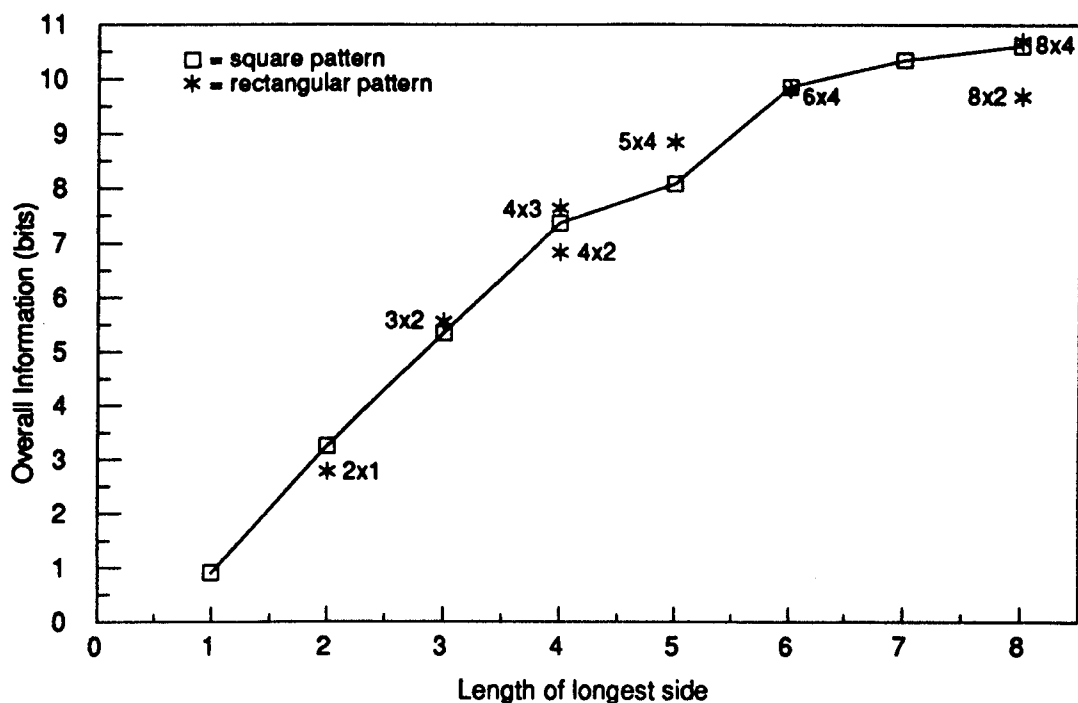


Figure 5.12. Variation of the overall information with change in the length of the boundaries.

In interpreting these results one must recall that the influence of the effects which were noted for rotational information have been diluted by the addition of translational information. Thus one may conclude:

- (i) That the length of the longest side is still an influential parameter for translational and for overall information.
- (ii) That the gain in rotational information when one side is shortened by one pixel, is largely cancelled and sometimes reversed by the loss of information of at least 10% - which the shortening must be causing in translational information.
- (iii) Thus, for translational information the length of both sides must contribute to the information. In fact, the difference between overall information I and average rotational information A which was defined as *net* translational information (τ) is roughly proportional to the peripheral length of the pattern as shown in Figure 5.13.

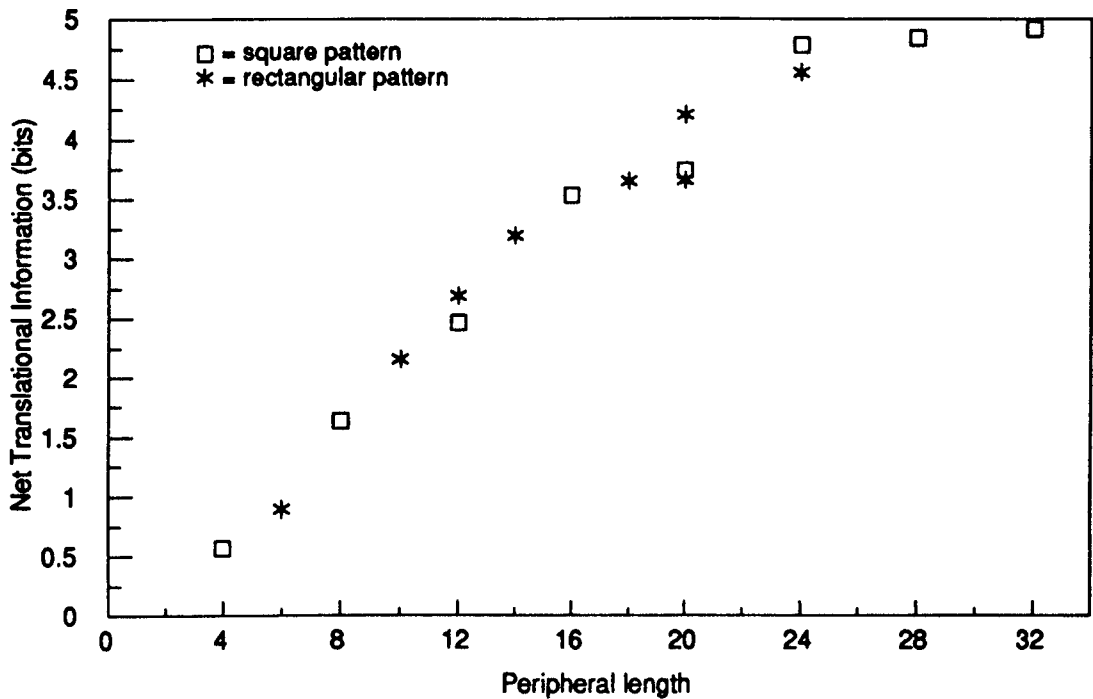


Figure 5.13. Variation of the net translational information with the peripheral length.

5.2.5. Shared Information (s)

We are now in a position to examine the value of shared information for the few patterns for which average translational information *T* has been assessed as well as average rotational information *A* and overall information *I*. The value of *s* may be readily deduced from equation 5.4 as:

$$s = A + T - I \tag{5.5}$$

Table 5.5 shows the values of *s* calculated for the four input patterns.

Input pattern	T (bits)	A (bits)	A+T (bits)	I (bits)	s (bits)	s I
4x2 rectangle	3.6848	4.1410	7.8258	6.8330	0.9928	0.1453
4x4 square	4.6588	3.8428	8.5016	7.3734	1.1282	.01530
8x2 rectangle	4.6000	6.0273	10.6273	9.6847	0.9426	0.0973
8x4 rectangle	5.5376	6.2511	11.7887	10.6992	1.0895	0.1018

Table 5.5. values of shared information

5.3. Information assessment of more detailed patterns

5.3.1. Patterns under study

The aim of this part of the investigation was to apply the information assessment methods to patterns with more detail which resemble some of the common types of patterns which one might encounter in general pattern recognition situations. However due to considerable volume of the computation involved it was necessary to economize in the size and complexities of the patterns used.

The patterns used may be divided into three groups. Group 1 was chosen to represent a somewhat gradual progress from simple cross to aircraft shape as shown in Figure 5.14. Group 2 consists of a total of 17 aircraft patterns, each of which has a different wing rake as a result of the wing tip moving with respect to the fuselage. The overall movement of the wing tip amounts to 2 pixel spacing units and three examples of these patterns are shown in Figure 5.14.

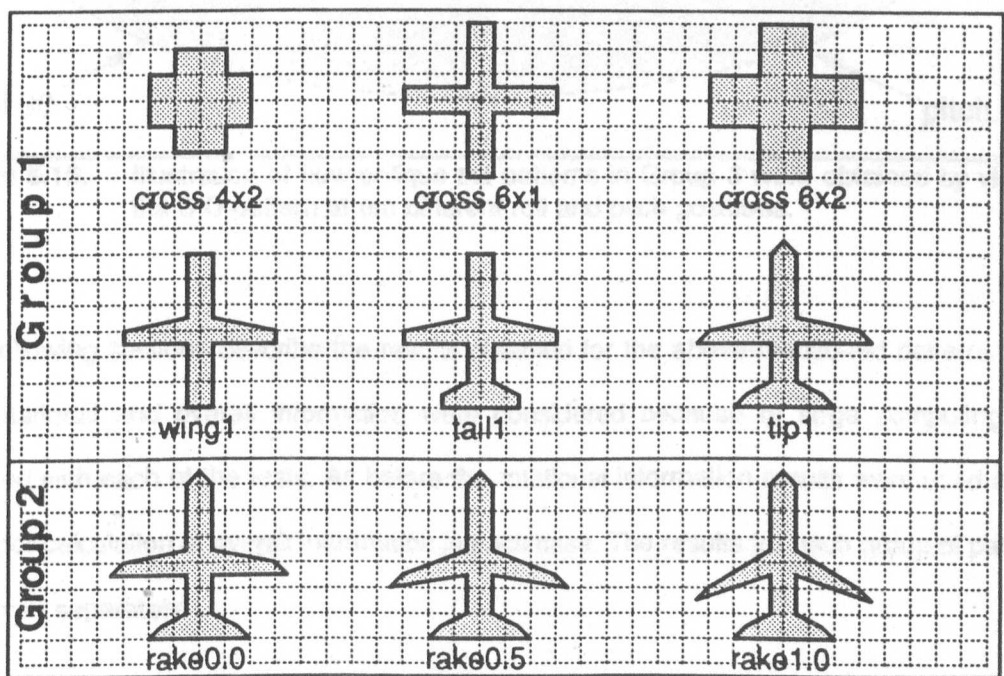


Figure 5.14. Two groups of patterns used. Group 1 consists of six patterns. Group 2 consists of 17 aircraft patterns with variations in rake of the wings; three examples are shown here.

The third group may be regarded as the *oblique set* and consists of ten two-dimensional views of a three dimensional aircraft shape at various roll and pitch inclinations as shown in Figure 5.15. For purpose of simplicity the dimensions of the 3-D shape were chosen to correspond with the patterns used in Group 2. For example, pattern roll 0 (or pitch 0) of this set is the same as pattern rake1.0 from Group 2. Furthermore, the dimensions of the tail fin of the aircraft were chosen to be the same as those of its tail plane.

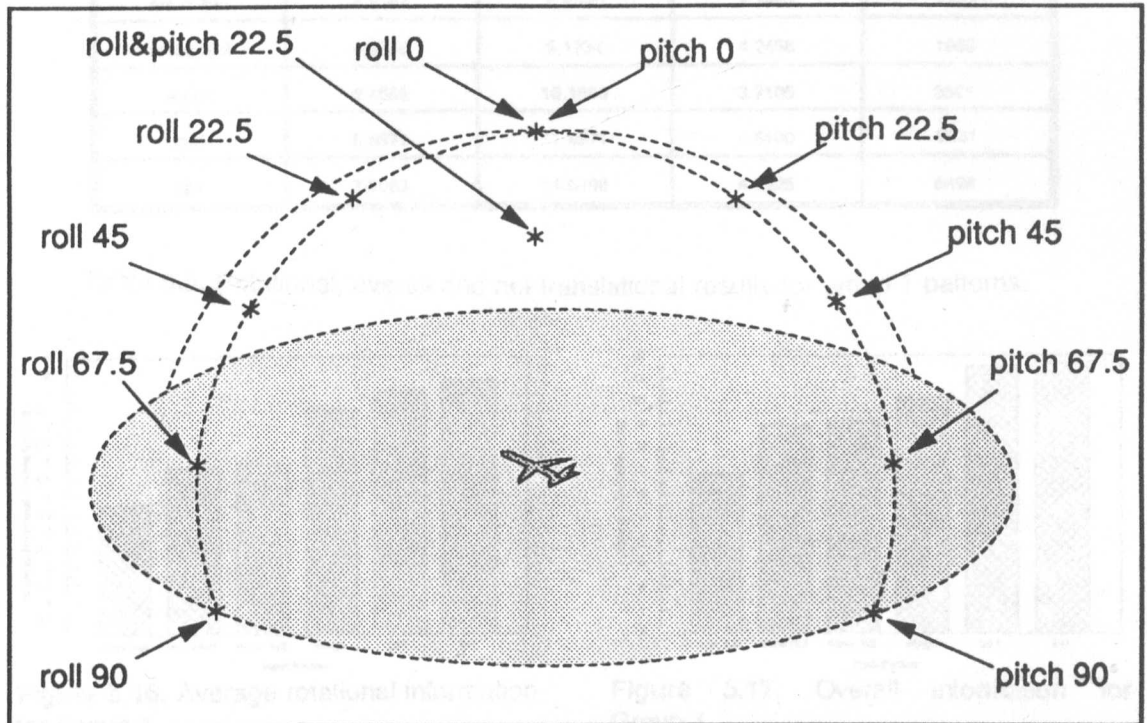


Figure 5.15. Illustration of how oblique set patterns in Group 3 were obtained by viewing the 3-D pattern at ten different roll and pitch positions.

The following sections describe the results obtained for the above-mentioned patterns. Only the rotational and overall information were considered because of large computing time involved with each of the tests. As before the rotational information results were used as the basis for calculation of overall information in each case. The results for each group of patterns are given separately.

5.3.2. Group 1

Results for the six patterns in Group 1 are shown in Table 5.5. and Figures 5.16 and 5.17.

Input pattern	Average rotational information (bits)	Overall Information (bits)	Net Translational Information (bits)	Number of unique sensor output patterns
cross4x2	3.7388	6.9093	3.1705	338
cross 6x1	4.8167	8.9820	4.1653	1703
cross 6x2	4.9268	9.1734	4.2466	1969
wing1	6.4558	10.1663	3.7105	3601
tail1	6.9871	11.4971	4.5100	9031
tip1	7.3083	11.6408	4.3325	8496

Table 5.6. Rotational, overall and net translational results for group 1 patterns.

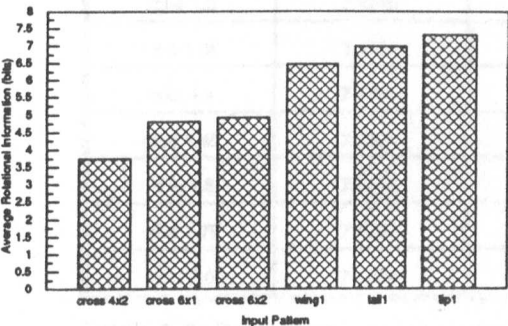


Figure 5.16. Average rotational information for Group 1.

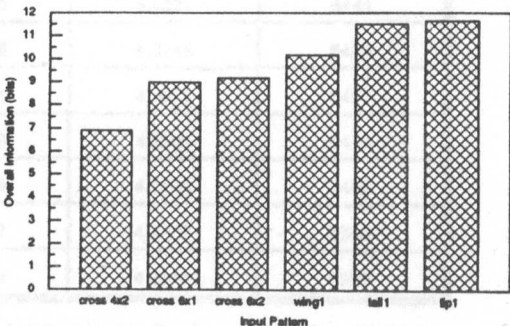


Figure 5.17. Overall information for Group 1.

The results are generally in line with the conclusions reached for squares and rectangles but it is evident that when the tips of the cross shaped figures are distinguished from each other as in wing1, tail1 and especially tip1, the rotational information increases, as might be expected by 1 to 2 bits. At the same time the net translational information decreases by up to 1 bit, presumably due to a loss of area in the more tenuous structure of the thin crosses.

5.3.3. Group 2

Results for group 2 are shown in Table 5.7. and Figures 5.18 and 5.19.

Input pattern	Average rotational information (bits)	Overall information (bits)	Net Translational information (bits)	Number of unique sensor output patterns
rake 0.0	7.3083	11.7469	4.4386	8496
rake 0.25	7.3513	11.8113	4.4600	8675
rake 0.5	7.3775	11.8712	4.4937	8711
rake 0.75	7.3591	11.8712	4.5121	8683
rake 1.0	7.4066	11.8738	4.4672	8510
rake 1.05	7.4096	11.8243	4.4147	8644
rake 1.1	7.4066	11.8343	4.4277	8586
rake 1.15	7.4190	11.8314	4.4124	8576
rake 1.2	7.4096	11.8309	4.4213	8511
rake 1.25	7.4186	11.8285	4.4099	8495
rake 1.3	7.4249	11.8270	4.4021	8444
rake 1.35	7.4304	11.8049	4.3745	8423
rake 1.4	7.4268	11.7941	4.3673	8463
rake 1.45	7.4324	11.7919	4.3595	8448
rake 1.5	7.5249	11.7855	4.2606	8409
rake 1.75	7.4397	11.7627	4.3230	8566
rake 2.0	7.4294	11.6642	4.2348	8573

Table 5.7. Rotational, overall and net translational results for group 2 patterns.

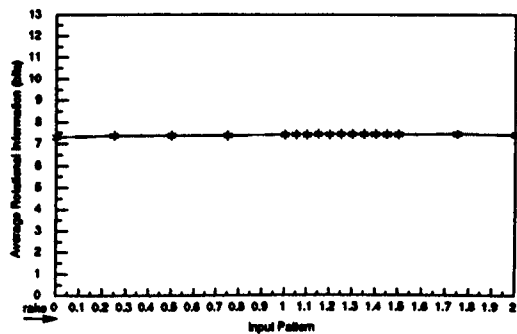


Figure 5.18. Average Rotational Information for Group 2.

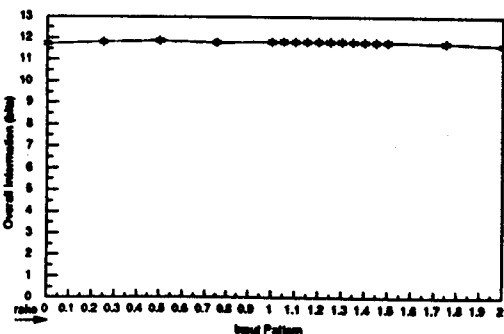


Figure 5.19. Overall Information for Group 2.

Again the results are in line with previous conclusions and show that Group 2 is a consistent set which will be analyzed in more detail in Chapter 6.

5.3.4. Group 3

Results for group 3 patterns are shown in Table 5.8. and Figures 5.20 and 5.21.

Input pattern	Average rotational information (Binary digits)	Overall information (bits)	Net translational information (bits)	Number of unique sensor output patterns
roll 0 pitch 0	7.4086	11.8243	4.4177	8510
roll 22.5	7.1701	11.8464	4.4763	7668
roll 45	6.9503	11.0624	4.1121	5272
roll 67.5	6.7747	10.3616	3.5869	3753
roll 90	7.7178	9.5489	1.8311	1935
pitch 22.5	7.0719	11.5733	4.5014	7265
pitch 45	6.9078	10.4921	3.5845	4028
pitch 67.5	5.7947	7.8088	2.0141	1297
pitch 90	5.0768	5.2043	0.1275	606
roll&pitch 22.5	6.9954	11.3804	4.3850	6352

Table 5.8. Rotational, overall and net translational results for group 3 patterns.

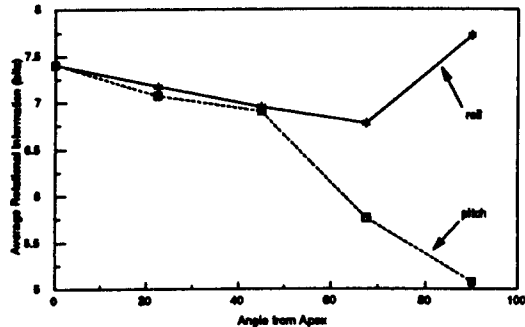


Figure 5.20. Average Rotational Information for Group 3.

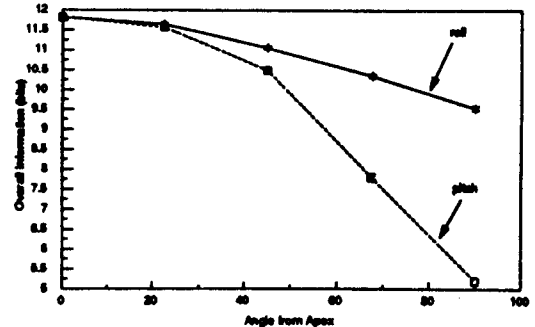


Figure 5.21. Overall information for Group 3.

Again the results are consistent with previous findings. The high figure for rotational information for roll 90 where the aircraft fuselage is seen sideways on is no doubt due to the fact that a long thin shape with head and tail distinguished acts like an arrow and forms a good *angular pointer*.

Chapter 6 - Analysis of Information Distinguishing Between Patterns

Previous chapters have assessed the information regarding position and orientation which may be obtained when an input image is placed in an arbitrary location on an array of sensors. This chapter is concerned with assessing that part of the information content of the sensor array output which enables different input images to be distinguished from one another. The principle adopted is to measure the increase in information in the sensor outputs when two or more patterns are presented in succession as the input image. The increase is measured by subtracting the average information measured for each image separately, from the combined information measured for the images when they are input in succession. The method is described in section 6.1.

To start this investigation a sequence of input images was required with one parameter changing progressively throughout. This was the purpose of creating the Group 2 patterns as described in Chapter 5. These are aircraft silhouettes for which only one attribute, the rake of the wings with respect to the fuselage, is changed from one pattern to the next, and their analysis is described in section 6.2.

A few input images were generated with other small variations in dimensions, such as change in width of wing of the aircraft silhouette. Section 6.3 shows that the information increment obtained is very much in line with the results described in section 6.2.

Section 6.4 of this chapter extends the investigation to the two-dimensional images which are representations of a three-dimensional aircraft shape, which were described in Chapter 5 as Group 3 patterns.

6.1. The comparison method

Preceding Chapters indicated that when assessing the information content of an input image, all the unique sensor output patterns associated with it were recorded, together with their respective probability of occurrence. The combined information for two or more input images is based on combining the relevant output pattern sets, to give a new set of unique sensor output patterns including all the output patterns for the separate sets. New values of probability of occurrence are evaluated for each output pattern in this combined set. For example, when combining the sets for two input images, the probability value for a sensor output pattern which exists only in one set will be divided by 2 to represent a true probability value for a sensor output pattern which now occurs within a combined set twice the size of the original set. For a sensor output pattern which exists in both sets, the new probability value is the sum of values from the two separate sets divided by 2.

Once a new *combined set* has been established, the information associated with it may be evaluated using similar techniques to those described in Chapter 4 and in Appendix 4. The total value of information in the combined set may be compared with the average value of the original sets, and the difference may be described as an *information increment* measuring the potential for distinguishing between input images. For example when comparing two input images, the value of *information increment* will be between 0 and 1. The lower limit represents a complete inability to distinguish them and the upper limit complete certainty of identification.

The *information increment* is a measure of the practicability of using sensor output patterns to identify the image that has been presented at the input by selecting it from a number of alternatives. The number of such *distinguishable patterns* is given by simply taking 2 to the power of the *information increment*. For example, when examining the sensor output patterns produced by two input images, if the incremental information increase is found to be equal to 0.95, the *distinguishable patterns* value is $2^{0.95} = 1.632$, indicating that the two input images

cannot be distinguished with certainty.

6.2. Accuracy of Discrimination between Patterns

The patterns in Group 2 as described in Chapter 5 were devised for this study so that only one attribute, namely rake of the wings with respect to the fuselage of the aircraft, is varied from one pattern to another. Owing to the extensive computing involved in evaluation of the information content of each pattern, it was necessary to be selective about the rake of wings chosen for these patterns. Wing rake is measured, for each input image, by the axial distance by which the wing tip lies aft of the position of the wing root at zero rake, measured in pixel spacing units. Nine patterns were chosen with the wing tip position ranging from 0.0 to 2.0 in 0.25 pixel steps. Eight more patterns were also studied so as to cover the range 1.0 to 1.5 in 0.05 pixel steps. This gave 17 patterns in total, and provided sufficient patterns for studies at different separations. *Separation* , for a set of input images is the difference in wing-tip position for the extreme members of the set.

6.2.1. Combining two Input Images

The first stage of this part of the work involved combining pairs of input images at different separations from 0.05 to 2.0 pixel spacing, and assessing the value of the information increment associated with that separation.

Figure 6.1 shows a scatter diagram of the values obtained for

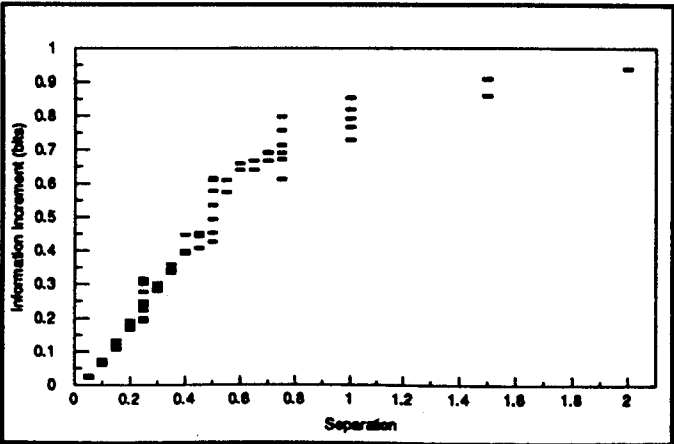


Figure 6.1. Scatter diagram of the information increment when combining two input images.

this part, and Figure 6.2 summarizes the results by providing a plot of average values of

information increment as a function of separation.

Two points are of interest, Firstly, the information appears roughly proportional to separation when the separation is small. This is not so surprising. Secondly the information becomes asymptotic to the value 1 bit for large separations. Since there are only two patterns, and 1 bit serves to distinguish precisely two patterns, it is not surprising that the information measured in the output never exceeds 1 bit.

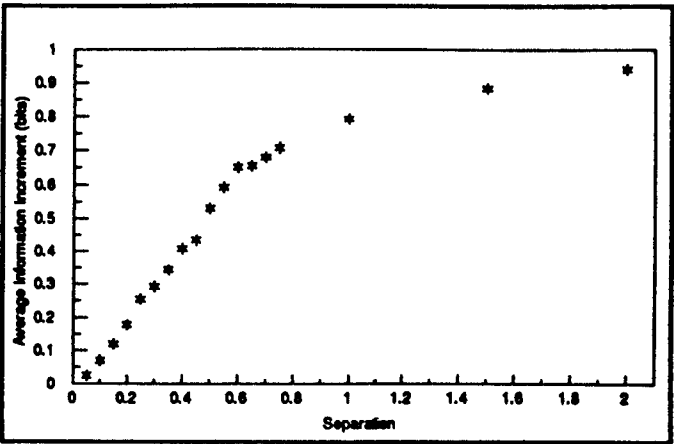


Figure 6.2. Plot of average information increment when combining two input images.

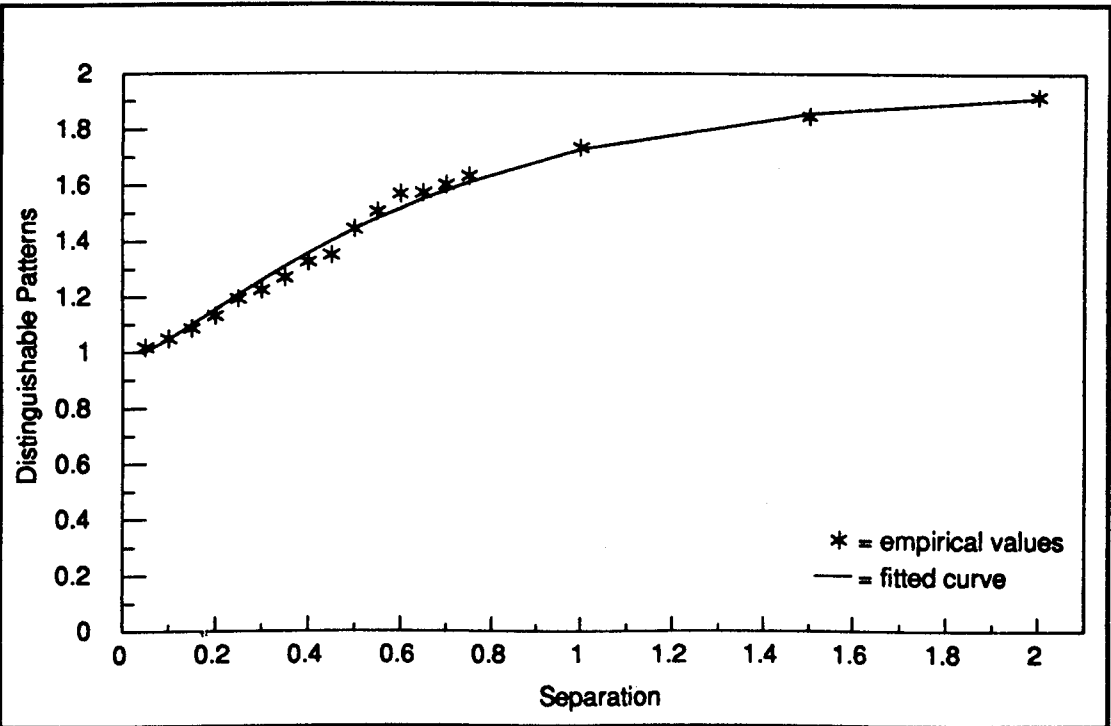


Figure 6.3. Plot of Distinguishable patterns against separation for two input images (A smooth curve has been fitted to assist further comparisons).

It was noted in section 6.1 that each value of information increment implies an ability to select one from a number of *distinguishable patterns*. Figure 6.3 illustrates the results in terms of this number. A smooth curve (a second order exponential) has been fitted to these values as guide of the trend of the results for use in future comparisons.

Again in this graph one may note that the number of distinguishable patterns rises approximately but not precisely linearly for small separations, and that it approaches 2 for large separations as might be expected. Since it cannot exceed 2 it is immediately evident that a pair of input images does not provide a good test for the information transmitting capability of the sensor array for large *separations*. To examine the full potential of the array it is necessary to have an input of larger groups of slightly differing input images as the *separation* increases. For each separation there is an optimum number of patterns in the input group.

6.2.2. Combining multiple input images

The comparison technique described in section 6.1 of this chapter may be used for combining any number of patterns. Table 6.1 shows some of the empirical results obtained when three, five and nine input images are combined. Figure 6.4 illustrates these results graphically. A very tentative attempt to derive a theoretical response for multiple input images from the results obtained for pairs of images was explored, and the predicted responses are plotted as fitted curves in Figure 6.4.

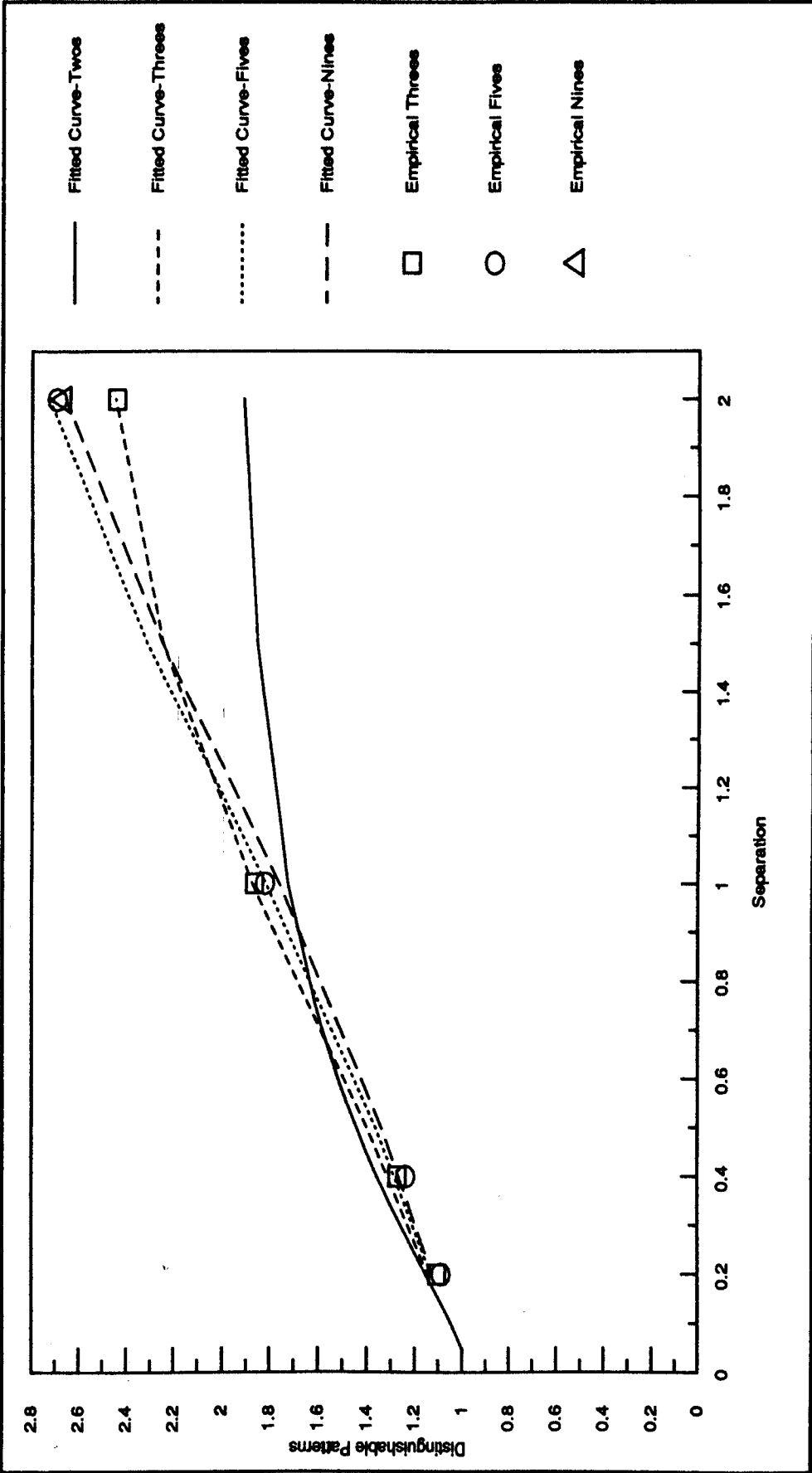


Figure 6.4. Empirical results and fitted curves for comparing multiple input images.

Separation ↓	Distinguishable Patterns			
	Combining two images	Combining three images	Combining five images	Combining nine images
0.2	1.131	1.107	1.089	-
0.4	1.327	1.273	1.239	-
1.0	1.731	1.863	1.820	-
2.0	1.918	2.441	2.695	2.667

Table 6.1. Summary of Empirical results.

In interpreting these results it can be seen that for small separations one may pick up the greatest amount of information by examining two input images at extreme sides of the separation range. For example, considering separations of up to 0.6, combining two input images produces the greatest value for *distinguishable patterns*. The values for combining three's and five's are somewhat smaller. In other words for small separations, two input patterns lying on the outer edges of the separation range produce sensor output patterns which are as dissimilar as possible. Considering more positions within this range of separation obscures the information available, and reduces the *information increment* assessment.

For larger separations the trend is somewhat different; the results show that one can increase the information by combining input images not only at the extreme positions, but also in between where further dissimilar output patterns may then be detected and used. This means that the information transmitting capability of a sensor array should be tested both at the edges and at the centre of the separation range. In Figure 6.4, three input images appear optimum between 0.7 and 1.2 separation, and five from 1.3 onwards. No doubt nine should be found optimum somewhere above a separation of 2 if results were available.

Considering the curves shown in Figure 6.4, one may see they may all be contained within an envelope which is the best measure of the information transmitting potential of the array. One may find a value for the slope of this envelope which has dimensions of *distinguishable*

patterns per separation, or more importantly the inverse of this slope gives *separation (in units of pixel spacing) per distinguishable pattern*. For the empirical results shown here, this value is approximately 1.2 pixel spacings per distinguishable pattern. In other words, this recognition system is capable of a high degree of discrimination between pairs of input images in which the wing tip has moved by at least 1.2 pixel units, and also some discrimination between triplets with the same separation. This result clearly illustrates the power of this technique in assessment of the ultimate limits of the recognition capability of any pattern recognition system based on the use of a sensor array. Thus, by comparing the overall performance of a pattern recognition system with this upper limit an *efficiency* may be assessed for the system.

6.3. Comparing very similar patterns

The results for wing tip movement that have just been examined in detail, provide a yardstick by which the results of other simple changes in shape can be judged. Figure 6.5 illustrates an example of three patterns studied here which are almost identical but for a small variation of 0.2 and 0.5 pixel units in the width of their wing tips shown in solid, dotted and dashed lines. Applying the information increment technique to these patterns gives the results shown in Table 6.2.

Change in wing tip width	Information increment	Distinguishable patterns
0.2	0.1600	1.117
0.5	0.5195	1.433

Table 6.2. Results for comparing very similar patterns.

It is interesting to note that similar results are obtained in Figure 6.3 and 6.4 for wing tip movement separation which is again 0.2 and 0.5 pixel units. This suggests that the *separation*

per distinguishable pattern for wing tip width may likewise be around 1.2 pixel spacing units.

In this case of course *separation* refers to a change in wing tip width.

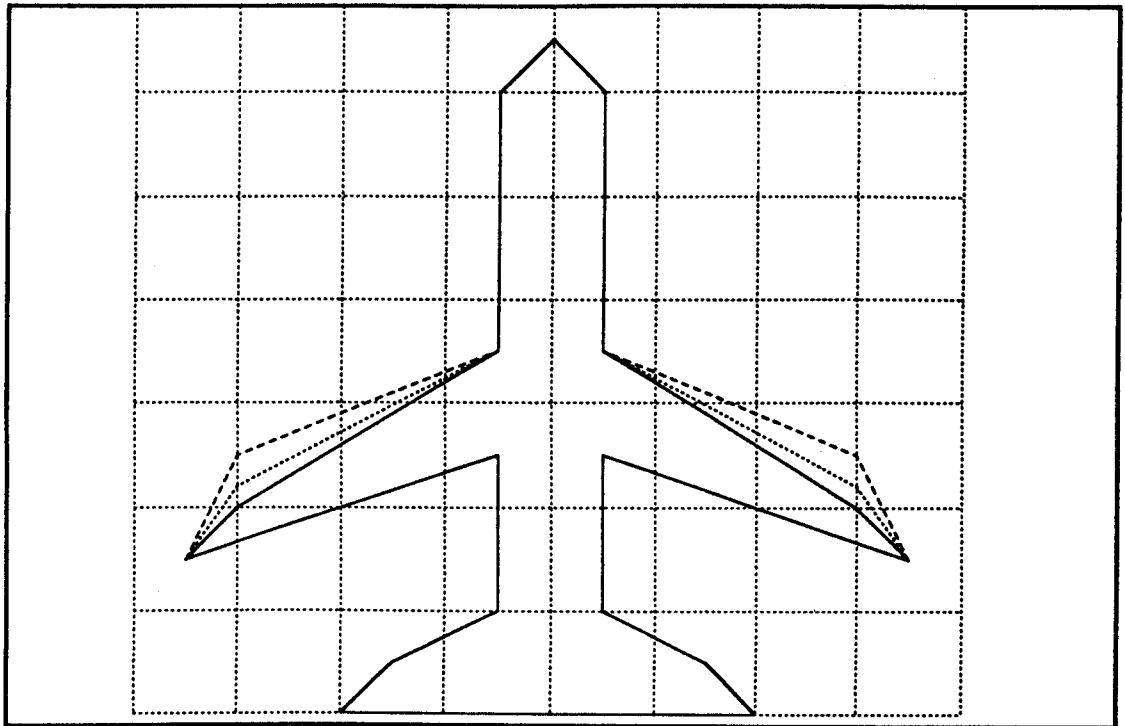


Figure 6.5. Small variation in the widths of wing tips.

6.4. Pitch and roll information carried by aircraft silhouettes

Group 3 patterns, as described in section 5.3.1 of Chapter 5, consist of two-dimensional silhouettes of a three-dimensional aircraft model viewed at various angles. The viewing positions were chosen, as shown in Figure 5.15, so that 5 side projections and 5 rear projections of the aircraft were obtained at equal angular separations (denoted by roll 0 to roll 90 and pitch 0 to pitch 90 respectively). In addition, another two-dimensional silhouette was obtained by viewing the aircraft at an oblique angle of 22.5° (denoted by roll & pitch 22.5).

It was found advantageous earlier in this chapter to use a comparison technique based on *distinguishable patterns* to assess the information available for discrimination between different positions of the wing tip. The first step in analyzing the pitch and roll images in Group 3 was therefore to apply this same technique in order to assess the information which permits

discrimination of pitch and roll angles. Appropriate silhouettes were combined in groups of twos, and where possible in threes and fives with angular separations ranging from 22.5° to 90°. Table 6.3 summarizes the results obtained, and Figures 6.6 and 6.7 illustrate the response of the recognition system in the form of plots of distinguishable patterns against angular separation derived as before.

Angular separation ↓		Distinguishable Patterns		
		Combining two images	Combining three images	Combining five images
R O L L	22.5	1.386	-	-
	45	1.852	1.869	-
	67.5	1.937	-	-
	90	1.952	2.411	2.748
P I T C H	22.5	1.471	-	-
	45	1.774	1.951	-
	67.5	1.918	-	-
	90	1.948	2.531	2.888

Table 6.3. Summary of results for Group 3 patterns.

By analyzing the empirical results here in a similar manner to that shown in section 6.2.2 of this chapter, the discrimination capability of the recognition system here may be assessed in terms of the change in roll and pitch angle per distinguishable

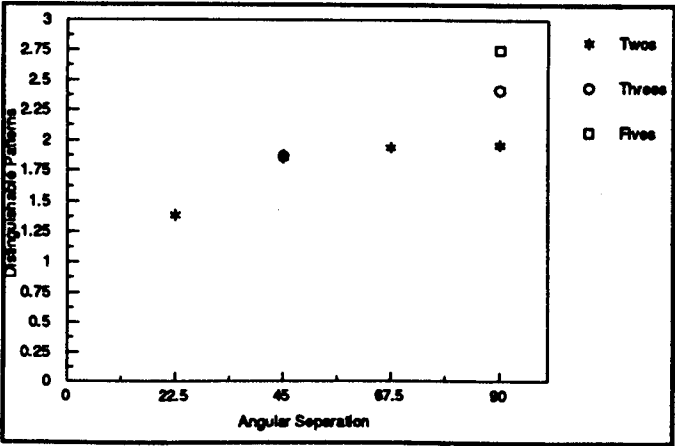


Figure 6.6. Empirical results for side views (roll set).

pattern. This may be derived by taking the reciprocal of the slope of the *envelope* in the graphs of Figures 6.6 and 6.7. In these graphs the *envelope* is not as clearly defined as in Figure 6.4 but it has been taken to mean a straight line through the uppermost points irrespective of whether they relate to two, three or five input images. For the roll set, this leads to a value of

51.5 degrees per distinguishable pattern. That is, the system is capable of a high degree of discrimination between patterns which are separated by 51.5 degrees or more. The comparable value for the pitch set is 47.7 degrees per distinguishable pattern.

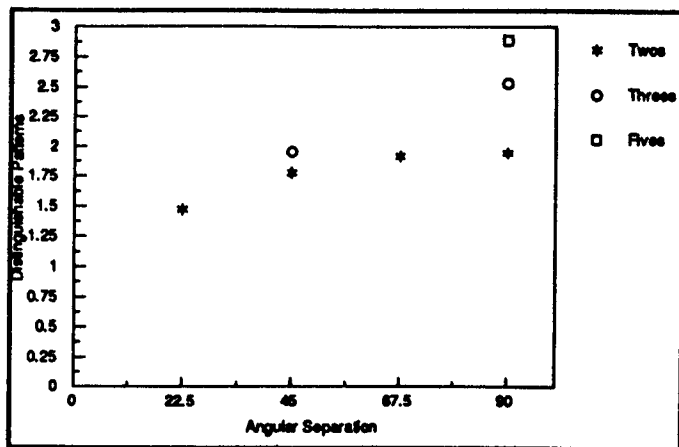


Figure 6.7. Empirical results for rear views (pitch set).

The discrimination appears slightly poorer with regard to roll. If we examine the separate results from which the averages in Table 6.3 were obtained, we find that this is partly due to the roll discrimination being very poor between 0° and 22.5°. Details are given in Tables 6.4, 6.5 and 6.6. This means that we are not dealing with a relatively homogeneous set of data as in the wing-tip analysis. Between 22.5° and 90° of roll, the discrimination improves to between 31° and 36°. In these circumstances the only really sound method of summing the roll and pitch information over the whole hemisphere shown in Figure 5.15 would be to carry out massive further analysis covering all possible combinations of pitch and roll. However, with the data at present available, there remains an uncertainty about the angular discrimination in the as yet unexplored areas of the hemisphere in Figure 5.15. If one assumes that the angular discrimination generally lies between the limits of 31° and 51.5°, one may estimate the number of distinguishable patterns over the whole hemisphere as between 27 and 10. The corresponding information available for angular discrimination in roll and pitch taken together, (with yaw also present in the side-view aspects) then lies between 4.7 bits and 3.3 bits. One further point that needs to be borne in mind is that for limited roll or pitch seen from directly above, roll to starboard and roll to port produce the same changes in the silhouette. So does a limited pitch in either nose-up or nose-down directions. The ambiguity thus introduced could reduce the information by a fraction of a binary digit.

Sets			Angular Separation	Comparison of two images		
				Information increment	Distinguishable Patterns	Angular range per distinguishable pattern
ROLL	0	22.5	22.5	0.1523	1.111	202.7
	22.5	45	22.5	0.7902	1.729	30.9
	45	67.5	22.5	0.7029	1.628	35.8
	67.5	90	22.5	0.7797	1.717	31.4
PITCH	0	22.5	22.5	0.3759	1.298	75.5
	22.5	45	22.5	0.7378	1.668	33.7
	45	67.5	22.5	0.7033	1.628	35.8
	67.5	90	22.5	0.4581	1.374	60.2

Table 6.4. Detailed results for combining two input images.

Sets				Angular Separation	Combining three input images		
					Information increment	Distinguishable Patterns	Angular range per distinguishable pattern
ROLL	0	22.5	45	45	0.6024	1.518	86.9
	45	67.5	90	45	1.2021	2.301	34.6
PITCH	0	22.5	45	45	0.9587	1.944	47.7
	45	67.5	90	45	0.9698	1.959	46.9

Table 6.5. Detailed results for combining three input images.

Sets			Angular Separation	Combining five input images		
				Information increment	Distinguishable Patterns	Angular range per distinguishable pattern
ROLL 0, 22.5, 45, 67.5, 90			90	1.4584	2.748	51.5
Pitch 0, 22.5, 45, 67.5, 90			90	1.5300	2.888	47.7

Table 6.6. Detailed results for combining five input images.

6.5. Comparison with a proposed pattern recognition method

One aim of the present study was to provide a standard against which the performance of actual pattern recognition methods could be tested for their efficiency of utilisation of the available information. To illustrate the way in which a comparison may be made, the conclusion regarding a pattern recognition method described by R.J. Petheram [12] may be quoted. This

method was tested on aircraft silhouettes with pitch and roll, and it was estimated that 5 bits of information regarding these angles were retained at the final output. This may be compared with the range of 3.3 to 4.7 bits estimated above. However, for a fair comparison one must also allow for the fact that the silhouettes studied here spanned about 7 pixel units in length and width, whereas the span of Petheram's was around 21.

Now it appeared that with the simple shapes studied in Chapter 5, the information picked up by a sensor array was proportional to the linear dimensions of the image rather than the area. If this also applies to aircraft silhouettes, then Petheram's method must have been using between 40% and 100% of the information available, depending on whether we regard 4.7 bits or 3.3 bits as more authentic. A more extensive study of silhouettes subject to pitch and roll is needed to confirm the appropriate value.

This comparison has necessarily been very tentative, and the assumptions that have been made need to be checked carefully. Nevertheless it does illustrate the potential value of being able to measure the information associated with a group of images forming the input to an array of sensors.

CHAPTER 7 - CONCLUSIONS AND FURTHER CONSIDERATIONS

7.1. Summary of the conclusions

The work described in the thesis was concerned with the use of information theory techniques in pattern recognition problems. Information content related to certain attributes, such as location and orientation, of a variety of input images was identified and assessed for the purpose of recognition and classification. Methods were also developed for assessment of the performance of pattern recognition systems.

7.1.1. Preliminary Investigation

Chapter 3 outlined the preliminary investigation into basic information assessment methods. It initially examined application of non-conditional and conditional entropy principles to simple binary patterns, in the form of a single black pixel and of two black pixels, as shown in Figures 3.1 and 3.2. Identical results were obtained using both non-conditional and conditional methods (4.0 bits and 4.5 bits of information for each pattern respectively). An L-shaped pattern of three pixels, as shown in Figure 3.3, was also considered. Again both methods resulted in the same value of information (5.12 bits). This means that both non-conditional and conditional entropy methods may be used for such basic assessments. Further considerations of this pattern indicated that information related to position and orientation of patterns may be evaluated separately (see section 3.1.4. and Appendix 1 for further detail). This led to further investigation of the positional (or translational) and orientational (or rotational) information content of images.

The second section of chapter 3 described how these information assessment techniques were further developed for evaluation of basic rotational and translational information content of a 4x2 rectangular image after it is input to a sensor array. The rotational information content of

the sensor array output patterns was found to be between 2.59 and 3.86 bits, depending on the position of the centre of gravity of the image within the pivotal pixel. The translational information content of the input image was found to be between zero and 4.44 bits, depending on the inclination of the image with respect to the pivotal pixel. Additionally the concept of maximal and minimal limits of information was discussed this provide a quick estimate of the order of magnitude of the information content of an input image.

The preliminary investigation showed that it was possible, though laborious to measure the rotational and translational information associated with simple binary patterns. It was then decided to extend this work to a wider range of images by seeking extensive computing facilities. This led to more advanced information assessment work the results of which are summarized in the next section.

7.1.2. Advanced Information assessment

7.1.2.1. Summary of the results

Chapter 4 described in detail the procedure of development of algorithms of the information assessment techniques established in Chapter 3. This facilitated more comprehensive studies to be carried out using the processing power of mainframe computers.

Chapter 5 described the investigation into assessment of information content of two-dimensional patterns. Distinctions between net translational, net rotational and overall information with consideration of the *shared information* were discussed in section 5.1 and in more detail in Appendix 3.

Section 5.2 of chapter 5 considered information assessment of simple binary images such as squares and rectangles as shown in Figures 5.2 and 5.3. Translational information content

results in the case of the 4x2 rectangle were found to be very close with those obtained in the preliminary investigation (maximum error was found to be around 0.02 bits). A few other patterns were also examined for translational information content with average values between 3.68 bits to 5.54 bits.

In case of rotational information, the values varied from 0.33 bits for a 1x1 square to 5.70 for an 8x8 square. Further analysis of the results showed that the length of the longest side of the input image is the most influential parameter in determining the rotational information content (see section 5.2.3.).

Assessment of the overall information revealed 0.91 bits for the 1x1 square to 10.62 bits for the 8x8 square. The value of the shared information for a few patterns was also calculated to be around 1 bit or 10% to 15% of the overall information, as shown in Table 5.4.

More detailed patterns were also studied in three major groups shown in Figures 5.14 and 5.15. Group 1 consisted of six patterns showing a gradual change from a cross to aircraft shape. Rotational information values for these patterns were found between 3.74 bits and 7.31 bits, and the overall information values were found to be between 6.91 to 11.64 bits.

Group 2 consisted of 17 aircraft patterns for which only one attribute, rake of the wings with respect to the fuselage of the aircraft, varied from one pattern to another. The values of information content were found to be consistent, with average rotational information value of 7.41 bits and average overall information value of 11.81 bits.

Group 3 patterns were two-dimensional views of a three-dimensional aircraft shape at various pitch and roll inclinations. It was found that both rotational and overall information values for the pitch views dropped more rapidly as the angle of viewing (measured from apex) was increased (rotational information value were between 7.41 bits to 5.08 bits compared with 7.41

bits to 5.79 bits for roll; overall information value were between 11.82 bits to 5.2 bits compared with 11.82 bits to 9.55 bits for roll). This may be explained when considering that the pitch views show a reduction in the length of the input image as the angle of viewing is increased.

7.1.2.2 Discussion and further conclusions

The computerization of the information assessment techniques produced accurate and reliable results. This facilitated detailed analysis of a variety of input images. Furthermore, the value of the earlier preliminary work was proved since it provided a useful check on the accuracy of the computer calculations.

The theoretical treatment of the net translational, net rotational, overall and shared information (section 5.1 and Appendix 3), and the empirical results were found to agree.

An interesting relationship between the *dips* in the translational information response and the sensor output pattern area domains were noted in section 5.2.2.2 (and Appendix 5), which agreed with the basic principles of information theory. That is, large area domains introduce uncertainty about the locations of the centre of gravity of the pattern within the pivotal pixel, and consequently this leads to a drop in the assessed information. Figures 5.6 and A5.1 illustrate this point.

Considering the results for the rotational and overall information assessment of the simple binary patterns (section 5.2.3 and 5.2.4), it was noted that the length of the longest side of the input image is the most influential parameter in determining both rotational and overall information. It was also shown that the net translational information is roughly proportional to the peripheral length of the pattern, since length of both sides of the pattern contribute to this information (see figure 5.13).

Analysis of the more detailed patterns (section 5.3) illustrated the power of the automated algorithms used. Data compression techniques were used for comparison and storage of the large number of the global sets discovered in these cases, which increased the speed of execution and reduced computer storage.

Results obtained for Group 1 patterns were found to be generally in line with the conclusions reached for squares and rectangles. Results for Group 2 patterns showed an expected consistency and were used later in further analysis of performance assessment of pattern recognition systems. Results for Group 3 patterns were largely in line with expectations given the shape of the input patterns produced at each viewing angle.

7.1.3. Assessment of performance of pattern recognition systems

Chapter 6 was concerned with the use of information assessment techniques to assess the recognition capability and efficiency of utilization of information of pattern recognition systems.

In the case of patterns with varying wing rakes (Group 2 patterns), it was found that the system under test was capable of a high degree of discrimination between pairs of input images in which the wing tip has moved by at least 1.2 pixel spacing units. Small variations in the width of the wing tip were also considered and the result was found to be generally in line with the previous findings.

In case of pitch and roll patterns (Group 3 patterns), it must be noted that a further study of combinations of pitch and roll would be desirable before drawing firm conclusions. However the data available at the present time was analyzed as well as could be managed to obtain an indication of what might be expected when more data becomes available.

The pattern recognition system under study in this case was found to be capable of distinguishing between patterns separated by 51.5° for roll and 47.7° for pitch views. Furthermore, considering a system as a hemisphere which contains roll, pitch and yaw views of the three-dimensional shape (as shown in Figure 5.15), it was estimated that the angular discrimination limits of 31° and 51.5° give rise to between 27 and 10 distinguishable patterns over the whole hemisphere. It was also estimated that the corresponding information available for angular discrimination in roll and pitch (and also yaw) taken together lies between 4.7 and 3.3 bits.

A comparison was also made with a proposed pattern recognition method by Petheram [12]. It was noted that Petheram's method which tested aircraft silhouettes with pitch and roll was estimated to retain 5 bits of information, which may be compared to the range of 3.3 bits to 4.7 bits estimated using the information assessment techniques. When considering that Petheram's input images were three times larger than those in Group 3, it may be estimated that Petheram's method uses between 40% and 100% of the information available. These results illustrate, although rather tentatively, the potential value of being able to measure the information associated with a group of images forming the input to an array of sensors.

7.2. Further development of the Investigation

It was already mentioned that the algorithms used were very computer intensive. This is partly due to the nature of the algorithms, which mainly involve manipulation of large arrays, and partly because some of the routines have evolved from an earlier part of the investigation and are rather less efficient when used for more complex tasks. Further refinement and improvement of the algorithms and programs would be possible and desirable. Efficient implementation of the algorithms on high performance parallel processors and workstations

would also be of great value to facilitate further investigation.

Considering the results of combining patterns (Chapter 6), further exploration of the theoretical link between pairs and multiple input patterns would be beneficial. Obtaining additional empirical results would also aid in substantiating any theoretical treatment.

Furthermore, considering the pairs curve in Figure 6.3, one can readily notice a low slope for small separation values (between 0.05 and 0.4 pixel units separation). One possible explanation of this effect may be due to the shared information between translation and wing-tip position. One could start by using only the rotational information for combining patterns in pairs. If the effect does not occur it may be argued that the effect has been due to the translational component of the shared information.

As mentioned earlier in this chapter and also in Chapter 6, information content results related to roll, pitch (and yaw) need to be assessed more thoroughly. It is envisaged that further refinement and implementation of the algorithms on a powerful workstation will facilitate more data of this kind to be obtained more rapidly.

7.3. Wider Implications of Information assessment methods

The feasibility, and the power of information assessment techniques in analysis of performance of pattern recognition systems has been demonstrated. Further work is needed in order to enhance the current algorithms to be more robust and flexible, so that they may be used in assessing the performance of various pattern recognition systems used in practical applications such as visual inspection and industrial automation.

It is also interesting to consider the possibility of using the global sets assembled in this study as a basis for a pattern recognition method in its own right. One possible realization may be through the use of parallel processing. Despite the computing cost of this method, implementation will be possible using parallel high performance processors that use sub-micron CMOS or GaAs technologies. This is made possible by the highly parallel nature of the algorithm, whereby one processor can be used for assessment of information at each sample point, and also rotational ranges within each sample points. Parallel implementation promises to be an exciting and challenging subject for future work.

References

1. Batchelor, B.G.; "Pattern recognition ideas in practice"; Plenum Press, 1978.
2. Patric, A.E.; "Fundamentals of pattern recognition"; Prentice-Hall, 1972.
3. Fu, K.S.; "Recent developments in pattern recognition"; IEEE Transactions on Computers, Vol.C-29; No.1 (Oct.1980); pp.845-854.
4. Fu, K.S.; "Syntactic methods in pattern recognition"; Academic Press, 1974.
5. Beurle, R.L.; Daemi, M.F.; Petheram, R.J.; "Final report of research into basic recognition processes at Nottingham University"; Report J/12/88 submitted to R.S.R.E. Malvern, March 1988.
6. Ballard, D.H.; Brown, C.M.; "Computer Vision"; Prentice-Hall, 1982.
7. Gonzalez, R.C.; Wintz, P. "Digital Image Processing"; Addison-Wesley, second edition; 1987.
8. Resenfeld, A.; "Picture Processing by Computer"; Academic Press, 1969.
9. Niblack, W ; "An introduction to digital image processing"; Prentice-Hall, 1986.
10. Fu, K.S.; "Digital pattern recognition"; Springer-Verlag, 1976.
11. Kulback, S.; "information theory and statistics"; Dover, 1968.
12. Petheram, R.J.; "Automatic pattern recognition"; Ph.D. Thesis, University of Nottingham; 1989.
13. Jourdain, G.; Tziritas, G.; "Communication in a fluctuating channel models and use of explicit or implicit diversity"; IEEE-ICASSP 82, vol.1, pp.113-16.
14. Gonzalez, R.C.; Safabakhsh, R.; "Computer Vision for Industrial inspection and Robot Control"; IEEE-COMPSAC 82, pp.594-600
15. Takagi, M.; "Biomedical image processing and pattern recognition"; Proc. of the fourth international conference on pattern recognition, Japan, 1978, pp.146-153.
16. Conners, R.W.; Harlow, C.A.; Dayer, S.J.; "Radiographic image analysis: past and present"; IEEE proc. of the sixth international conference on pattern recognition, Munich, 1982, pp.1152-1169.

17. Chen, T.M.; Staelin, D.H.; Ronald, B.A.R.P.S.; "Information content analysis of landsat image data for compression"; IEEE Trans. on Geoscience and Remote Sensing, Vol.GE-25, no.4 (July 87), pp.499-501.
18. Christopoulos, C; Thomas, D.W.P.; Wright, A.; "Signal processing and discriminating techniques incorporated in a protective scheme based on travelling waves"; IEE Proceedings, Vol.136, Pt.C, no.5 (Sept.1989), pp.279-288.
19. Likens, W.C.; Jones, H.W.; Shameson, L.; "Advanced communication technologies for image processing"; Proc. of IEEE conf. on spatial information technologies for remote sensing today and tomorrow, 1984, pp.4-9.
20. Fu, K.S.; "Pattern recognition for visual inspection"; SPIE, Vol.336, pp.12-19.
21. Ullmann, J.R.; "Pattern recognition techniques"; Butterworth, 1973.
22. Fu, K.S.; "Sequential Methods in pattern recognition and machine learning"; Academic Press, 1968.
23. Chen, C.H.; "Statistical pattern recognition"; Hyden, 1973.
24. Fu, K.S.; "Syntactic pattern recognition and applications"; Prentice-Hall, 1982.
25. Meisels, A.; Kandel, A.; Gecht, G.; "Entropy and the recognition of fuzzy letters"; Fuzzy sets and systems (Netherlands), vol.31, no.3 (July 1989), pp.297-309.
26. Farag, R.F.H.; "An information theoretic approach to image partitioning"; IEEE Trans. on Systems, Man and Cybernetics, vol.SMC-8, no.11 (Nov.78), pp.829-833.
27. Pavlidis, T.; "Algorithms for graphics and image processing"; Computer science Press, 1982.
28. Verhagen, C.J.D.M.; "Some general remarks about pattern recognition: its relation with other disciplines, a literature survey"; Pattern Recognition, vol.7 (1975), pp.109-116.
29. Kanel, L.; "Patterns in pattern recognition: 1968-74"; IEEE Trans. on Information Theory, vol.IT-20, no.6, Nov.1974, pp.697-722.
30. Wong, E.; "Recent progress in stochastic processes- A survey"; IEEE. trans. on information theory, vol.IT-19, no.3 (May 73), pp.262-275
31. Simon, J.C.; "Recent progress to formal approaches of pattern recognition and scene

- analysis"; Pattern Recognition, vol.7 (1975), pp.117-124.
32. Toussaint, G.T.; "Recent progress in statistical methods applied to pattern recognition"; Proc. of the second international joint conference on pattern recognition, 1974, Denmark, pp.479-88.
 33. Thomason, M.G.; "Syntactic methods in pattern recognition"; Proc. of the NATO advanced study institute: Pattern recognition theory and applications, 1981, pp.119-137.
 34. Fu, K.S.; "Hybrid approaches to pattern recognition"; Pattern recognition theory and applications (editors: J. Kittler, K.S. Fu and L.F. Pau), Reidel publishing company, 1982, pp.139-155.
 35. Blahut, R.E.; "Principles and practice of information theory"; Addison-Wesley, 1987.
 36. Shannon, C.E.; "A mathematical theory of communication"; Bell Sys. Tech. J., 27 (1948), pp.379-423, 623-656.
 37. Nyquist, H. "Certain factors effecting telegraph speed"; Bell. Sys. Tech. J., vol. 3 (April 1924), pp.324-353.
 38. Hartley, R.V.L.; "Transmission of Information"; Bell Sys. Tech. J., vol.7 (July 1928), pp.535-563.
 39. Fisher, R.A.; "Theory of statistical estimation"; Proc. Cambridge Phil. Soc., 22 (1925), pp.700-725.
 40. Wiener, N.; "Extrapolation, interpolation and smoothing of stationary time series"; MIT Press, & Wiley, New York 1949.
 41. Kotel'nikov, V.A.; "The theory of optimum noise immunity"; Ph.D. dissertation, Molotov Energy Institute, Moscow, 1947, Translated by R.A. Silverman, Mc Graw- Hill, New York, 1959.
 42. Hamming, R.W. "Error detecting and error correcting codes"; Bell Sys. Tech. J., vol.29 (April 1950), pp.147-16.
 43. Roden, M.S.; "Analogue and digital communication systems"; Prentice-hall, 1979.
 44. McEllice, R.J.; "Encyclopedia of mathematics and its application: The theory of information and coding"; Addison-Wesley, 1977.

45. Gabor, D.; "Theory of communication"; J. Inst. Elec. Eng. (London), vol 93, pt.3 (Sept. 1946), pp.429-457.
46. Pierce, J.R.; "The early days of information theory"; IEEE Trans. on information theory, vol.IT-19, no.1 (Jan. 1973), pp.3-8.
47. Longo, G.; "The information theory approach to communications"; Spriner-Verlag, 1977.
48. Billingsley, F.C.; "Digital image processing for information extraction"; The Institute of Physics conference series no. 13: 'Machine perception of pattern and pictures', April 1972, pp.337-361.
49. Thompson, A.; "A measure of shared information in class of patterns"; Pattern Recognition, Vol.12 (1980), pp.369-379.
50. Shore J.E.; "Minimum cross-entropy pattern classification and cluster analysis"; IEEE Trans. on pattern analysis and machine intelligence, vol. Pami-4, no.1 (Jan 1982), pp.11-17.
51. Altes, R.A.; Connelly, S.F.; Utilization of information measures for feature selection and dimensionality reduction"; IEEE International symposium in information theory, 1982.
52. Emptoz, H.; "non-probabilistic entropies and indetermination measures in the setting of fuzzy set theory"; Fuzzy sets and systems, vol.5 (1981), pp.307-317.
53. Chuchadeyev, D.N.; "An informational approach in pattern recognition theory"; Soviet Automatic Control, vol.14, no.3 (May 1982), pp.5-16.
54. Chang, S.K.; Yang, C.C.; "Picture information measures for similarity retrieval"; IEEE COMPSAC (1982), pp.464-9.
55. Van Gool, L.; Dewaele, P.; Oosterlinck, A.; "Texture analysis Anno 1983"; Computer Vision, Graphics, and Image Processing, Vol.29 (1985), pp.336-357.
56. Wong, A.K.C.; Sahoo, P.K.; "A gray level threshold selection method based on maximum entropy principles"; IEEE Trans. Sys., Man and Cyber., vol. 19, no.6 (July 89), pp.866-71.
57. Zhuan Ji-Ming, Yu Ying-Lin; "A new approach to image restoration by maximum entropy and evaluation of PSF of an image"; CA-DSP'89, Proc. of 1989 international

- Symposium on computer architecture and digital signal processing, Hong Kong, vol.1, pp.579-83.
58. Huck, F.O.; Fales, C.L.; Park, S.K.; "Information theory analysis of sensor array imaging system for computer vision"; SPIE, vol.397, pp.82-97.
 59. Nishihara, N.K.; "Hidden information in early visual processing"; SPIE, vol.360, pp.76-87.
 60. Ottinen, P.T.; Saarelma; " Information content in images"; Journal of Imaging tech., vol.14,no.1 (Feb. 1988), pp. 15-19.
 61. Pal, N.R.; Pal, S.K.; "Object-background segmentation using new definition of entropy"; IEE Proceedings, vol.136, pt.E, no.4 (July 1989), pp.284-295.
 62. Cencor, Y.; Elfiring, T.; Herman, G.T.; "Methods for entropy maximization with applications in image precessing"; Proc. of the third Scandinavian conference of image analysis, Denmark, 1983, pp. 296-301.

Appendix 1 - Detailed Calculations of the Information Contents of Simple Binary Images

This Appendix explains the details of calculation of the information content of simple binary images described in Chapter 3.

A1.1. Single black pixel on white background

The first case considered was the image of a single black pixel in a 4 by 4 grid of white background as shown in Figure A1.1. The following assumptions were made about this case:

Assumptions

1. The image is binary and no noise is present.
2. The black square occupies an integral pixel.
3. No part of the image lies outside the grid.
4. The image can appear in any of the 16 possible positions with equal probability.

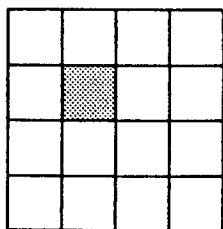


Figure A1.1. The single black pixel.

For this simple case, it can readily be seen that the size of the sample set is 16 which is the number of the possibilities of the black square appearing in any of the positions on the grid.

The information conveyed by detection of the black square in a position may be measured by simply applying the basic entropy formula as shown in equation A1.1:

$$H(x) = - \sum_{i=1}^n p(x_i) \log_2 \frac{1}{p(x_i)} \quad (\text{A1.1})$$

where, $p(x_i)=1/16$, and $n=16$

therefore, $H(x) = 16 \times 1/16 \log_2 16$

$H(x) = \log_2 16$

$H(x) = 4$

Obviously, the conditional entropy formulae are not applicable in this case as there is only one black pixel present.

A1.2. Two black pixels

In this case, two black pixels were considered on a 4 by 4 noise-free grid as shown in Figure A1.2. The assumptions are similar to those of the first case:

Assumptions

1. The image is binary and no noise is present.
2. The image occupies integral number of pixels.
3. No part of the image lies outside the 4 by 4 grid.
4. The 2 black pixels forming the image can lie in both horizontal and vertical orientation as well as at any position within the grid with equal probabilities.
5. The size of the sample set is 24, with 12 possibilities in horizontal and 12 possibilities in vertical orientation, resulting a probability of $p(x) = 1/24$ for any sample set.

6. Scanning of the image is performed in a similar manner to that of a raster scan, ie. starting from top left hand pixel, from left to right and top to bottom.
7. For purpose of application of conditional entropy formulae, we call the upper most or the left hand side black pixel x_1 , and the other black pixel x_2 . This means that the first black pixel discovered by virtue of the scanning algorithm described in 6 above is termed x_1 (see Figure A1.3).

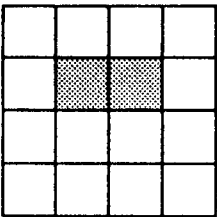


Figure A1.2. The two black pixels.

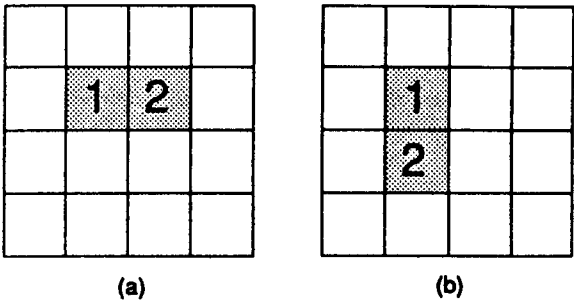


Figure A1.3. Identification of the first scanned black pixel as x_1 and the other as x_2 - (a) left-hand side case, (b) upper-most case.

The basic entropy measurement formula (equation A1.1) can easily be implemented. As already mentioned, $p(x_i) = 1/24$ in this case, therefore,

$$H(X) = 24 \times 1/24 \log_2 24$$

$$H(X) = \log_2 24 = 4.5850$$

In this case the conditional entropy formula can be applied to assess the information conveyed by discovering the first pixel and then the second pixel given the position of the first pixel. In notation this can be described as:

$$H(X) = H(x_1) + H(x_2|x_1)$$

$$H(X) = \sum_{x_1, x_2} \left[p(x_1) \log_2 \frac{1}{p(x_1)} + p(x_2|x_1) p(x_1) \log_2 \frac{1}{p(x_2|x_1)} \right]$$

It is imperative to avoid duplication of the measurements, which is an easy mistake to make if a record of the number of the possibilities (or samples) that have been considered for a defined set of measurements is not kept. In order to avoid this problem a simple scanning algorithm may be adopted which uses the usual raster scan to detect the first pixel, then it considers the two positions to the right or below the first pixel for the second pixel; and never looks at the positions to the *left* or *above* the first pixel.

Figure A1.4 shows the possibilities which exist when the above mentioned scanning algorithm is used.

ii	ii	ii	i
ii	ii	ii	i
ii	ii	ii	i
i	i	i	0

Figure A1.4. Number of x_2 positions possible for any x_1 , when using raster scanning algorithm for the position of x_2 .

Clearly it can be seen that there are 9 x_1 positions for which two possibilities of x_2 exist; and 6 positions for which only one x_2 position is possible. Therefore in the former case, probability of occurrence of x_2 given x_1 , ie $p(x_2 | x_1) = 1/2$; and in the latter case $p(x_2 | x_1) = 1$.

The calculation of the information contents by the conditional entropy method are as follows:

	9 positions		6 positions
$H(X)=$	{ 2 x_2	}{+{ 1 x_2	}
	{ 9 X 2/24 X $\log_2 12$	}	{ 6 X 1/24 X $\log_2 24$
$H(X_2 X_1)=$	{ 9 X 2 X 2/24 X $1/2 \log_2 2$	}	{ 6 X 1 X 1/24 X $1 \log_2 1$
	3/4 $\log_2 12$	+	1/4 $\log_2 24$
	3/4 $\log_2 2$	+	0
	3/4 $\log_2 24$	+	1/4 $\log_2 24$
	<u>= $\log_2 24$</u>		

Clearly the calculation of the information contents in both conditional and non-conditional cases agree.

A1.3. Three black pixels in L-shape

A1.3.1. The 4 by 4 grid

In this case three black pixels were arranged such that they formed an L-shape in a 4 by 4 grid as shown in Figure A1.5.

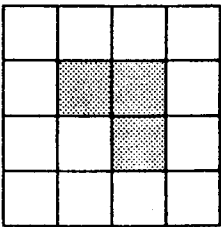


Figure A1.5. The L-Shape.

Assumptions

1. The image is binary and no noise is present.
2. The image occupies integral number of pixels.
3. No part of the image lies outside the 4 x 4 grid.
4. The L-shape image can lie in any position and orientation within the grid with equal probabilities, thus resulting in a sample size of 36 and sample point probability of 1/36.
5. Initial raster scan is performed to detect the first pixel of the L-shape which is then termed as x_1 . Clearly, this will then be the top left hand pixel of the L-shape.

The independent test may be performed easily by considering the possible 36 positions and orientations of the L-shape:

$$n = 36 ; p(x_i) = 1/36$$

therefore, $H(X) = 36 \times 1/36 \log_2 36$

$$H(X) = \log_2 36$$

or, $H(X) = 5.17$

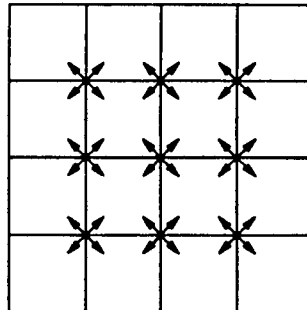


Figure A1.6. Demonstration of the 36 possible positions and orientations of the L-shape.

The conditional entropy technique may also be used to measure the information conveyed by the L-shape. However scanning the grid is still important so that duplication may be avoided.

By taking into account the information from left to right scan, when a black pixel is discovered it could obviously be the top left hand pixel.

Fig A.7. shows the possibilities for x_2 patterns given each x_1 positions. It can be seen that the total number is 36.

3	4	4	1
3	4	4	1
3	4	4	1
0	0	0	0

Figure A1.7. Number of possibilities of x_2 given x_1 in a 4x4 grid.

The calculations using the conditional entropy are as follows:

TOTAL
3 positions
{
3 x_2
}
{
9
}
= 36

}+{
6 positions
4 x_2
}
{
24
}
}+{
3 positions
1 x_2
}
{
3
}

For x_1

$H(X_1)=$
{ 3 X 3/36 \log_2 12
}
}+{
6 X 4/36 \log_2 9
}
}+{
3 X 1/36 \log_2 36
}

=
{ 1/4 \log_2 12
}
}+{
2/3 \log_2 9
}
}+{
1/12 \log_2 36
}

For x_2 & x_1

$H(X_2|x_1) =$
{ 9X3/36X1/3X \log 12
}
}+{
24X4/36X1/4 \log 4
}
}+{
3X1/36X1 \log 1
}

=
{ 1/4 \log_2 3
}
}+{
2/3 \log_2 9
}
}+{
1/12 \log_2 36
}

Therefore,

$H(X)$
= $H(X_1)$ + $H(X_2)$

= \log_2 36

= 5.1699

Clearly, this result agrees with the independent measure of information.

A1.3.2 The 5 by 5 grid

In order to show that the foregoing was not a coincidence, let's consider the same L-shape in a 5 by 5 grid, where we have $p(x_1) = 1/64$.

Non-Conditional entropy

$$\begin{aligned} H(X) &= 64 \times 1/64 \log_2 64 \\ &= \log_2 64 \\ &= 6 \end{aligned}$$

Conditional entropy

As seen in Figure A1.8;

3	4	4	4	1
3	4	4	4	1
3	4	4	4	1
3	4	4	4	1
0	0	0	0	0

Figure A1.8. Number of possibilities of x_2 given x_1 in a 5x5 grid.

$$\begin{aligned} & \begin{array}{ccc} 4 \text{ positions} & 12 \text{ positions} & 4 \text{ positions} \end{array} \\ & \left\{ \begin{array}{l} 3 \ x_2 \\ 12 \end{array} \right\} + \left\{ \begin{array}{l} 4 \ x_2 \\ 48 \end{array} \right\} + \left\{ \begin{array}{l} 1 \ x_2 \\ 4 \end{array} \right\} \\ & = 64 \text{ possibilities} \end{aligned}$$

For x_1

$$\begin{aligned} H(X_1) &= \left\{ 4 \times \frac{3}{64} \log_2 \frac{64}{3} \right\} + \left\{ 12 \times \frac{4}{64} \log_2 \frac{16}{4} \right\} + \left\{ 4 \times \frac{1}{64} \log_2 \frac{64}{1} \right\} \\ &= \left\{ \frac{3}{16} \log_2 \frac{64}{3} \right\} + \left\{ \frac{3}{4} \log_2 16 \right\} + \left\{ \frac{1}{16} \log_2 64 \right\} \\ &= 4.2028 \end{aligned}$$

For x_2

$$\begin{aligned} H(X_2) &= \left\{ 12 \times \frac{3}{64} \times \frac{1}{3} \log_2 3 \right\} + \left\{ 48 \times \frac{4}{64} \times \frac{1}{4} \log_2 4 \right\} + \left\{ 4 \times \frac{1}{64} \times 1 \log_2 1 \right\} \\ &= \left\{ \frac{3}{16} \log_2 3 \right\} + \left\{ \frac{3}{4} \log_2 4 \right\} + \left\{ 0 \right\} \\ &= 1.7971 \end{aligned}$$

Therefore,

$$\begin{aligned} H(X) &= H(X_1) + H(X_2) \\ H(X) &= 6 \end{aligned}$$

APPENDIX 2 - Details of Calculation of Basic Rotational and Translational Information Content

This Appendix is a detailed explanation of calculation of rotational and translational information content of a simple, two level (binary) 4x2 rectangular input image which was used in the preliminary investigation described in Chapter 3.

A2.1. Calculation of rotational information content.

In this section detailed calculations of information content associated with rotation of the rectangular input image are shown. There were four cases considered when the input image was rotated about its centre of gravity while keeping the position of the centre of gravity fixed in relation to the pixel array. These are labelled as Set IA, IB, IC, and ID as shown in Figure A2.1.

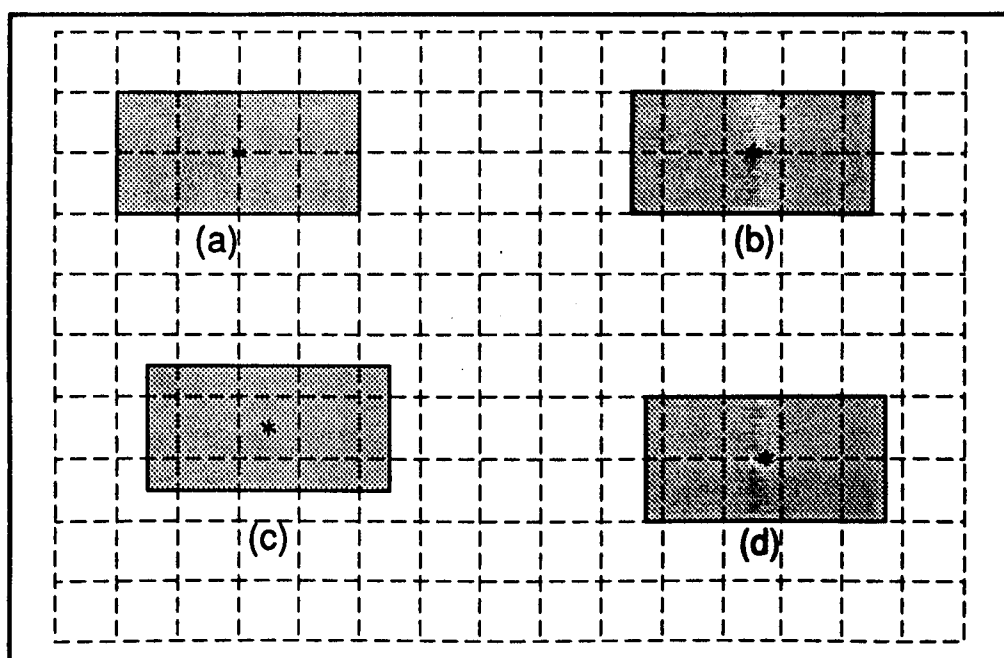


Figure A2.1. Position of centre of gravity of each sample set (each square represents one pixel).

- (a): Sample set IA
- (b): Sample set IB
- (c): Sample set IC
- (d): Sample set ID

For each of the four cases considered in this section, two figures and one table are shown. The first figure shows the rectangular input image as it is subjected to rotation through 180 degrees and the respective sensor output patterns (sensor response) at the specified intervals. The second figure shows the complete set of uniquely numbered sensor output patterns, and the respective range of angles over which each sensor pattern exists. The table for each case, shows the steps taken in calculation of the rotational information content for each case.

A2.1.1. Set IA

In Set IA, two types of calculations were made, one assuming that the sensor array behaves like a set of area detectors, and the other assuming that the sensors array behaves like a set of point detectors. The results obtained when area detectors were used are shown in Figures A2.1(a), A2.2(a), and Table A2.1(a). The results obtained when point detectors were used are shown in Figures A2.1(b), A2.2(b), and Table A2.1(b).

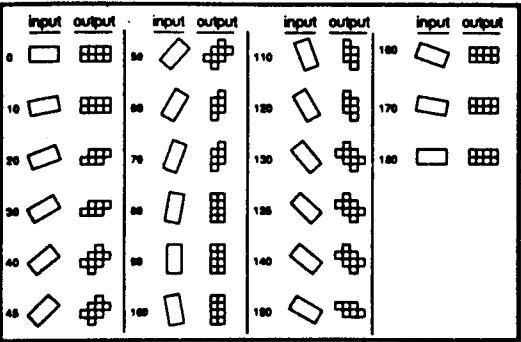


Figure A2.1(a). Case IA - response of the area sensor array.

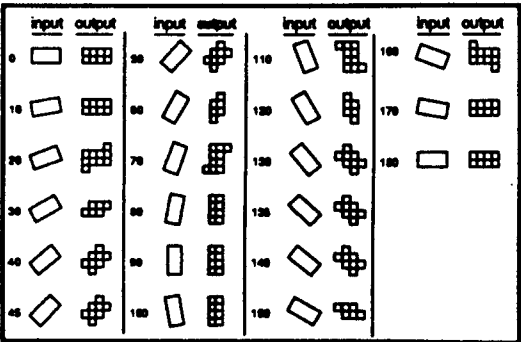


Figure A2.1(b). Case IA - Response of point sensor array.

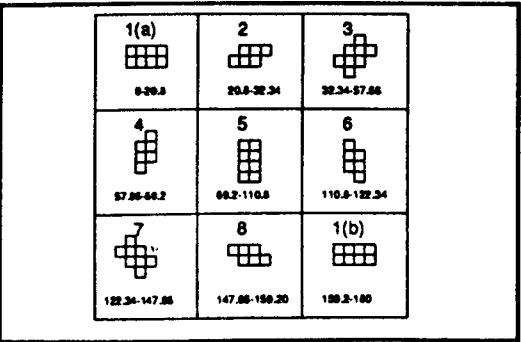


Figure A2.2(a). Set IA - The set of sensor output patterns produced using area sensors.

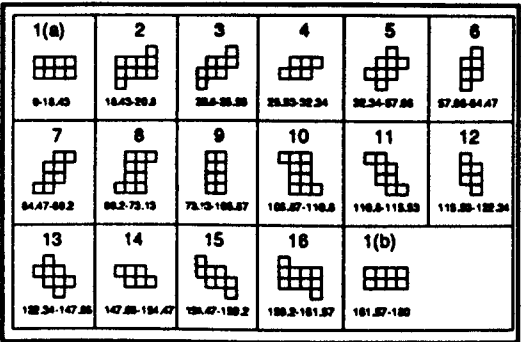


Figure A2.2(b). Set IA - The set of sensor output patterns using point detectors.

x_i	Range R (degrees)	$P(x_i)$	$\log \frac{1}{2 p(x_i)}$	$H(X) = \sum p(x_i) \log \frac{1}{2 p(x_i)}$	$H(X) / R$
x_1	41.6	0.2311	2.1134	0.4884	0.0117
x_2	11.54	0.0641	3.9635	0.2541	0.0220
x_3	25.32	0.1403	2.8334	0.3975	0.0157
x_4	11.54	0.0641	3.9635	0.2541	0.0220
x_5	41.6	0.2311	2.1134	0.4884	0.0117
x_6	11.54	0.0641	3.9635	0.2541	0.0220
x_7	25.32	0.1403	2.8334	0.3975	0.0157
x_8	11.54	0.0641	3.9635	0.2541	0.0220
TOT.	180	1.0000	-	2.7882	-

Table A2.1(a). Case IA - Rotational Information Assessment Results
When Area Detectors Are Used.

x_i	Range R (degrees)	$P(x_i)$	$\log \frac{1}{2 p(x_i)}$	$H(X) = \sum p(x_i) \log \frac{1}{2 p(x_i)}$	$H(X) / R$
x_1	36.86	0.2048	2.2879	0.4686	0.0127
x_2	2.37	0.0132	6.2433	0.0824	0.0348
x_3	4.73	0.0263	5.2488	0.1380	0.0292
x_4	6.81	0.0378	4.7255	0.1786	0.0262
x_5	25.32	0.1407	2.8293	0.3981	0.0157
x_6	6.81	0.0378	4.7255	0.1786	0.0262
x_7	4.73	0.0263	5.2488	0.1380	0.0292
x_8	3.93	0.0218	5.5195	0.1203	0.0306
x_9	33.74	0.1874	2.4158	0.4527	0.0134
x_{10}	3.93	0.0218	5.5195	0.1203	0.0306
x_{11}	4.73	0.0263	5.2488	0.1380	0.0292
x_{12}	6.81	0.0378	4.7255	0.1786	0.0262
x_{13}	25.32	0.1407	2.8293	0.3981	0.0157
x_{14}	6.81	0.0378	4.7255	0.1786	0.0262
x_{15}	4.73	0.0263	5.2488	0.1380	0.0292
x_{16}	2.37	0.0132	6.2433	0.0824	0.0348
TOT.	180	1.0000	-	3.3893	-

Table A2.1(b). Case IA - Rotational Information Assessment results
When Point Detectors are used.

A2.1.2. Set IB

Results for this set are shown in Figures A2.3, A2.4 and Table A2.2.

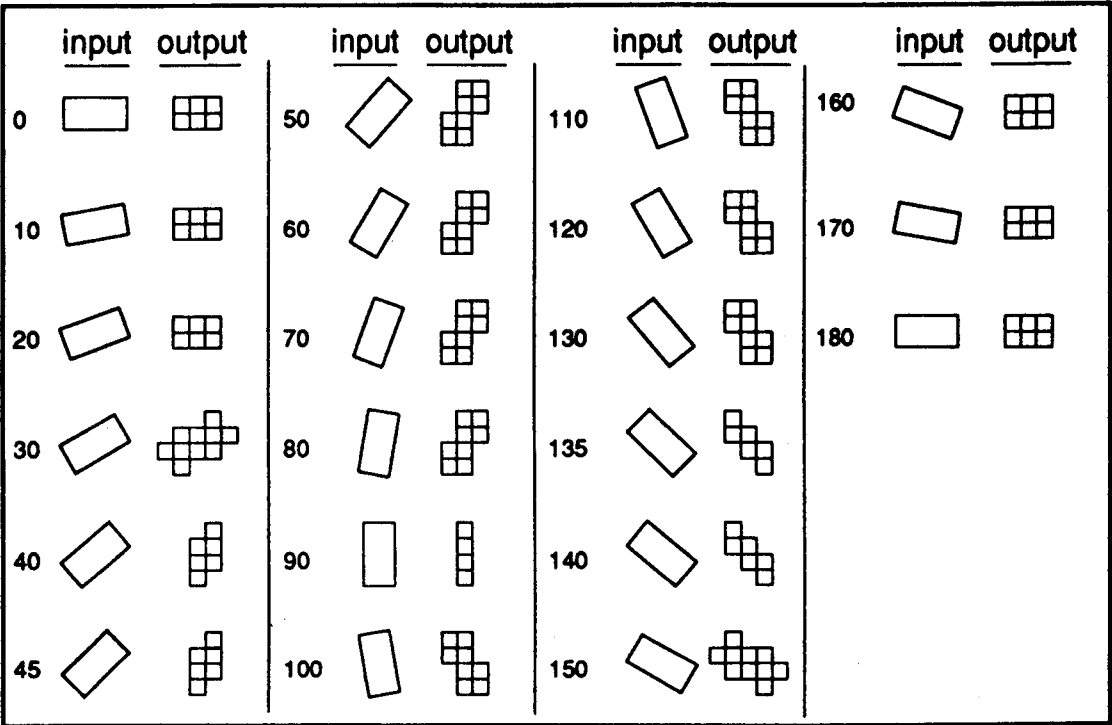


Figure A2.3. Case IB - Response of point sensor array.

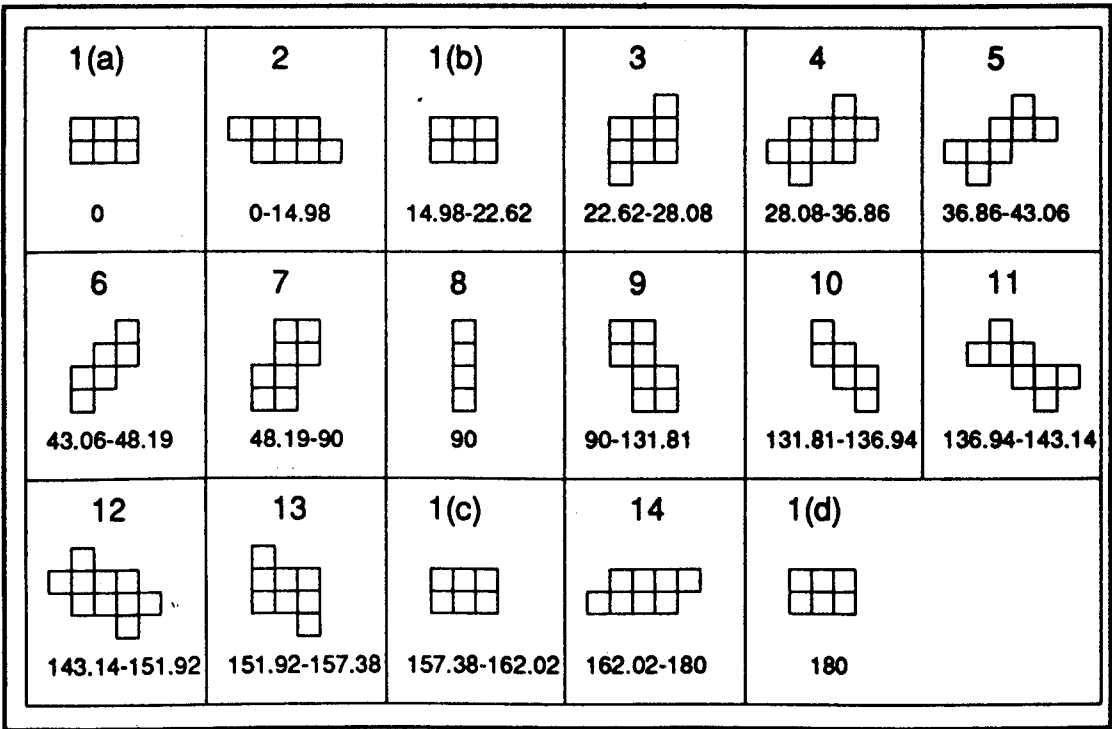


Figure A2.4. Case IB - The set of sensor output patterns.

x_i	Range R (degrees)	$P(x_i)$	$\log \frac{1}{2 p(x_i)}$	$H(X) = \sum p(x_i) \log \frac{1}{2 p(x_i)}$	$H(X) / R$
x_1	15.28 ⁹	0.0849	3.5581	0.3021	0.0198
x_2	14.98	0.0832	3.5873	0.2985	0.0199
x_3	5.46	0.0303	5.0445	0.1528	0.0280
x_4	8.78	0.0488	4.3570	0.2126	0.0242
x_5	6.2	0.0344	4.8614	0.1672	0.0270
x_6	5.13	0.0285	5.1329	0.1463	0.0285
x_7	41.81	0.2323	2.1059	0.4892	0.0117
x_8	0	0	-	-	-
x_9	41.81	0.2323	2.1059	0.4892	0.0117
x_{10}	5.13	0.0285	5.1329	0.1463	0.0285
x_{11}	6.2	0.0344	4.8614	0.1672	0.0270
x_{12}	8.78	0.0488	4.3570	0.2126	0.0242
x_{13}	5.46	0.0303	5.0445	0.1528	0.0280
x_{14}	14.98 ⁹	0.0832	3.5873	0.2985	0.0199
TOT.	180	1.0000	-	3.2353	-

Table A2.2.

Case IB - Rotational Information Assessment results
When Point Detectors Are Used.

A2.1.3. Set IC

Results for this set are shown in Figures A2.5, A2.6, and Table A2.3.

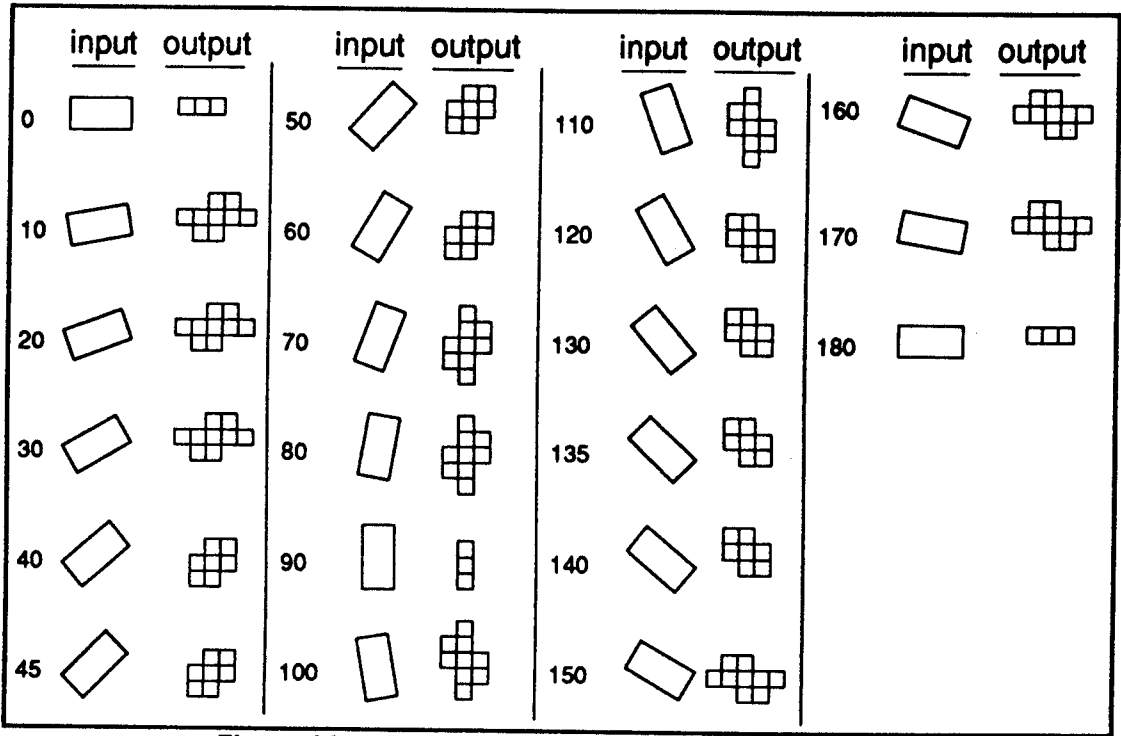


Figure A2.5. Case IC - response of point sensors array.

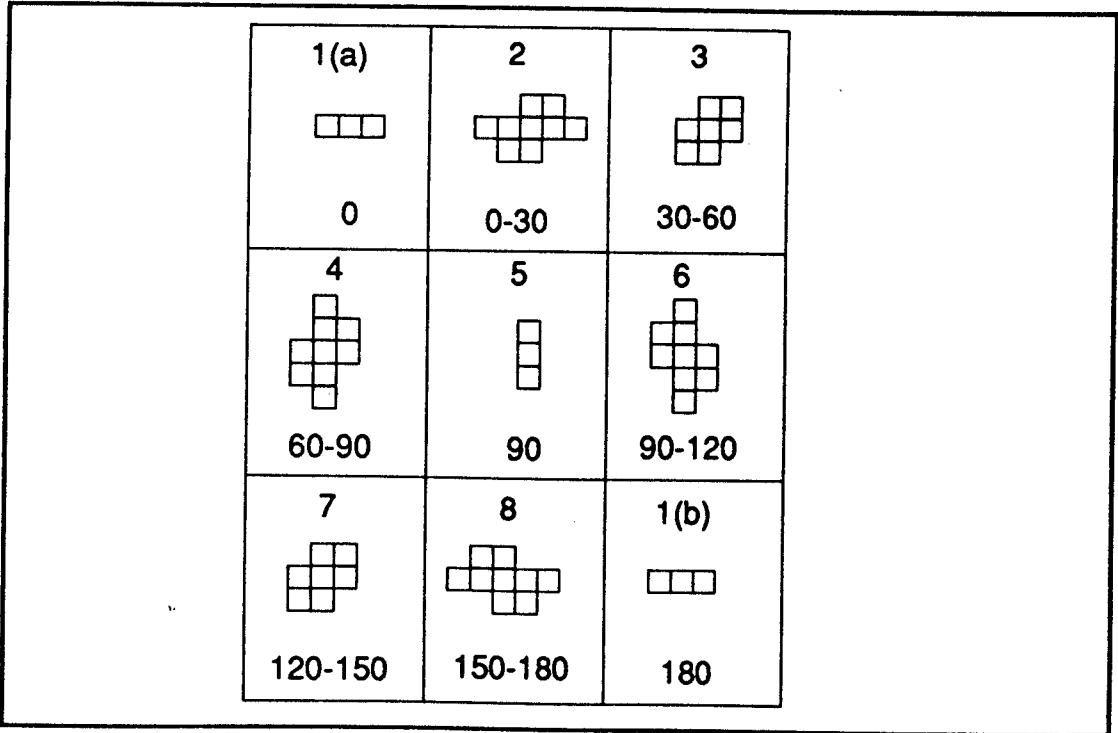


Figure A2.6. Set IC - The set of sensor output patterns.

x_i	Range R (degrees)	$P(x_i)$	$\log_2 \frac{1}{p(x_i)}$	$H(X) = \sum p(x_i) \log_2 \frac{1}{p(x_i)}$	$H(X) / R$
x_1	0	0	-	-	-
x_2	30	1/6	2.5850	0.4308	0.0144
x_3	30	1/6	2.5850	0.4308	0.0144
x_4	30	1/6	2.5850	0.4308	0.0144
x_5	0	0	-	-	-
x_6	30	1/6	2.5850	0.4308	0.0144
x_7	30	1/6	2.5850	0.4308	0.0144
x_8	30	1/6	2.5850	0.4308	0.0144
TOT.	180	1.0000	-	2.5850	-

Table A2.3. Case IC - Rotational Information Assessment results When Point Detectors Are Used.

A2.1.4. Set ID

The results for this set are presented in Figures A2.7, A2.8 and Table A2.4.

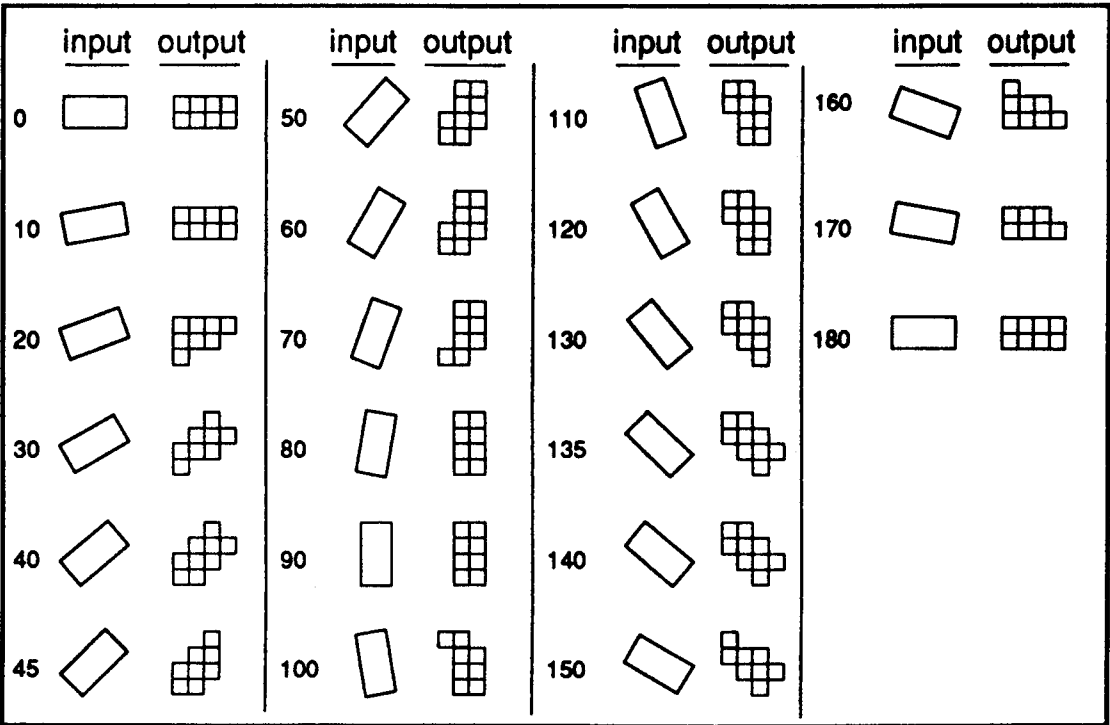


Figure A2.7. Set ID - response of point sensor array.

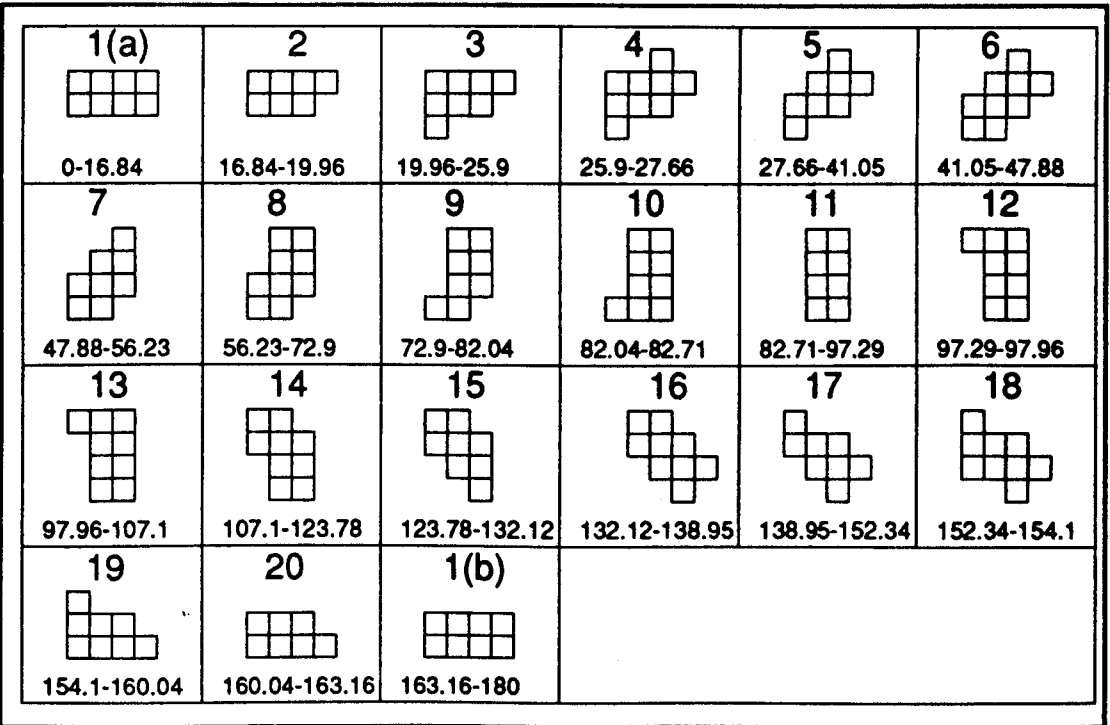


Figure A2.8. Set ID - The set of sensor output patterns.

x_i	Range R (degrees)	$P(x_i)$	$\log \frac{1}{2 p(x_i)}$	$H(X_i) = p(x_i) \log \frac{1}{2 p(x_i)}$	$H(X_i) / R$
x_1	33.68	0.1871	2.4181	0.4525	0.0134
x_2	3.12	0.0173	5.8503	0.1012	0.0324
x_3	5.94	0.0330	4.9214	0.1624	0.0273
x_4	1.76	0.0098	6.6763	0.0654	0.0372
x_5	13.39	0.0744	3.7488	0.2789	0.0208
x_6	6.83	0.0379	4.7200	0.1789	0.0262
x_7	8.35	0.0464	4.4301	0.2056	0.0246
x_8	16.67	0.0926	3.4327	0.3179	0.0191
x_9	9.14	0.0508	4.2997	0.2184	0.0239
x_{10}	0.67	0.0037	8.0696	0.0299	0.0446
x_{11}	14.58	0.0810	3.6259	0.2937	0.0201
x_{12}	0.67	0.0037	8.0696	0.0299	0.0446
x_{13}	9.14	0.0508	4.2997	0.2184	0.0239
x_{14}	16.67	0.0926	3.4327	0.3179	0.0191
x_{15}	8.35	0.0464	4.4301	0.2056	0.0246
x_{16}	6.83	0.0379	4.7200	0.1789	0.0262
x_{17}	13.39	0.0744	3.7488	0.2789	0.0208
x_{18}	1.76	0.0098	6.6763	0.0654	0.0372
x_{19}	5.94	0.0330	4.9214	0.1624	0.0273
x_{20}	3.12	0.0173	5.8503	0.1012	0.0324
TOT.	180.00	1.0000	-	3.8634	-

Table A2.4.

Case ID - Rotational Information Assessment Results
When Point Detectors Are Used.

A.2.2. Calculation of Translational Information Content

In this section details of assessment of information content associated with translation of the rectangular input image is presented. There were five cases considered when the input image was translated within the pivotal pixel while maintaining a fixed inclination to the pixel array. Input images inclined at 0 degrees, 30 degrees, 45 degrees, and 90 degrees were considered. The results are labelled as Set IIA, IIB, IIC and IIE respectively. The 60 degree case was deduced from the 30 degree set by symmetry and is labelled as set IID, but not shown in detail here.

A2.2.1 - Set IIA: object Inclined at 0 degrees

In this case there can only be one sensor pattern associated with each pivotal pixel with a probability of one. This is because the probability of occurrence of other sensor patterns is zero. Therefore the measure of the fine translation information is zero. This is the expected result, as no information is conveyed by the occurrence of a certain event. Figure A2.9. shows the set of sensor output patterns and their respective areas of occurrence in the pixel array.

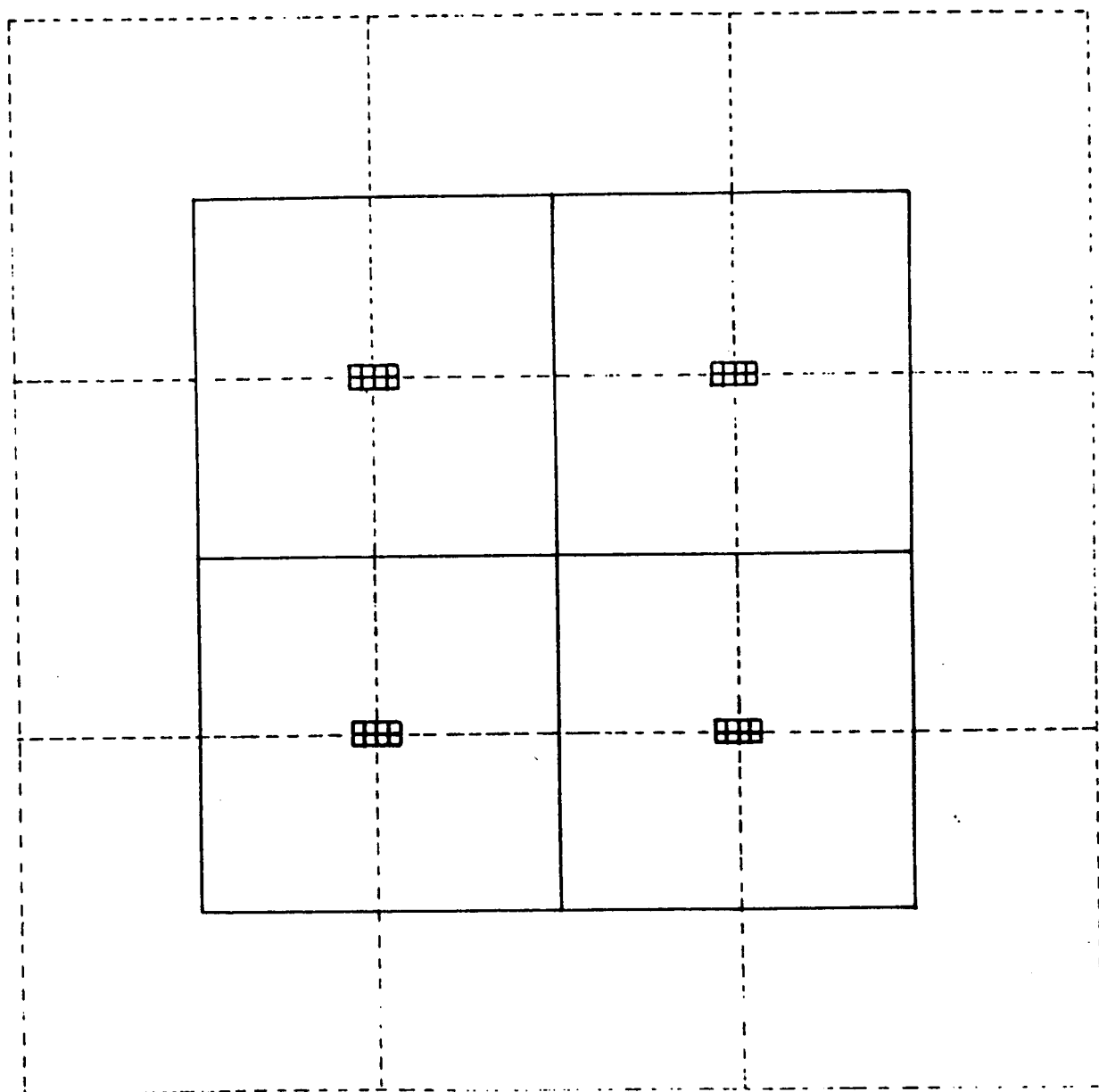


Figure A2.9. CaseIIA - Rectangular image subjected to translation and the sensor patterns arising when point sensors are used.

Each square with broken line represents one pixel, the solid lines denote the enclosed areas in which a specific sensor pattern occurs. The sensor patterns are shown within the enclosed area in which they occur.

A2.2.2 - Case IIB: object Inclined at 30 degrees

In this case there are 29 different sensor patterns attributed to each pixel. Figure A2.10. shows the uniquely numbered set of sensor output patterns, and their respective areas of occurrence in the pixel array. The detailed calculations of the translational information content are shown in Table A2.5.

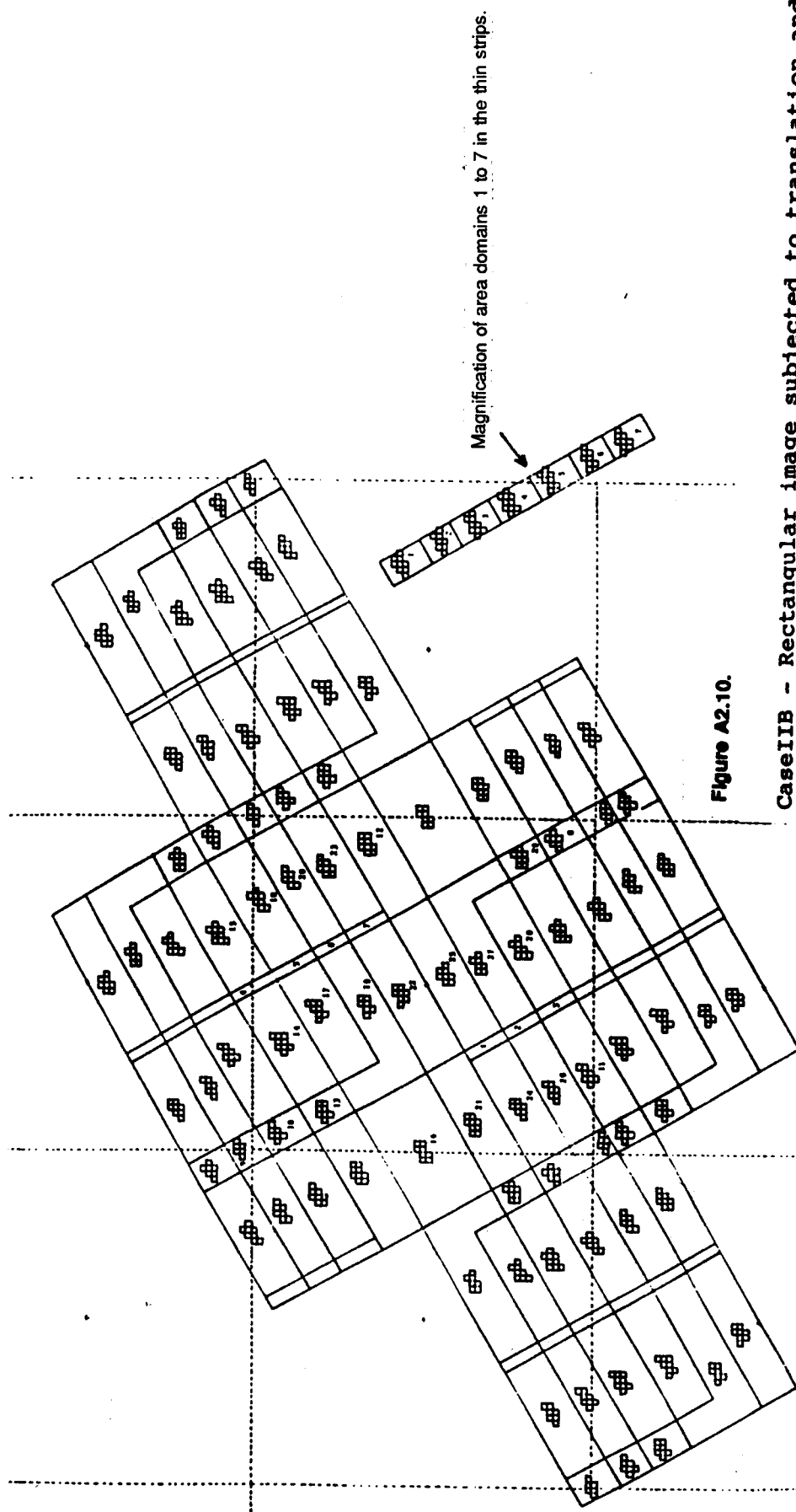


Figure A2.10.

CaseIIB - Rectangular image subjected to translation and the sensor patterns arising when point sensors are used.

Each square with broken line represents one pixel, the solid lines denote the enclosed areas in which a specific sensor pattern occurs. The sensor patterns are shown within the enclosed area in which they occur. The number shown against each sensor pattern identifies it as a unique sensor pattern attributable to the central pixel.

x_i	Range R (unit area)	$p(x_i)$	$\log \frac{1}{2 p(x_i)}$	$H(X) = \sum p(x_i) \log \frac{1}{2 p(x_i)}$	$H(X) / R$
x_1	0.0048	0.0048	7.6999	0.0370	7.6999
x_2	0.0035	0.0035	8.1499	0.0287	8.1499
x_3	0.0048	0.0048	7.6999	0.0370	7.6999
x_4	0.0048	0.0048	7.6999	0.0370	7.6999
x_5	0.0048	0.0048	7.6999	0.0370	7.6999
x_6	0.0035	0.0035	8.1499	0.0287	8.1499
x_7	0.0048	0.0048	7.6999	0.0370	7.6999
x_8	0.0131	0.0131	6.2499	0.0821	6.2499
x_9	0.0096	0.0096	6.6999	0.0644	6.6999
x_{10}	0.0131	0.0131	6.2499	0.0821	6.2499
x_{11}	0.0490	0.0490	4.3500	0.2133	4.3500
x_{12}	0.0538	0.0538	4.2150	0.2270	4.2150
x_{13}	0.0131	0.0131	6.2499	0.0821	6.2499
x_{14}	0.0490	0.0490	4.3500	0.2133	4.3500
x_{15}	0.0490	0.0490	4.3500	0.2133	4.3500
x_{16}	0.0933	0.0933	3.4225	0.3192	3.4225
x_{17}	0.0490	0.0490	4.3500	0.2133	4.3500
x_{18}	0.0490	0.0490	4.3500	0.2133	4.3500
x_{19}	0.0587	0.0587	4.0916	0.2400	4.0916
x_{20}	0.0359	0.0359	4.7999	0.1723	4.7999
x_{21}	0.0538	0.0538	4.2150	0.2270	4.2150
x_{22}	0.0622	0.0622	4.0075	0.2492	4.0075
x_{23}	0.0490	0.0490	4.3500	0.2133	4.3500
x_{24}	0.0490	0.0490	4.3500	0.2133	4.3500
x_{25}	0.0622	0.0622	4.0075	0.2492	4.0075
x_{26}	0.0359	0.0359	4.7999	0.1723	4.7999
x_{27}	0.0587	0.0587	4.0916	0.2400	4.0916
x_{28}	0.0490	0.0490	4.3500	0.2133	4.3500
x_{29}	0.0131	0.0131	6.2499	0.0821	6.2499
TOT.	1.0000	1.0000	-	4.4381	-

Table A2.5.

Case IIB - Translational Information Assessment
Results When Point Detectors Are Used.

A2.2.3 - Case IIC: object Inclined at 45 degrees

In this case the number of sensor patterns which are attributable to each pixel is 8. Figure A2.11 shows the uniquely numbered set of sensor output patterns and their respective areas of occurrence in the pixel array. Table A2.6. shows the detailed calculations of the translational information content in this case.

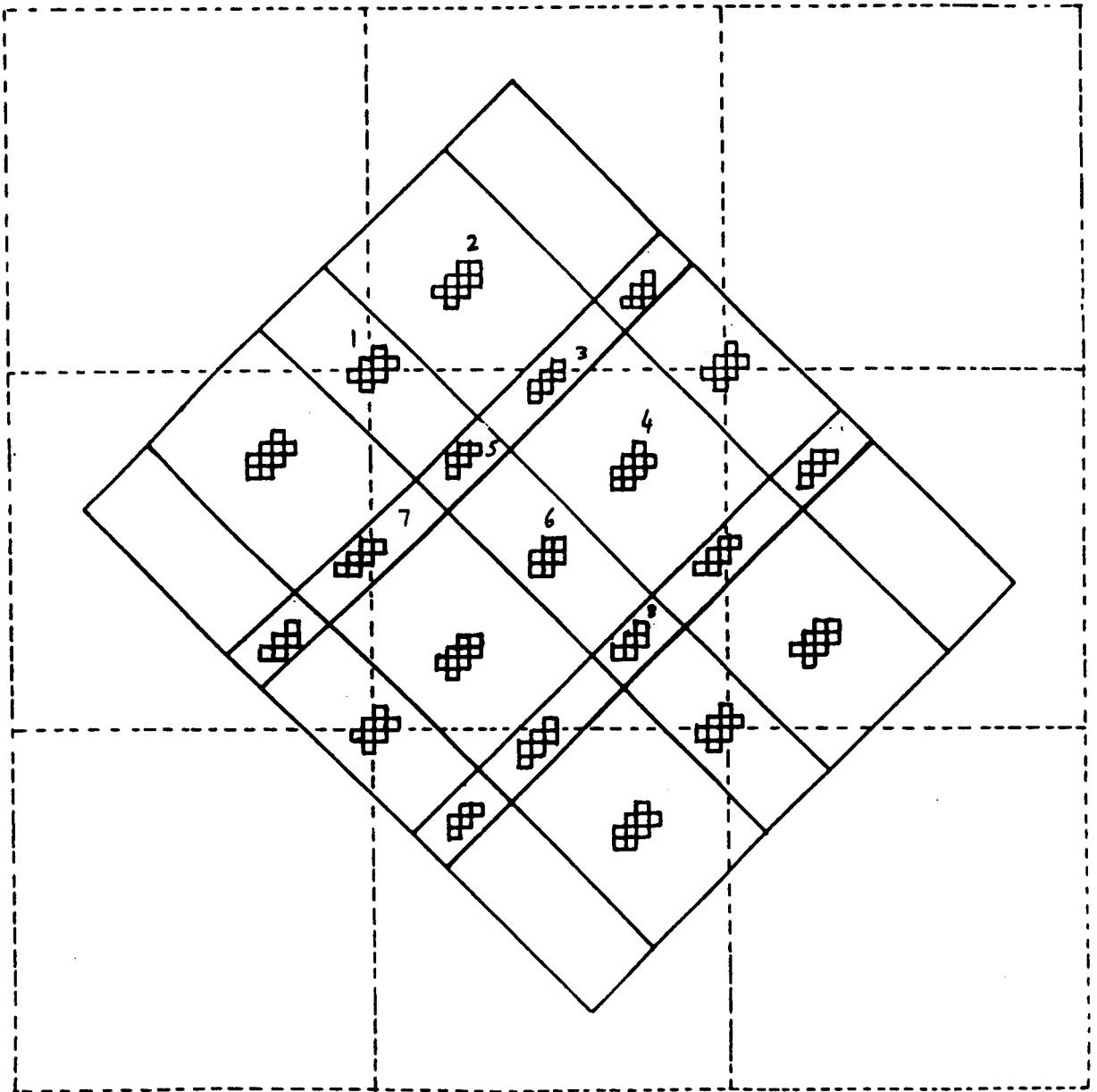


Figure A2.11. CaseIIC - Rectangular image subjected to translation and the sensor patterns arising when point sensors are used.

Each square with broken line represents one pixel, the solid lines denote the enclosed areas in which a specific sensor pattern occurs. The sensor patterns are shown within the enclosed area in which they occur. The number shown against each sensor pattern identifies it as a unique sensor pattern attributable to the central pixel.

x_i	Range R (unit area)	$P(x_i)$	$\log_2 \frac{1}{p(x_i)}$	$H(X) = \sum_i p(x_i) \log_2 \frac{1}{p(x_i)}$	$H(X) / R$
x_6	0.1458	0.1454	2.7821	0.4045	2.7706
x_2	0.2670	0.2663	1.9087	0.5083	1.9037
x_4	0.2670	0.2663	1.9087	0.5083	1.9037
x_8	0.0313	0.0312	5.0036	0.1561	5.0359
x_5	0.0313	0.0312	5.0036	0.1561	5.0359
x_3	0.0573	0.0571	4.1302	0.2358	4.1375
x_7	0.0573	0.0571	4.1302	0.2358	4.1375
x_1	0.1458	0.1454	2.7821	0.4045	2.7706
TOT.	1.0028	1.0000	-	2.6094	-

Table A2.6. Case IIC - Translational Information Assessment
Results When Point Detectors Are Used.

A2.2.4. - Case IID: object Inclined at 90 degrees

As for case IIA, in this case there can only be one sensor pattern associated with each pixel with a probability of one. This is because the probability of occurrence of other sensor patterns is zero. Therefore the measure of the fine translation information is zero. This is the expected result, as no information is conveyed by the occurrence of a certain event. Figure A2.12. shows the set of sensor output patterns and their respective areas of occurrence in the pixel array.

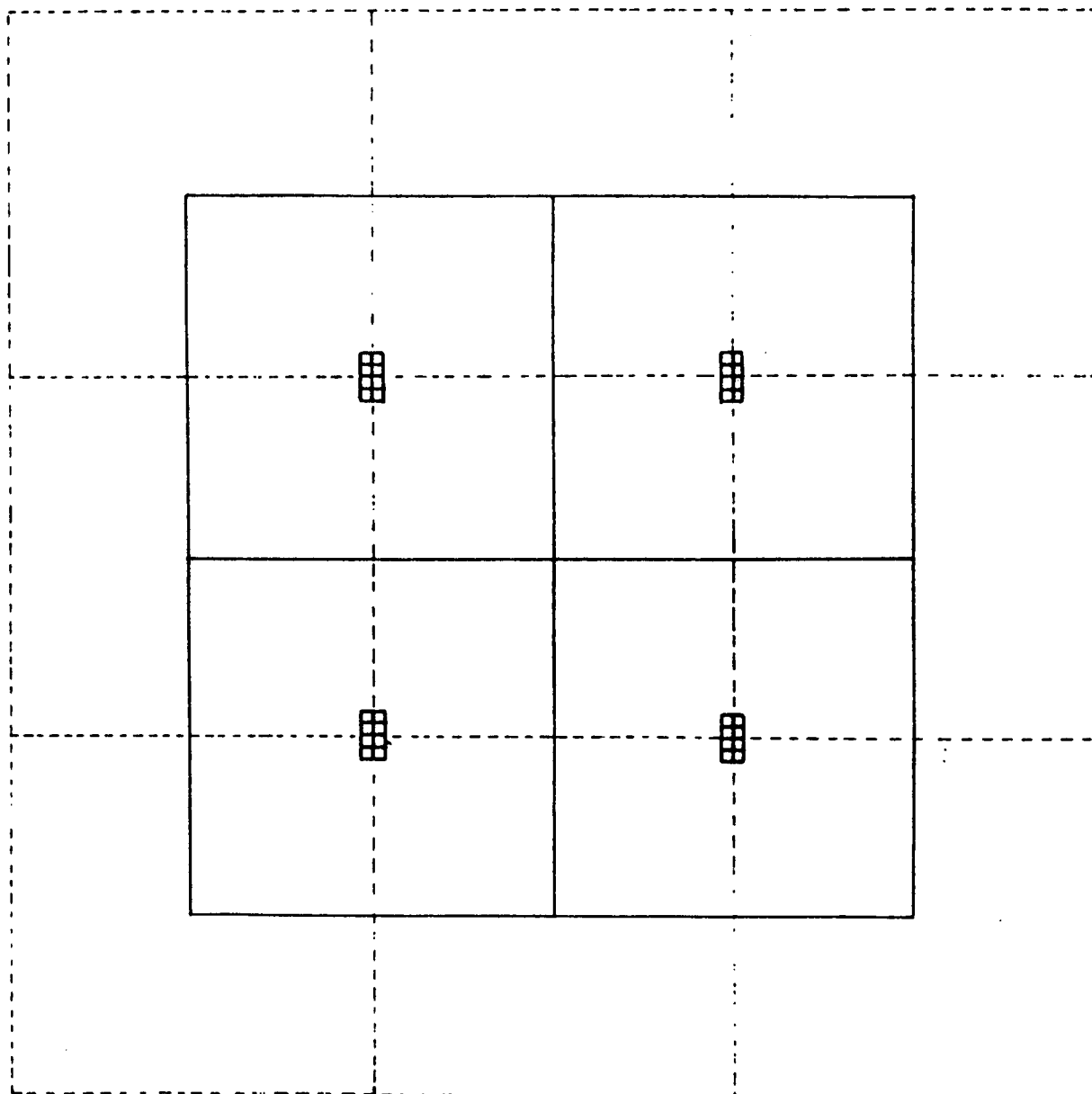


Figure A2.12. CaseIIE - Rectangular image subjected to translation and the sensor patterns arising when point sensors are used.

Each square with broken line represents one pixel, the solid lines denote the enclosed areas in which a specific sensor pattern occurs. The sensor patterns are shown within the enclosed area in which they occur.

APPENDIX 3 - Translation, Rotation and Total Information

(Private Communication from Professor R.L. Beurle)

This Appendix describes in detail the theory behind translation, rotation and total information content as described in Chapter 5.

1. Fig 4.1 is a map of pixel output patterns vs position denoted by axis Z and angle θ . The scales Z and θ are made up of m and n elements respectively, corresponding to the positions and angles for which the output patterns have been determined and their extent. (Z may represent a co-ordinate x + iy in two dimensions).
2. A, B & C show three out of many possible shapes denoting the areas occupied by individual patterns. The scales are chosen so that equal area denotes equal probability of occurrence.
3. Translation Information is assessed by summing $p_i \log \frac{1}{p_i}$ for all patterns for a given value of θ (i.e. along a horizontal line). To find the mean value for all θ , the result is then summed vertically and divided by n.

Thus, the contribution of pattern A or pattern B to the mean is

$$\frac{q}{n} \frac{p}{m} \log \frac{m}{p} = \frac{pq}{mn} (\log m - \log p)$$

For pattern C, the assessed contribution is $\frac{u}{n} \frac{1}{m} \log m$

4. For Rotation Information we have likewise

$$\text{For A or B } \frac{pq}{mn} (\log n - \log q)$$

$$\text{For C, } \frac{u}{mn} \log n$$

5. For overall Information we sum $p_i \log \frac{1}{p_i}$ over the whole area giving

$$\text{For A or B } \frac{pq}{mn} \log \frac{mn}{pq}$$

$$\text{For C } \frac{u}{mn} \log \frac{mn}{u}$$

6. The excess of Translation + Rotation Information over overall Information is

$$\text{For A or B } \frac{pq}{mn} (\log m + \log n - \log p - \log q)$$

$$- \frac{pq}{mn} (\log m + \log n - \log p - \log q)$$

$$= 0$$

$$\begin{aligned} \text{For C } & \frac{u}{mn} (\log m + \log n) - \frac{u}{mn} (\log m + \log n - \log u) \\ &= \frac{u}{mn} \log u \end{aligned}$$

7. Conditional Entropy Explanation

The conditional entropy of Z , given that C is known, represents the remaining uncertainty about Z which may be resolved if θ is also given. Thus, one of the u possible values of Z is selected by the knowledge of the true value of θ (out of u possibilities), taken in conjunction with the configuration of the area C on the pixel pattern map and

$$p(Z/C) = \frac{1}{u}$$

$$\text{But } p(C) = \frac{u}{mn}$$

$$\text{Therefore } H(Z/C) = \sum_{u \text{ terms}} \left(\frac{u}{mn} \cdot 1 \cdot \log u \right) = \frac{u}{mn} \log u$$

8. An Alternative

Another way of showing that the result obtained in 6. represents the information provided by a knowledge of θ which enables Z to be defined more precisely is to argue:-

When pattern C occurs, which it does with a frequency of $\frac{u}{mn}$, a knowledge of the value of θ allows the selection of the true value of Z from the u possible values. This uses $\log u$ bits of information. Since this only occurs with a frequency of $\frac{u}{mn}$, the contribution that this correlation between θ and Z makes to the overall average information is

$$\frac{u}{mn} \log u$$

This also applies if it is the value of Z which is known and is used to identify θ more precisely.

9. Accuracy of determination of Z without a knowledge of θ (or vice versa)

The knowledge provided by the configuration of C is only useful if we know either θ to enable us to pinpoint Z more precisely, or Z enabling us to identify θ more precisely. Without this information we are no better off than we would be with a square map area for C . Then the useful *overall* information provided by C would be $\frac{u}{mn} \log \frac{mn}{u^2}$. This is equal to the *overall* information less the result in 6.

$$\frac{u}{mn} \log \frac{mn}{u} = \frac{u}{mn} \log u - \frac{u}{mn} \log \frac{mn}{u^2}$$

Overall Information Result in 6 Useful or "net" component
of *overall* Information

THUS:

If we write the sum of such terms as $\frac{u}{mn} \log u$ as S .

Gross Overall Information

$$\begin{aligned}
 &= \text{Net overall information} + s \\
 &= \text{Gross Translation Information } T \\
 &\quad + \text{Gross Angular Information } A \\
 &\quad - s
 \end{aligned}$$

therefore,

Net overall information

$$\begin{aligned}
 &= (T - s) \\
 &\quad + (A - s)
 \end{aligned}$$

$$\begin{aligned}
 &[= \text{Net translation Information } \tau] \\
 &[= \text{Net Angular Information } \alpha]
 \end{aligned}$$

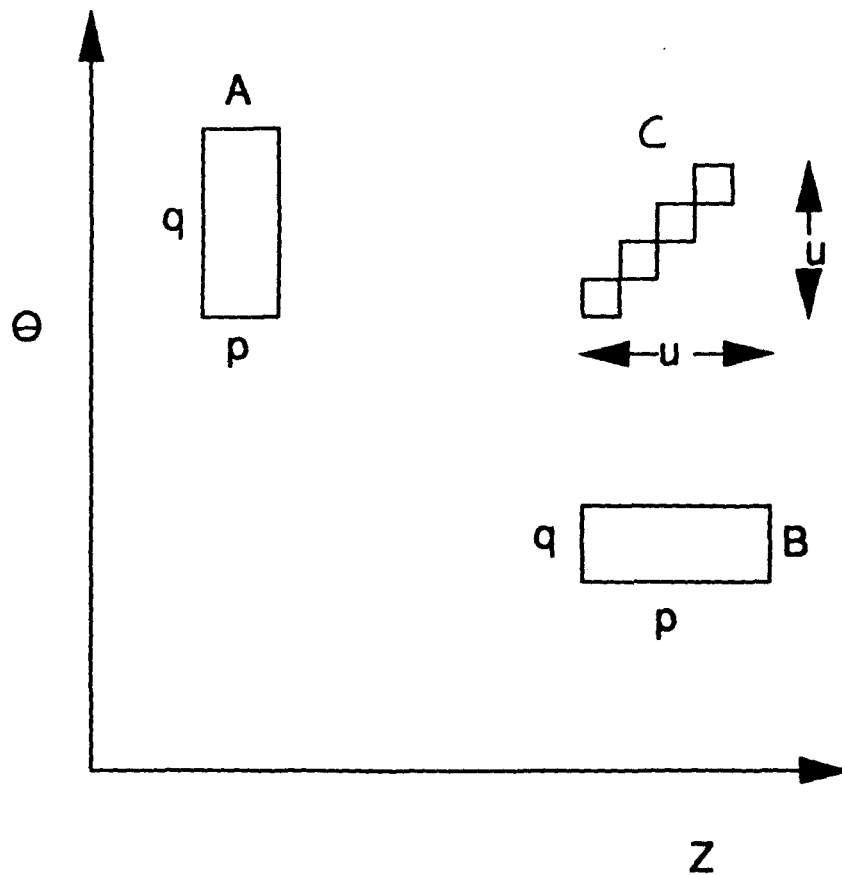


Figure A3.1.

Appendix 4 - Computer Calculation of Fine Translational Information Content

This Appendix describes details of the procedure used in computing fine translational information content of images shown in chapter 5.

A4.1. Details of calculations

As a typical example, consider the 4x2 rectangular pattern when it is oriented at 30 degrees. Using the technique described in Chapter 4 (section 4.2) all the unique sensor output patterns discovered are classified and labelled by comparing them with the set of unique sensor output patterns discovered in other orientations. Figure A4.1 shows the sensor output patterns found in this example, the number next to each sensor output pattern in this Figure being the label (i) used by the computer for purpose of identifying each unique sensor output pattern.

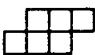
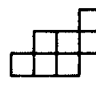
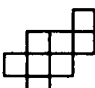
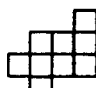
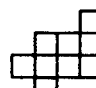
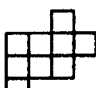
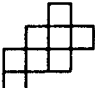
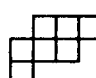
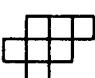
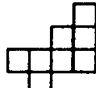
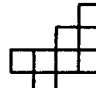
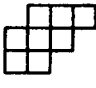
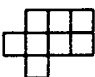
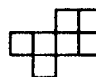
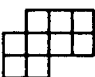
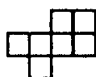
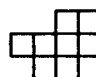
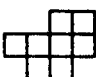

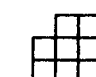
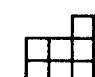
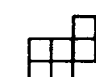


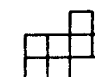
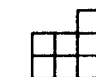
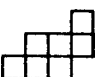
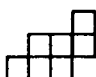
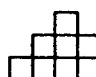
 52	 46	 53	 48	 64	 51
 54	 43	 56	 65	 57	 58
 8	 66	 11	 13	 67	 14
 12	 15	 17	 16	 70	 60
 61	 21	 71	 72	 62	

Figure A4.1. Sensor output patterns for 4x2 rectangle oriented at 30 degrees.

The area of the domain occupied by each unique sensor output pattern is also evaluated using the method described in Chapter 4. The second column in Table A4.1 lists the areas found in this example. The probability of occurrence of each unique sensor output pattern $p(x_i)$ may then be calculated by dividing its respective domain area by the total area of the pivotal pixel, which is 1,048,576 ($=1024 \times 1024$). Clearly the sum of these probabilities will be 1 as shown in the third column of Table A4.1. The information associated with each unique sensor output pattern may then be calculated using the standard relationship shown in equation A4.1.

$$H(x_i) = -p(x_i) \log_2 \frac{1}{p(x_i)} \quad (A4.1)$$

Consequently the total information at 30 ° may be calculated by summing all these individual information values using equation A4.2.

$$H(X) = -\sum_{i=1}^n p(x_i) \log_2 \frac{1}{p(x_i)} \quad (A4.2)$$

This is the fine translational information content of the 4x2 rectangular pattern when oriented at 30 degrees as shown in the fourth column of Table A4.1, which in this case is 4.4381.

Sensor Pattern (i)	area	$p(x_i)$	$H(x_i)$
52	10087.0030	0.0096	0.0646
46	37642.2081	0.0358	0.1723
53	51420.3008	0.0490	0.2133
48	51419.8618	0.0490	0.2133
64	5043.7588	0.0048	0.0376
51	51420.3584	0.0490	0.2133
54	51419.8187	0.0490	0.2133
43	37641.3306	0.0358	0.1723
56	13776.8674	0.0131	0.0821
65	5043.2632	0.0048	0.0376
57	51419.4231	0.0490	0.2133
58	51419.4231	0.0490	0.2133
8	13776.5280	0.0131	0.0821
66	3681.8827	0.0035	0.0267
11	56463.8218	0.0538	0.2276
13	61506.5038	0.0587	0.2400
67	5043.2632	0.0048	0.0376
14	65186.4486	0.0622	0.2482
12	87797.3256	0.0833	0.3182
15	65186.8675	0.0622	0.2482
17	56463.8784	0.0538	0.2276
16	61506.8848	0.0587	0.2400
70	5042.3857	0.0048	0.0376
60	51418.4358	0.0490	0.2133
61	51420.3584	0.0490	0.2133
21	13777.5837	0.0131	0.0821
71	3680.9473	0.0035	0.0267
72	5042.3857	0.0048	0.0376
62	13777.5837	0.0131	0.0821
Total	1048572.6456	1.0000	4.4381

Table A4.1. Translational information results for 4x2 pattern at 30°.

A4.2. Summary of the results

Table A4.2 shows the results obtained for the 4x2, 8x2 and 8x4 rectangles, and the 4x4 squares. These are the values used for plotting Figure 5.6 in Chapter 5.

Pattern→	4x2	4x4	8x2	8x4
Orientation ↓				
0	0.0112	0.0204	0.0112	0.0112
1	0.5290	0.7928	1.0832	1.3480
2	0.9777	1.4710	1.8888	2.4183
3	1.3852	2.0818	2.8145	3.3730
4	1.7708	2.6556	3.2518	4.2254
5	2.1362	3.1931	3.7942	4.9829
6	2.4809	3.6925	4.2249	5.5819
7	2.8034	4.1507	4.5015	5.9878
8	3.1021	4.5642	4.5855	6.1398
9	3.3750	4.9299	4.7513	6.2995
10	3.6202	5.2448	4.8955	6.3314
11	3.8354	5.5050	4.8041	6.4509
12	4.0177	5.7076	5.0585	6.4703
13	4.1631	5.8473	5.2112	6.3743
14	4.2634	5.9146	4.4592	5.3333
15	4.2882	5.8980	5.1002	6.3631
16	4.4068	5.6837	5.6534	6.1138
17	4.4524	5.8779	5.4986	6.6558
18	4.4123	5.5048	5.3148	6.1855
19	4.4635	5.5559	5.4379	6.3405
20	4.4989	5.6970	5.6588	6.5545
21	4.3794	5.7473	5.2788	6.5198
22	4.4529	5.6148	5.1180	6.2580
23	4.4615	5.3154	5.2223	6.2834
24	4.4878	4.8410	5.3487	6.1801
25	4.2780	4.1343	5.4540	5.3889
26	3.9116	3.4888	4.8380	4.2801
27	3.8428	3.3896	4.6744	4.0396
28	4.1375	3.7122	5.4985	4.8816
29	4.3932	4.5407	5.4035	5.9998
30	4.4381	5.1374	4.8587	6.3554
31	4.5208	5.5480	5.0955	6.2489
32	4.4285	5.7870	5.1529	6.4857
33	4.4797	5.8399	5.0289	6.4003
34	4.5154	5.7846	4.7557	6.0617
35	4.5252	5.7819	5.2584	6.3812
36	4.4056	5.4435	4.9993	6.2212
37	4.2084	4.8537	4.1124	5.0978
38	4.3585	5.5398	5.1692	6.4895
39	4.3833	5.7520	5.2147	6.5872
40	4.3382	5.6522	5.8086	6.4853
41	4.1395	5.5094	5.5161	6.4323
42	3.8539	5.2978	5.0170	6.3589
43	3.6785	4.8582	4.8058	6.0110
44	3.3268	4.1478	4.0892	5.0636
45	2.5891	2.8556	2.5587	2.8252
TOTAL	169.503	214.3069	211.5988	254.7313
AVERAGE	3.684847	4.658845	4.599973	5.537636

Table A5.2. Summary of translational information results.

The *probability volume* of each unique sensor output pattern may be calculated by summing the probabilities in each orientation, and dividing by the total range of orientations.

Appendix 5 - Translational Information Dips **in Simple Images**

It was noted in Chapter 5 (section 5.2.2.) that when assessing fine translational information, at certain orientations dips in values of the information were encountered, as shown in figure 5.6. This effect may be attributed to interaction between the boundaries of the pattern under test and the pixel centres. In most orientations, as the pattern is translated horizontally its boundaries cross one pixel centre at any one time. This leads to a gradual change in the sensor output patterns since they change by one pixel only when the of the pattern moves from one area domain to the next.

However, at certain orientations, the boundary (or boundaries) of the pattern may be inclined so that as the pattern is translated horizontally, the boundary crosses two or more pixel centres simultaneously. This means that the sensor output pattern changes by more than one pixel as the centre of gravity of the pattern moves from one area domain to the next. In such a case, when the whole area of the pivotal pixel is considered, fewer sensor output patterns are encountered, and on average each sensor output pattern spans a larger area domain.

These large area domains introduce uncertainty about the locations of the centre of gravity of the pattern within the pivotal pixel, and consequently this leads to a drop in the assessed information.

This effect may be observed by considering the computer generated area domain maps shown in figure A5.1. This shows the results obtained for the 4 x 2 rectangular pattern as its orientation passes through 45°. It can clearly be seen that the lines defining the boundaries between area domains move close to each other until they touch at 45° inclination and form 8 unique large area domains.

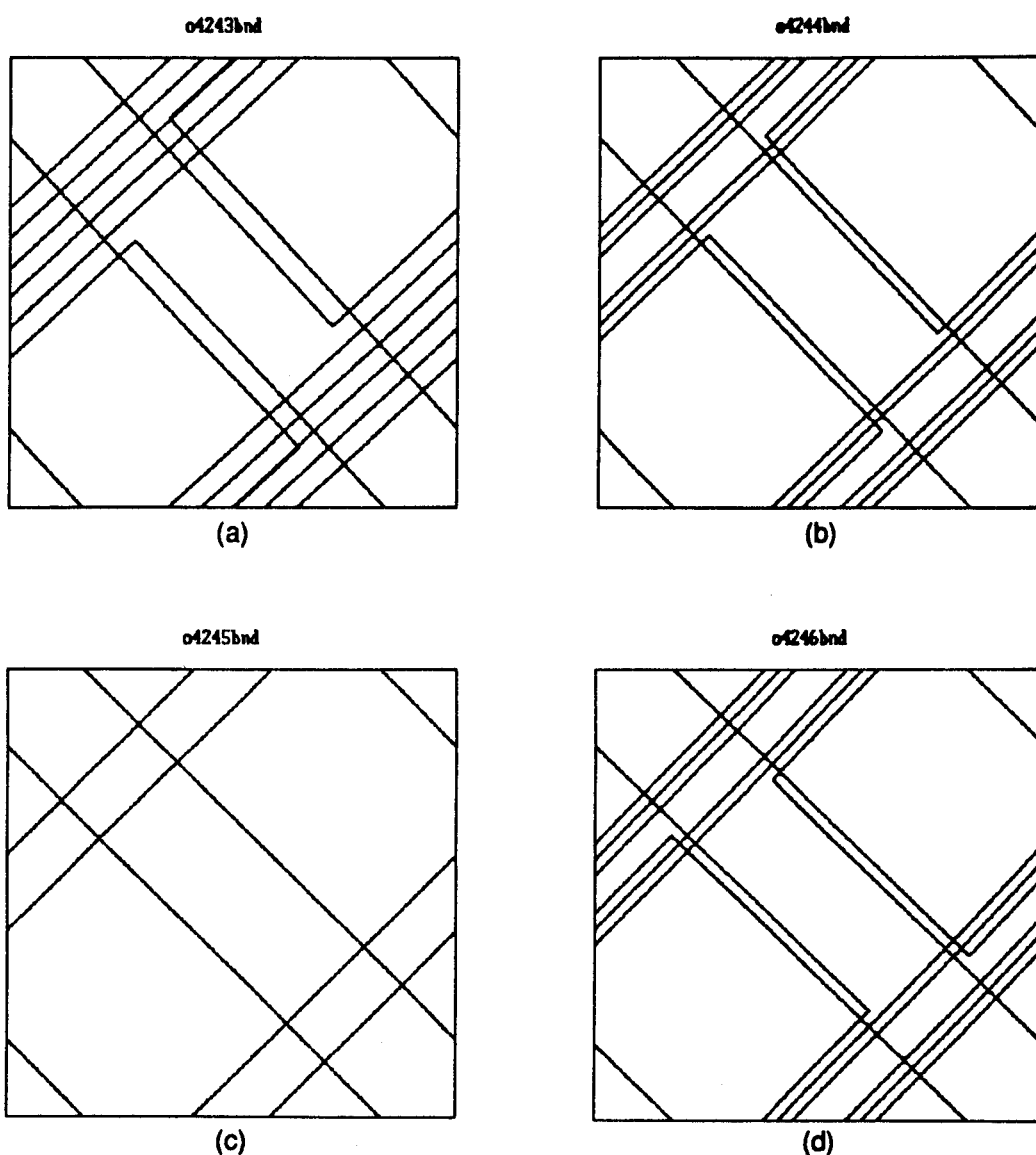


Figure A5.1. Area Domain maps for the 4x2 rectangle inclined at
 (a) 43 degrees
 (b) 44 degrees
 (c) 45 degrees
 (d) 46 degrees

A5.1 Calculation of critical Inclinations and lengths boundaries

By considering Figure A5.2, the angles at which an inclined boundary crosses more than one pixel centre simultaneously may be calculated together with the minimum length of the boundary required for each case to occur. Table A5.1 summarizes this information.

From these values one may expect to see 'dips' in the values of the information for the patterns that meet the requirements. For instance, in the case of 8 x 2 and 8 x 4 rectangular patterns, one expects to see

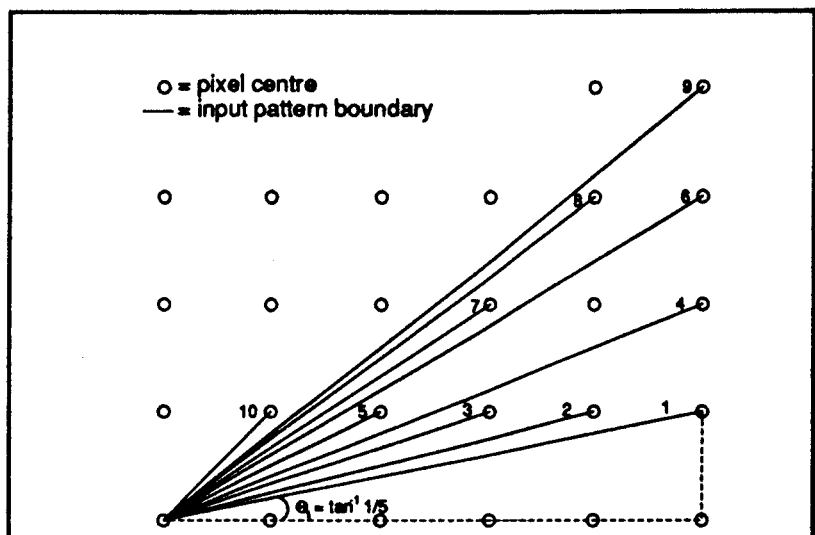


Figure A5.2. Interaction between the pixel centres and the pattern boundary.

dips at the angles listed in table A5.1. Figure A5.3 confirms this theory. One may also expect dips at angles at which opposite sides of a rectangle cross pixel centres simultaneously. An example is that for sides separated by two or four pixel units 36.87° is a critical angle with an equivalent *minimum length* of only one or two units.

Case No.	$\tan \theta$	θ	Minimum Length
1	1/5	11.31	5.10
2	1/4	14.04	4.12
3	1/3	18.43	3.16
4	2/5	21.80	5.39
5	1/2	26.57	2.27
6	3/5	30.96	5.83
7	2/3	33.69	3.61
8	3/4	36.87	5.00
9	4/5	38.66	6.40
10	1/1	45	1.00

Table A5.1 Critical inclinations and lengths of boundaries.

Dips at 0°, 26.57°, 36.27° and 45° are more prominent since more than two pixel centres are

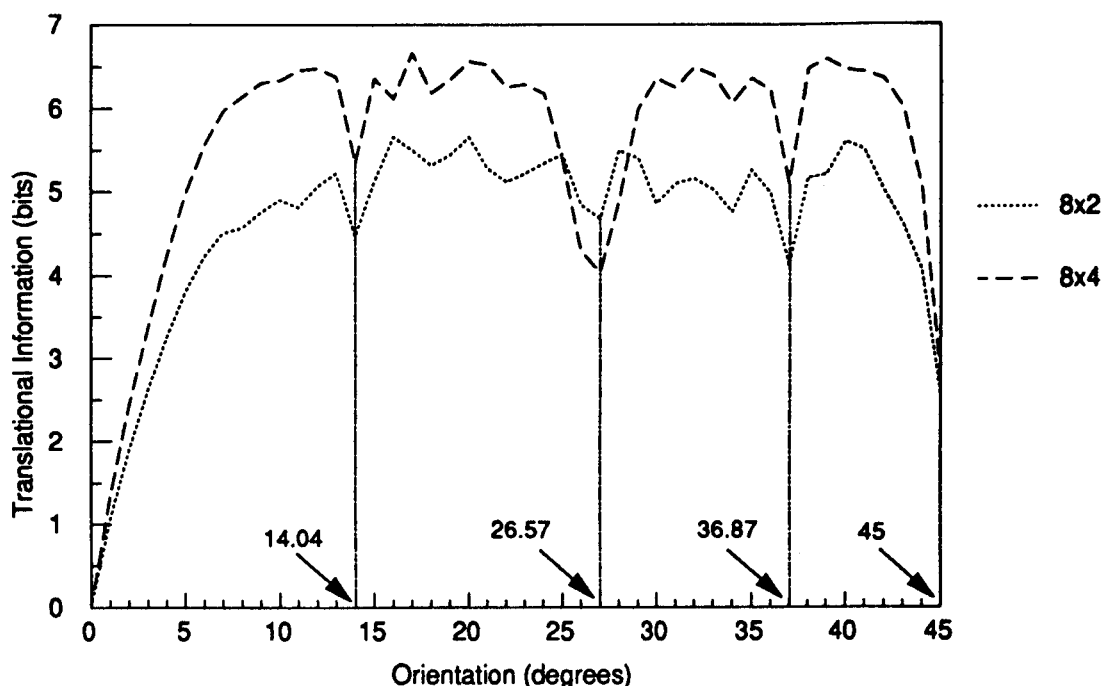


Figure A5.3. Translational Information *dips* for 8x2 and 8x4 rectangles.

crossed by the patterns' boundaries simultaneously. Similarly, when considering the 4 x 2 and 4 x 4 patterns as shown in Figures A5.4, dips present at 0°, 26.57°, 36.87° and 45° are explicable in terms of either single sides or opposite sides crossing pixel centres.

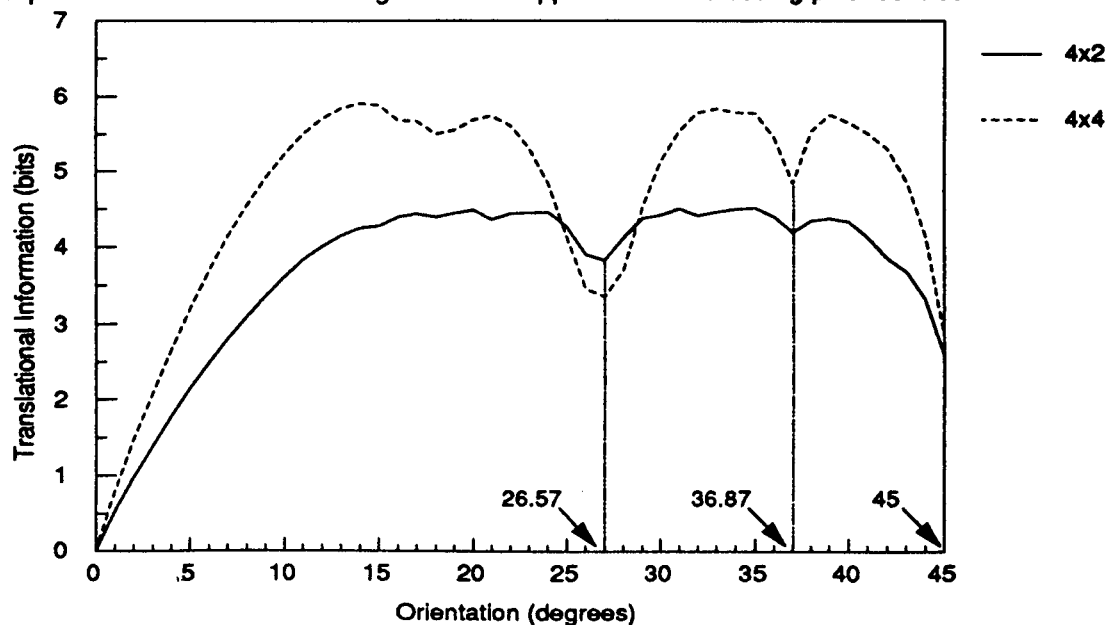


Figure A5.4. Translational information *dips* for 4x2 rectangle and 4x4 square.